INVESTIGATION OF W-BEAM ENERGY-ABSORBING GUARDRAIL END TERMINAL SAFETY PERFORMANCE USING FINITE ELEMENT MODELING

Yunzhu Meng

Dissertation submitted to the faculty of the Virginia Polytechnic Institute and State University in partial fulfillment of the requirements for the degree of

Doctor of Philosophy
In
Biomedical Engineering

Costin D. Untaroiu, Chair
Warren N. Hardy
Zachary R. Doerzaph
Stefan M. Duma
Yong W. Lee

July 18th, 2022
Blacksburg, VA

Keywords: Roadside safety; Occupant safety; Computational biomechanics; Finite Element

INVESTIGATION OF W-BEAM ENERGY-ABSORBING GUARDRAIL END TERMINAL SAFETY PERFORMANCE USING FINITE ELEMENT MODELING

Yunzhu Meng

ABSTRACT

Guardrails were designed to deter vehicle access to off-road areas and consequently prevent hitting rigid fixed object alongside the road (e.g., trees, utility poles, traffic barriers, etc.). However, guardrails cause 10% of deaths of vehicle-to-fixed object crashes which has attracted attention in the highway safety community on the vehicle-based injury criteria used in guardrail regulations. The objectives of this study were 1) to develop and validate a Finite Element (FE) model of the ET-Plus, a commonly used energy-absorbing guardrail end terminal; 2) to examine the conditions of in-service end terminals, and to evaluate the performance of the damaged relative to undamaged end terminals in simulated impacts; 3) to investigate both full-body and body region driver injury probabilities during car-to-end terminal crashes using dummy and human body FE models; to analyze the relationship between the vehicle-based crash severity metrics used currently in regulations and the injury probabilities assessed using biomechanics injury criteria; and 4) to quantify the influence of pre-impact conditions on injury probabilities.

In this dissertation, an ET-Plus FE model was developed based on publicly available data on ET-Plus dimensions and material properties. The model was validated against the NCHRP-350 crash tests. The developed ET-Plus model was used to develop to five damaged ET-Plus whose damage patterns were identified based on an investigation of in-service end terminals mounted along U.S. roads. It was observed that damaged end terminals usually increase collision severity compared to undamaged end terminals. Meanwhile, a total of 40 FE impact simulations between a car with a dummy/human body model in the driver seat and an end terminal model were performed in various configurations. The vehicle-based severity metrics were observed to be correlated to full-body and certain body-region injury risks while no head injury risk could be predicted. The results pointed out that more advanced vehicle-based metrics should be proposed and investigated to improve the predictability in terms of occupant injury risks in the crash tests. The simulation models could also supplement crash compliance tests of new hardware designs, by investigating their safety performance for a large variety of pre-impact conditions, observed in traffic accidents, but not included the compliance tests.

INVESTIGATION OF W-BEAM ENERGY-ABSORBING GUARDRAIL END TERMINAL SAFETY PERFORMANCE USING FINITE ELEMENT MODELING

Yunzhu Meng

GENERAL AUDIENCE ABSTRACT

Guardrails were designed to deter vehicle access to off-road areas and consequently prevent hitting rigid fixed object alongside the road (e.g., trees, utility poles, traffic barriers, etc.). However, guardrails cause 10% of deaths of vehicle-to-fixed object crashes which has attracted attention in the highway safety community on the vehicle-based injury criteria used in guardrail regulations. The objectives of this study were 1) to develop and validate a Finite Element (FE) model of a commonly used energy-absorbing guardrail end terminal; 2) to examine the conditions of in-service end terminals, and to evaluate the performance of the damaged relative to undamaged end terminals in simulated impacts; 3) to investigate both full-body and body region driver injury probabilities during car-to-end terminal crashes using dummy and human body FE models; to analyze the relationship between the vehicle-based crash severity metrics used currently in regulations and the injury probabilities assessed using biomechanics injury criteria; and 4) to quantify the influence of pre-impact conditions on injury probabilities.

In this dissertation, a numerical model was developed based on publicly available data on end terminal dimensions and material properties. The model was validated against the NCHRP-350 crash tests. The developed ET-Plus model was used to develop to five damaged ET-Plus whose damage patterns were identified based on an investigation of in-service end terminals mounted along U.S. roads. It was observed that damaged end terminals usually increase collision severity compared to undamaged end terminals. Meanwhile, a total of 40 impact simulations between a car with a dummy/human body model in the driver seat and an end terminal model were performed in various configurations. The vehicle-based severity metrics were observed to be correlated to full-body and certain body-region injury risks while no head injury risk could be predicted. The results pointed out that more advanced vehicle-based metrics should be proposed and investigated to improve the predictability in terms of occupant injury risks in the crash tests. The simulation models could also supplement crash compliance tests of new hardware designs, by investigating their safety performance for a large variety of pre-impact conditions, observed in traffic accidents, but not included the compliance tests.

Acknowledgements

I would like to express my deepest appreciation to my advisor, Dr. Costin Untaroiu, for all his invaluable help and encouragement, in addition to the other members of my committee Dr. Warren N. Hardy, Dr. Zachary R. Doerzaph, Dr. Stefan M. Duma, Dr. Yong W. Lee.

I would also like to thank the various organizations (e.g., IIHS, GHBMC, NHTSA) who have sponsored my research. Furthermore, many thanks to my lab mates. Thank you so much for all your friendship and help throughout this process. I would like to acknowledge my family for their enduring support of me.

Table of Contents

List of figures

List of tables

Attribution

Several colleagues aided in the writing and research behind my chapters presented as part of this dissertation. A brief description of their contributions is included here.

Chapter 3:

Wen Hu, Ph.D., is currently a Senior Research Transportation Engineer at Insurance Institute for Highway Safety (IIHS). Dr. Hu served as a co-author on this paper and helped to review and edit the paper draft.

Costin D. Untaroiu, Ph.D., is an associate professor at Virginia Tech. Dr. Untaroiu supervised, conceptualized, and helped review and edit the paper draft.

Chapter 4:

Wen Hu, Ph.D., is currently a Senior Research Transportation Engineer at IIHS. Dr. Hu served as a co-author on this paper and helped to review and edit the paper draft.

Costin D. Untaroiu, Ph.D., is an associate professor at Virginia Tech. Dr. Untaroiu supervised, conceptualized, and helped review and edit the paper draft.

Chapter 5:

Costin D. Untaroiu, Ph.D., is an associate professor at Virginia Tech. Dr. Untaroiu supervised, conceptualized, and helped review and edit the paper draft.

1. Introduction

1.1 Background

Although fatalities caused by collisions with fixed objects have decreased from 10,550 in 1979 to 8,603 in 2020 in the United States, the percentage of crash fatalities recorded in these collisions of all traffic fatalities has remained around 20% [1]. The guardrails were designed to deter vehicle access to off-road areas and consequently prevent hitting rigid fixed objects alongside the road (e.g., trees, utility poles, etc.). However, the guardrail became a hazardous part because it caused 893 fatalities in 2020 in the U.S., which was 10% of all the fatalities involved in collision with fixed-objects [1]. Meanwhile, the crashes with guardrail end terminals were observed to be more severe than ones with guardrail barrier. In the end terminal crashes, both occupant injury risk and the rollover probability were reported to be higher than in the guardrail crashed with 5.1 times, and 6.7 times, respectively [2]. Therefore, the safety performance evaluation of guardrail end terminals recently attracted attention in the highway safety community [3].

All the newly installed guardrail end terminals have to show the ability to protect occupants of impacted vehicles according to a set of test procedures required for all the highway safety products outlined by the National Cooperative Highway Research Program (NCHRP) [4] and recently the American Association of State Highway and Transportation Officials (AASHTO) Manual for Assessing Safety Hardware (MASH) [5]. Since the MASH guideline was developed by updating the NCHRP-350 guideline, several NCHRP-tested guardrail end terminals were not required to be tested under MASH conditions [5, 6]. Therefore, it is questionable if these end terminals have a proper safety performance under the MASH test conditions. Meanwhile, the crash tests were performed under simplified crash conditions. The performance of these devices under real-world conditions could differ from the crash test results due to factors such as impact conditions, site conditions, and installation or maintenance issues [7]. It has been observed that some in-service guardrail end terminals are improperly installed or maintained [8]. The performance of damaged end terminals is unknown and needs to be evaluated to better understand how damages contribute to crash outcomes.

Historically, occupant injury risk was assessed based on the flail-space model (FSM) to evaluate the end terminal safety performance during crash tests. In this simplified injury model, the

occupant was modeled as a point mass based on a conservative assumption that the occupant is unrestrained during the crash [9]. While anthropomorphic test devices (ATD) were commonly used in other regulation crash tests (e.g. Federal Motor Vehicle Safety Standards (FMVSS)) to evaluate occupant protection [10-12], no ATD data was measured during the NCHRP or MASH tests [4, 5]. Therefore, full-body injury risks could be evaluated but not individual body region risks. Meanwhile, the availability of airbags (100%) in current vehicles and high seat belt usage rates (~90%) challenge the validity of the FSM model proposed in 1981, when there was only a 20% seatbelt usage rate [13, 14]. Several studies showed that the FSM has little ability to assess occupant injury [15, 16]. Generally, it was accepted that the vehicle-based crash severity metrics (such as FSM) provide a more conservative injury assessment than dummy-based criteria [17-19]. Thus, to better understand the relationship between vehicle-based metrics (e.g., FSM) and dummy-based injury assessments, more research was required.

Finite Element (FE) simulations were widely used in traffic safety research to help better understand vehicle collisions at significantly reduced costs compared to physical crash tests. Several FE models had been developed for guardrail systems [20, 21], and non-energy-absorbing guardrail end terminals [22]. However, little effort had been spent on the numerical modeling of energy-absorbing guardrail end terminals, which is the most advanced end terminal design. A previous study developed a simplified FE model of the Sequential Kinking Terminal-30 (SKT-30) energy-absorbing guardrail end terminal [23]. However, the models of the deflector plane and impact head were validated separately, without evaluating the whole end terminal system during a full vehicle collision. Therefore, a FE model for an energy-absorbing guardrail end terminal was needed. The model would help investigate device performance in crash situations that are impractical to test physically as well as the effects of site characteristics on device performance. The simulation models would also supplement crash tests to certify new hardware designs.

Dummy models were widely used to assess injuries on component levels in varied traffic crashes [24-28]. However, there were no simulation-based studies developed to evaluate the occupant risk in the crashes involving a guardrail end terminal. The previous studies focused on either the general safety performance of a guardrail [29-31] or the occupant risk assessments during the crashes with guardrail barriers (not end terminal systems) [25, 27, 32-34]. The employment of

the occupant dummy model would increase the accuracy of occupant injury risk assessment. Component-level injury risks would also be evaluated based on the simulations.

1.2 Project aims

To better understand the vehicle-to-end terminal impacts and the injury criteria used to evaluate the safety performance of end terminals, four aims to this study were defined as follows (Figure 1-1):

(1) Development and validation of a FE model for the most common energy-absorbing guardrail end terminal using along U.S. roads

Overview: A FE model of an ET-Plus end terminal was developed and was validated based on NCHRP-350 test data. The overall kinematics of vehicle model showed agreement to test data.

(2) Examination of damaged ET-Plus performance using FE models and investigation of the effects on the occupant injury risk of the end terminal damages
Overview: Five damaged ET-Plus FE models were developed to investigate possible changes in their safety performance relative to an undamaged ET-Plus model. It was found that the performance of ET-Plus guardrail end terminals was adversely affected by the minor and severe damage examined.

(3) Injury assessment using dummy models during car-to-end terminal crashes
Overview: Car-to-end terminal crash FE simulations involving a dummy model were performed for the first time. The driver injury risks during a crash with ET-Plus were evaluated on both full-body and component levels. Statistical analysis was performed to compare the vehicle-based crash severity metrics and dummy-based injury criteria based on 20 crash simulations

(4) Injury assessment using human body models during car-to-end terminal crashes
Overview: Twenty FE crash simulations involving end terminal, vehicle, and belted human body model was performed. It was observed that current vehicle-based assessment methods could predict full-body occupant injury risks and certain body-region injury risks while no head and brain injury could be predicted

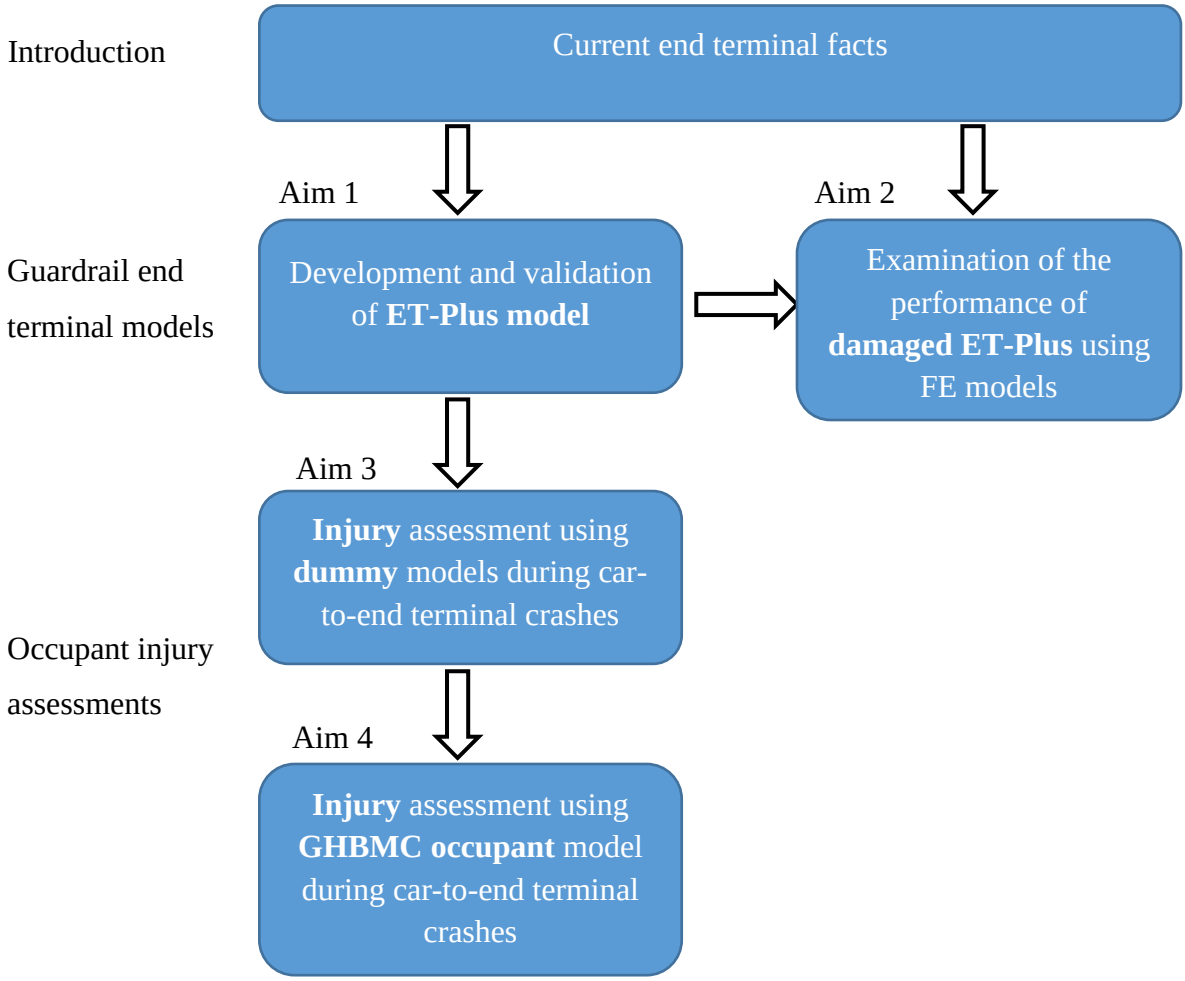

Figure 1-1 Framework of this study

2. A Review of guardrail end terminals mounted on along U.S. roads

Section 2 is based in part on the previously published article

"Meng, Y., Hu, W., & Untaroiu, C. (2020). An examination of the performance of damaged energy-absorbing end terminals. *Accident Analysis & Prevention*,147, 105789."

2.1 Main features of W-beam guardrail end terminals

W-beam guardrail end terminals may be classified as either energy-absorbing (Figure 2-1a) or non-energy absorbing (Figure 2-1b). Non-energy absorbing guardrail end terminal was primarily developed to avoid spearing during a crash. In addition to avoiding spearing, energy-absorbing end terminals tries also to reduce the possibility of penetration during end-on impacts. They

dissipate significant amounts of energy and consequently reducing the distance traveled by striking vehicles post-impact while keeping the rate of deceleration tolerable for the occupants.

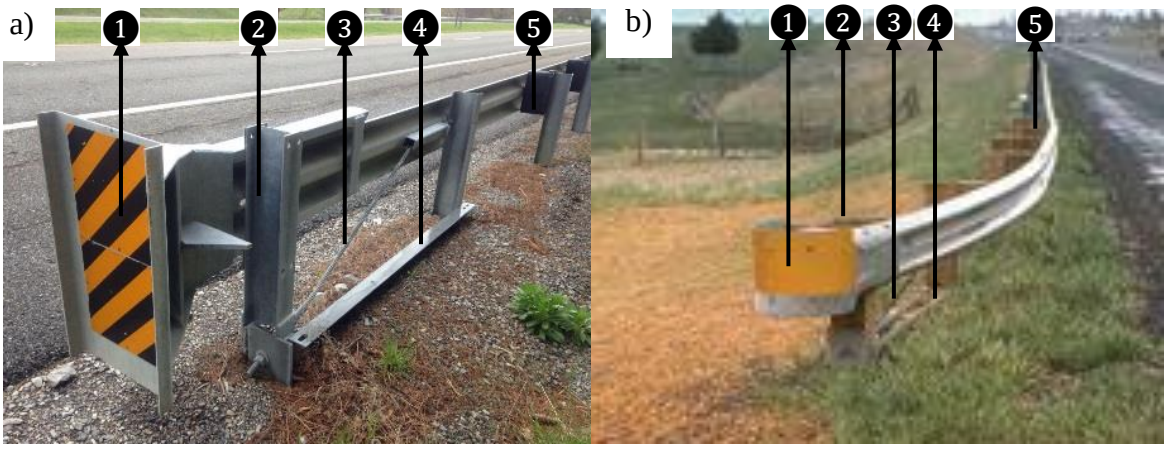

❶ Impact head ❷ Post ❸ Anchor cable ❹ Ground strut ❺ Block-out

Figure 2-1 Main features of guardrail end terminals: a) energy-absorbing; b) non-energy-absorbing

Impact heads, anchor cables, ground struts, posts, and block-outs are the main components of W-beam guardrail end terminals (Figure 2-1). These components can be used to distinguish different systems in the field. Energy-absorbing guardrail end terminals (Figure 2-1a) typically have a large, conspicuous impact head covering the end of the rail that dissipates vehicle energy by deforming the barrier and keeps the guardrail from penetrating the vehicle. Non-energy-absorbing end terminals (Figure 2-1b), by contrast, generally have a simpler end cap.

An anchor cable is a cable connecting the base of the first post to the top of the second post. The purpose of the anchor cable is to provide tension in the rest of the guardrail system, which is necessary for the guardrail to function properly. Both leading and trailing ends of guardrails typically have anchor cables on high-speed roads, while the anchor cables may not be necessary if the guardrails are installed on low-speed roads. The anchor brackets that connect anchor cables to the guardrail are often distinctive and are thus useful for identifying different end terminal systems. A ground strut is a beam normally connecting the first and second posts at ground level which is included in most of the end terminal systems. Similar to an anchor cable, it helps provide tension in the guardrail.

The number and type of posts can be used to identify guardrail end terminals in the field. Posts can be categorized as either standard posts or breakaway posts. Standard posts are designed not to break during a crash (e.g. made of steel), while breakaway posts are designed to break (e.g. made of wood). The posts are numbered from 1 starting closest to the impact head.

2.2 Estimation of the distribution of guardrail end terminal systems

Two databases, National Automotive Sampling System – Crashworthiness Data System (NASS-CDS) and the Second Strategic Highway Research Program - Roadway Information Database (SHRP2-RID), were used to estimate the distribution of guardrail end terminal systems along U.S. roads. The NASS-CDS collects detailed crash data for a nationally representative sample of police-reported tow-away crashes involving passenger vehicles (NHTSA 2015). The system primarily focuses on vehicle and occupant data; NASS-CDS coding for struck objects does not identify specific end terminal systems or, until recently, differentiate the end of the guardrail from the face. However, crash site photographs are available for the majority of cases in NASS-CDS, so these photographs were inspected manually to identify end terminal systems involved in a crash. A total of 3,270 crashes involving one or more fixed objects were selected from the NASS-CDS (case years: 2000-2014). Manual inspection of the crash site photos revealed that in 724 cases a vehicle struck a W-beam guardrail end terminal. The type of W-beam guardrail end terminal was identified for 674 of these cases based on the identification features discussed in previous sections (Table 2-1). Each case in NASS-CDS is a probability sample, so it has a sample weight factor to reflect national estimates (Agresti 1996). The weight factors were applied, and the weighted percentage of each identified guardrail end terminal was calculated (Table 2-1). Overall, energy-absorbing end terminals correspond to 36% of all the W-beam guardrail end terminals involved in tow-away crashes. ET-Plus was the most common W-beam guardrail end terminal in all crashes, while the BCT was the most common non-energy-absorbing end terminal. However, the safety performance of all the end terminals systems were considered to be the same in this study. Since the NASS-CDS database only involves the tow-away crashes, the end terminals with a better safety performance may be more common than estimated. While no qualitative comparison was performed to evaluate the safety performance difference of the end terminals, the data shown in Table 2-1 was considered acceptable.

Table 2-1 Distribution of end terminal systems involved in passenger vehicle tow-away crashes, 2000-2014

End terminal	Frequency	Unweighted Percentage	Weighted percentage
Energy absorbing guardrail end terminals			
ET-2000	72	10%	4%
ET-Plus	182	25%	27%
FLEAT	25	3%	3%
SKT	24	3%	2%
Subtotal	303	42%	36%
Non-energy absorbing guardrail end terminals			
BCT	141	19%	22%
MELT	17	2%	4%
SRT-350	90	12%	13%
Turndown	123	17%	20%
Subtotal	371	51%	58%
Not identified	50	7%	6%
Total	724	100%	100%

The guardrail end terminals identified in the NASS-CDS cases were all involved in crashes. To estimate the guardrail end terminal system distribution among those installed on the roads, the SHRP2-RID was used. The database compiles data from the SHRP2 mobile data collection project, existing roadway data, and supplemental data such as crash data and traffic information. The mobile data collection project covered more than 25,000 miles of roads between 2011 and 2013 in the six Naturalistic Driving Study (NDS) sites in Florida, Indiana, New York, North

Carolina, Pennsylvania, and Washington. Information of various road features, including the type of guardrail end terminals, was collected by the mobile data collection vehicles. In each vehicle, a calibrated camera was used to capture images every 20 feet and correspond the images with Global Positioning System (GPS) information. The images were post-processed to capture road features. NDS sites spanned a variety of land uses, both urban and rural roads were investigated in all the six sites. Pennsylvania, Indiana and New York sites have higher percentage of rural roads than the other three sites. Among the 52,542 end treatments recorded in the database, 47% (24,872) were W-beam guardrail end terminals; 21% (10,865) were coded as "Continuous" which was the connection part between two barriers; 17% (8,915) were attached to fixed objects; 11% (5,733) were end terminals of other types of guardrails (e.g. box beam); 2% (908) were coded as "None" and had no end terminal treatment; and 2% (1,249) were unknown treatments. Of the 24,872 recorded W-beam guardrail end terminals, 22,521 were the commonly used systems as described earlier, and 2,351 were rarely used in the U.S. (e.g. end piece). Only the distribution of the 22,521 commonly used W-beam guardrail end terminals was examined (Table 2-2). The names of these end terminals were recorded in SHRP2-RID, but these names did not match their commonly used names exactly. To solve the problem, 200 samples were randomly selected for each of the SHRP2-RID named guardrail end terminal systems, and location information was used to identify the samples on Google Street View. Based on the review of photos of each sample obtained from Google Street View, the system names used in SHRP2-RID were matched to the common names, as shown in Table 4. For example, the SKT, ET-2000 and ET-Plus were all classified as Tangential End Treatments (TET) end terminals in SHRP2-RID.

Among the W-beam guardrail end terminals identified in SHRP2-RID, SRT-350 was the most common system in Florida, Pennsylvania, and Washington. The SKT, ET-2000 and ET-Plus were considered as one type (TET) and were the most common type in North Carolina. Turndowns were the most common in Indiana and New York. Overall, 37% of identified W-beam guardrail end terminals had energy-absorbing designs. SRT-350 and TET (the SKT, ET-2000 and ET-Plus) were the most common systems, with each comprising 24% of the total, and turndowns closely following with 23% of the total.

Table 2-2 Distribution of end terminal systems along sample roads in SHRP2-RID, 2011-2013

SHRP2-RID name	End terminal (commonly used name)	State						Total (%)
		FL	IN	NC	NY	PA	WA	
Energy absorbing guardrail end terminal								
GR-9-350	FLEAT	363	531	825	135	730	333	2,917 (13%)
TET	SKT, ET-2000, and ET-Plus	195	827	1992	560	1208	603	5,385 (24%)
Non-energy absorbing guardrail end terminal								
FET	BCT and MELT	622	156	1435	2	87	1262	3,564 (16%)
GR-11	SRT-350	1476	80	338	70	1918	1566	5,448 (24%)
Cut Slope, GR-8 and GR-5	Turndown	6	1154	207	1747	1707	386	5,207 (23%)
Total (%)		2,662 (12%)	2,748 (12%)	4,797 (21%)	2,514 (11%)	5,650 (25%)	4,150 (19%)	22,521 (100%)

2.3 Conclusion

Guardrail end terminals are important to roadway safety, but limited research has been performed on them, possibly due to a lack of information available on existing end terminals on roads. This study summarized the design and main features of the most common W-beam guardrail end terminals. The NASS-CDS and SHRP2-RID were used to estimate the distribution of different guardrail end terminals on U.S. roads. Based on the review of NASS-CDS cases, the ET-Plus was the most common W-beam guardrail end terminals among those involved in crashes. According to the data from SHRP2-RID, the SRT-350 and the TET, which includes SKT, ET-2000 and ET-Plus, were the most common systems overall.

The estimated distributions of W-beam guardrail end terminal systems differed between the NASS-CDS and SHRP2-RID. The NASS-CDS includes a nationally representative sample of

police-reported tow-away crashes. Guardrail terminals that are frequently involved in these crashes as well as the terminals that are used in more crash-prone areas may be overrepresented in NASS-CDS compared with SHRP2-RID. On the other hand, SHRP2-RID database includes the end terminals installed only on the roads in six study sites. As a result, it is not a representative sample of the roads nationwide. For a more accurate estimation of end terminal distributions on U.S. roads, a larger road network would need to be investigated.

Data related to guardrail end terminals and other roadside hardware are key components necessary for roadside safety research, especially the research related to the in-service end terminals (e.g. evaluating the performance of in-service end terminals; determining the location and type of end terminals to be used). The paper provides information to help practitioners identify different guardrail end terminal systems in the field. The distribution data summarized in the study additionally offers preliminary information on existing guardrail end terminals, and could be used as a starting point to develop roadside safety research needs and identify research subjects.

3. Development and validation of the ET-Plus model

This section is based in full on the previously published article

"Meng, Y., Hu, W., & Untaroiu, C. (2019). Finite Element modeling of an energy-absorbing guardrail end terminal. *SAE International Journal of Commercial Vehicles* 12 (02-12-04-0021), 271-280"

3.1 Introduction

Although fatalities caused by collisions with fixed-objects have decreased from 10,550 in 1979 to 7,833 in 2017 in the United States, the percentage of crash fatalities recorded in these collisions has remained around 20% [35]. To keep vehicles within their roadway, and consequently prevent them from colliding with dangerous obstacles on the road side, traffic

barrier systems are usually installed along highways. However, 9% of traffic fatalities recorded in collisions with fixed-object were caused by traffic barriers in 2017[35].

A guardrail end terminal is designed to protect vehicle occupants by preventing vehicle penetrations during end terminal collisions. All new guardrail end terminals must pass test procedures for all the highway safety products recommended by National Cooperative Highway Research Program (NCHRP) [4] and recently the American Association of State Highway and Transportation Officials (AASHTO) Manual for Assessing Safety Hardware (MASH) [36] to be installed along U.S roads. However, the consequences of vehicle collisions with end terminals could be severe; 113 deaths occurred in these crashes in 2017. The performance of guardrail end terminals has been evaluated in ongoing In-Service Performance Evaluation (ISPE) [37]. However, data collection for ISPE are time-consuming and expensive.

Finite Element (FE) simulations are widely used in traffic safety research to help better understand vehicle collisions with reasonable accuracy and to significantly reduce costs compared with physical crash tests and crash investigations. Several FE models have been developed for guardrail systems [20, 21], and non-energy-absorbing guardrail end terminals [22, 23]. However, little effort has been spent on the numerical modeling of energy-absorbing guardrail end terminals, which is the most advanced end terminal design. A previous study developed a simplified FE model of the Sequential Kinking Terminal-30 (SKT-30) energy-absorbing guardrail end terminal [23]. However, the models of deflector plane and impact head were validated separately, without to evaluate the whole end-terminal system during a full vehicle collision. The main objective of this study is to develop and validate a FE model of the ET-Plus, a commonly used energy-absorbing guardrail end terminal.

3.2 Methods

3.2.1 Development of ET-Plus model

Impact heads, anchor cables, ground struts, posts, and block-outs are the main components of an ET-Plus guardrail end terminal (Fig. 1a). The geometric model of each component (except the anchor cable) was developed in the Rhino software (Robert McNeel & Associates, Seattle, WA, USA) by using dimensional data collected from published ET-Plus drawings [38] or measured from an ET-Plus product mounted in Blacksburg, VA. (Figure 3-1).

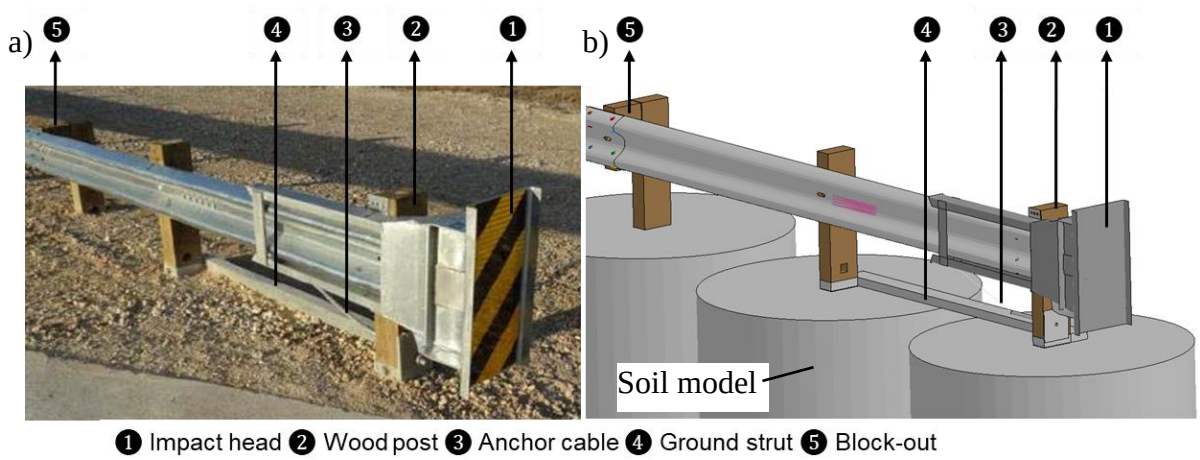

Figure 3-1 ET-Plus components: a) product; b) FE model

The developed component models were meshed in the Hypermesh software (Altair HyperWorks, Troy, MI). A geometry clean-up were performed, if it is necessary, to ensure the surface continuity and to remove unnecessary details such as small holes in posts. Since the impact head and rail parts have large dimension-to-thickness ratios, they were modeled using shell elements with an assigned thickness which would improve the model's computational efficiency [39]. The impact head part was meshed using quadrilateral elements with a size of approximately 10×10 mm. Meanwhile, manual improvements were performed to ensure the element quality [40].

While the impact head was meshed by quadrilateral elements, other components (wood post, ground strut, and block-outs) were meshed using hexahedral elements. The mechanical and failure responses of wood posts and blocks are critical to the overall impact simulation. Therefore, the mesh size (20 mm) was chosen based on a mesh convergence study performed in LS-DYNA FE software (LSTC, Livermore, CA) [20]. On the other hand, the soil material model (MAT 147, LS-DYNA Library) only constrains the post (no failure assigned), so a relatively large mesh size (100 mm) was used. The anchor cable and cable holder were meshed using a combination of shell, solid, and beam elements due to its complicated geometry. The main part of the anchor cable was modeled using a beam element with a circular cross-sectional area.

All the material models of the end terminal system were selected from the LS-DYNA material library (Table 3-1). The steel parts (impact head, guardrail, and ground strut) and the anchor

cable were assigned an elasto-plastic material (MAT 024) and an elastic material (MAT 001), respectively [41]. A wood material (MAT 143) was assigned to the models of the guardrail posts and block-outs [42, 43].

Table 3-1 Material properties used in ET-Plus model

Component	Density (kg/m^3)	Elastic modulus (MPa)	Yield stress (MPa)	Poisson's ratio	Reference
Impact head, guardrail, and ground strut	7.86×10^3	2×10^5	415	0.33	[44]
Wood post and block-outs	6.731×10^2	Parallel: 1.135×10^4 Perpendicular: 247	Parallel: 40 (tension) 13 (compression) Perpendicular: 0.96 (tension) 2.57 (compression)	0.16	[42, 43]
Anchor cable	7.89×10^3	2×10^5	NA	0.3	[44]

The six welded plates of the end terminal impact head were connected using node coupling welding constraints (*Constrained_spotweld in LS-DYNA). Since no failure in the bolt part was observed in the damaged end terminals from crash tests [38], all the bolts in the system were simplified as rigid constraints (*Constrained_nodal_rigid_body in LS-DYNA). Appropriate contacts were defined between the end terminal parts to avoid self-penetration during collision simulations. The static and dynamic friction coefficients between steel parts (ET-Plus and rails) were defined as 0.6 and 0.4, respectively [45]. Similarly, the static and dynamic friction coefficients between the steel and wood parts were set as 0.2 and 0.1 [45].

3.2.2 Energy absorbing mechanism verification

The ET-Plus model was impacted by a cylindrical impactor (Figure 3-2) to verify qualitatively its responses during a frontal collision, including its energy absorbing mechanism. The impactor has a mass corresponding to a mid-size truck (2000 kg), and its diameter (800 mm) was selected to be slightly larger than the impact head length. A contact was defined between the impactor and the end terminal model, and a prescribed 100 km/h initial velocity was assigned to the impactor.

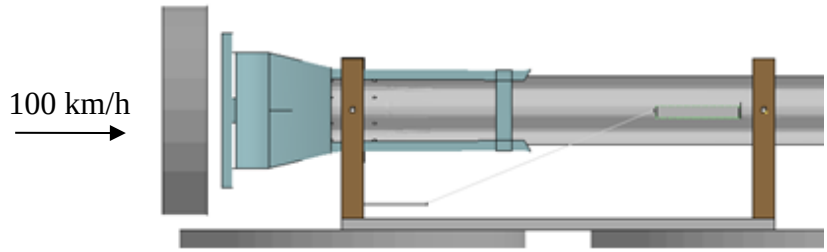

Figure 3-2 ET-Plus - cylinder impactor collision

3.3.3 Validation of ET-Plus model

Among the NCHRP test procedures (NCHRP-350), test 27-30 and 31-30 were developed for guardrail end terminals, and their test conditions were used in the FE simulations to validate the ET-Plus model (Table 3-2) [38]. A vehicle model of 1997 Geo Metro [46] impacted the ET-Plus model with an impact velocity of 102.5 and 102.8 km/h, which were the same as the velocities recorded from test 27-30 and 31-30, respectively. As in the NCHRP 350 tests, the center line of the vehicle model was parallel to the guardrail with an offset of ¼ vehicle width (~397 mm) (Figure 3-3). The vehicle interior parts (seats, steering wheel, etc.) were not modeled, so the weight of the dummy used in the tests was added to the vehicle floor (*Element_mass_node_set in LS-DYNA). The main difference between the two simulations was the guardrail height, as shown in Table 3-2.

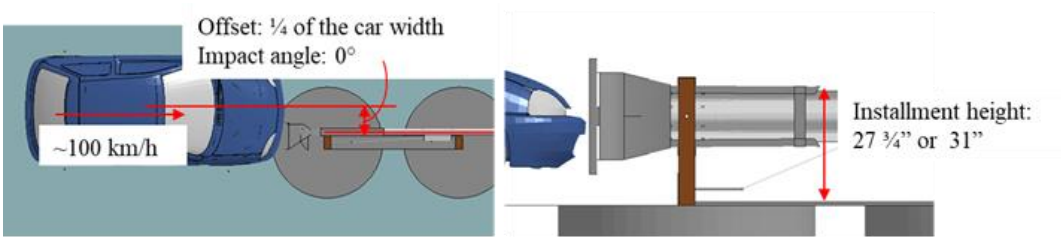

Figure 3-3 Vehicle – ET-Plus collision simulation setup

Slight differences were observed between the pre-impact velocities and angles recorded in both NCHRP 350 tests and their corresponding target values (100 km/h and 0°). In the simulations, these parameters were identical to the ones recorded from each test (Table 3-2).

Table 3-2 Simulation setup parameters [38, 47]

	Guardrail height (in)	Pre-impact velocity (km/h)	Pre-impact angle (degree)	Pre-impact offset	Dummy position
Test 27-30	27 ¾	102.5	0.1	¼ vehicle width	Driver
Test 31-30	31	102.8	0.2	¼ vehicle width	Driver

The ET-Plus model was validated qualitatively and quantitatively. The vehicle response in simulation was recorded and compared with the photos taken during the tests qualitatively. The time histories of yaw, pitch and roll angles were recorded, the 50ms moving average accelerations were calculated and compared to the test results.

3.3.4 Model Robustness Evaluation

Six FE crash simulations with a vehicle pre-impact velocity close to U.S. highway speed limit were performed based on the NCHRP 350 27-30 test conditions. Specifically, 97 km/h (60 mph), 100 km/h (62 mph), 103 km/h (64 mph), 106 km/h (66 mph), 109 km/h (68 mph), and 113 km/h (70 mph) were used. Vehicle velocity [48, 49] and acceleration [50] were reported to be correlated to the occupant injury. Therefore, in addition to the model stability, the vehicle post-impact velocity (measured at the vehicle CG) and acceleration (measured based on velocity during a collision) were recorded during each simulation. The vehicle post-impact velocities were defined as the vehicle CG velocity at the end time of vehicle-end terminal contact. The vehicle acceleration was calculated as the ratio of the velocity difference (initial velocity vs. post-impact velocity) and the time interval of vehicle-to-end terminal contact.

3.3Results

3.3.1 FE Model of ET-Plus end terminal

The ET-Plus FE model consists of 21 parts, 208,782 nodes, and 181,205 elements (49,700 shell elements, 131,504 solid elements, and 1 beam element). The ET-Plus FE model dimensions matched well with the dimensions collected from the ET-Plus product (Table 3-3 and Figure 3-4). Additionally, more than 99.99% elements passed the quality criteria (Table 3-4) [40].

Table 3-3. ET-Plus dimensions: product vs. FE model

	Mass (kg)	Length (m)	Impact head size (mm×mm)
ET-Plus product	79	1.44	711 ×381
FE model	78	1.43	711 ×381

a) b)

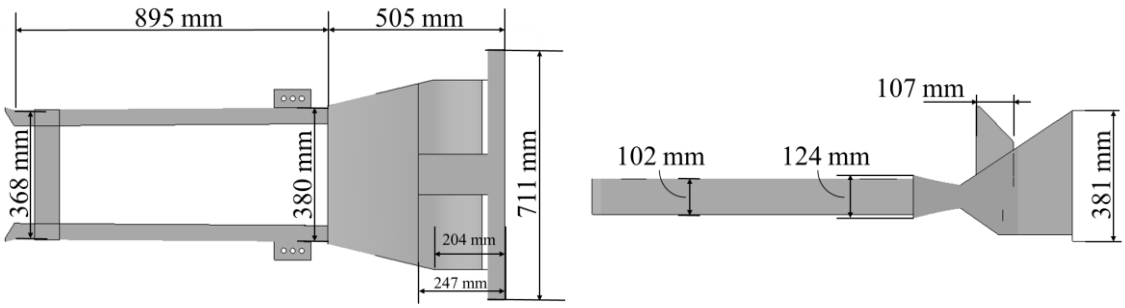

Figure 3-4 ET-Plus impact head dimensions: a) side view; b) top view

Table 3-4 Element quality

Element type	Mesh quality criterion	Min (m) / Max (M) in the model	Allowable limit*	Number of elements under allowable limit (%)
Shell (49,700)	Jacobian	0.434 (m)	0.3	0 (0%)
	Warpage	25 (M)	10	4 (0.008%)
	Aspect Ratio	9.26 (M)	10	0 (0%)
Solid (131,504)	Jacobian	0.53 (m)	0.3	0 (0%)
	Warpage	35 (M)	10	4 (0.003%)
	Aspect Ratio	2.59 (M)	10	0 (0%)

* Note: Allowable limit was referred from [39]

A significant deformation of the end terminal head model was observed during the FE simulation with the cylindrical impactor (Figure 3-5). Meanwhile, the rail model extruded through the impact head model with no failing elements. While post #1 broke at about 0.005 s after the impact, post #2 swung during simulation until a complete fracture was observed around 0.09 s. The impactor velocity decreased until rest (0.175 s) and then moved backward until the end of the crash simulation (0.8 s). Overall, the end terminal model reduced the impactor kinetic energy in a controlled manner by the deformation of rail without any end rail spearing.

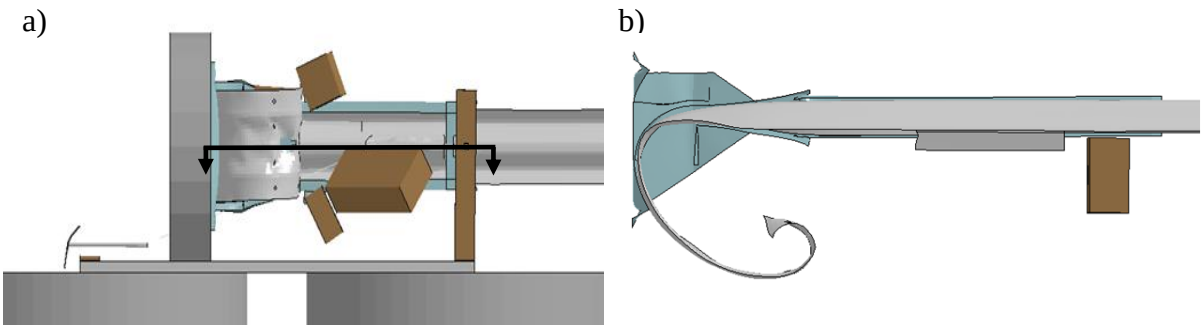

Figure 3-5 ET-Plus responses to the collision with simple impactor: at 0.055 s: a) side view; b) cross sectional view

3.3.2 Model Validation in Car – ET-Plus Collisions

3.3.2.1 Test 27-30 FE simulation

During the NCHRP-350 27-30 simulation, the vehicle front end impacted the ET-Plus model and then rotated clockwise as in the crash test (Figure 3-6). The vehicle bumper model was in contact with the end terminal head till 0.38 s after the initial impact, then the vehicle model started moving backward toward the traffic lane. The vehicle stopped at around 1.04 s, and the maximum distance from the middle line of the barrier was 3.8 m. Overall, the vehicle model decelerated in a controlled fashion, and it remained on the road after the collision.

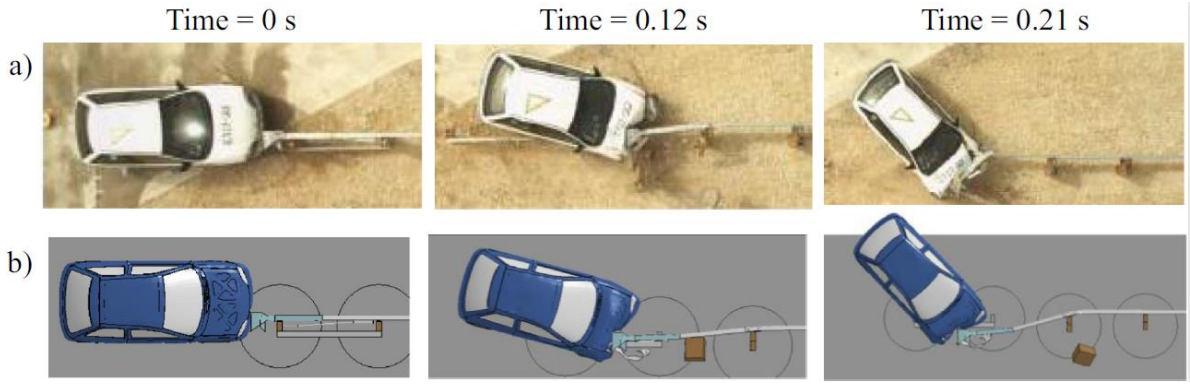

Figure 3-6 NCHRP 350 27-30 test versus FE simulation: a) experiment; b) simulation

The time histories of yaw angles recorded in the simulation showed good agreement with test data [38] (Figure 3-7). However, the time histories of roll angles matched well only within the first 0.5 second and the ones of pitch angles matched only within 0.2 second after the end-terminal impact. Since the test was performed only once, and both roll and pitch angles showed relatively low peak values in the tests (< 7°), the simulation results were considered to be acceptable.

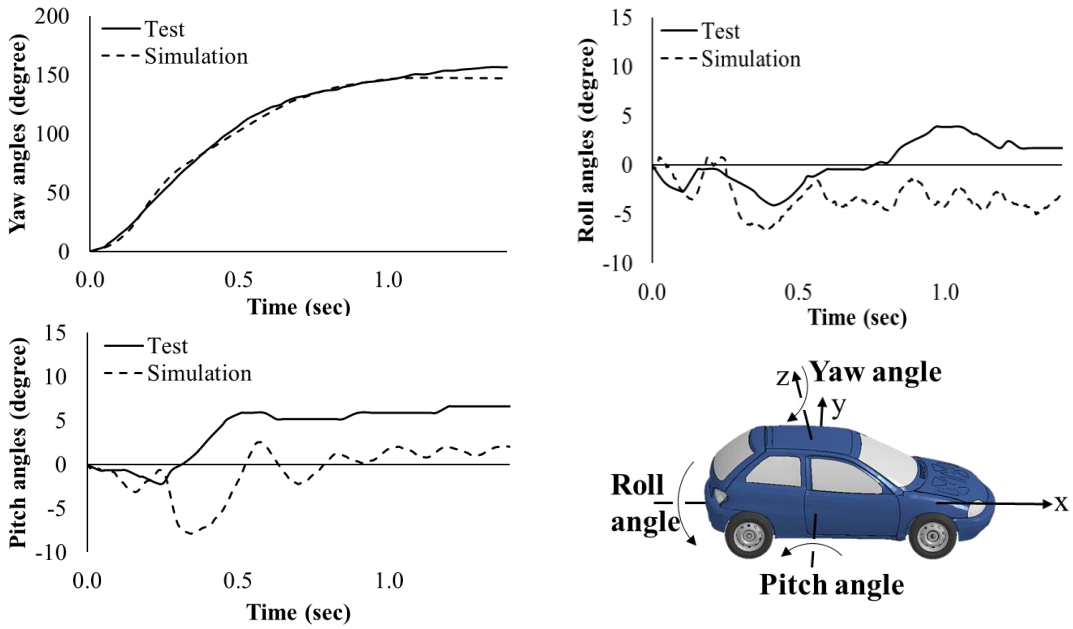

Figure 3-7 Vehicle yaw, roll, and pitch angles by time after initial impact during the NCHRP 350 27-30 simulation

3.2.2 Test 31-30 FE simulation

In the NCHRP 350 31-30 simulation, the vehicle model pushed initially the end terminal head along the guardrail (first 0.23 s), then a backward motion of the vehicle model was observed. Overall, the vehicle rotated clockwise and remained upright during the simulation, which is a good agreement to the recorded test data (Figure 3-8).

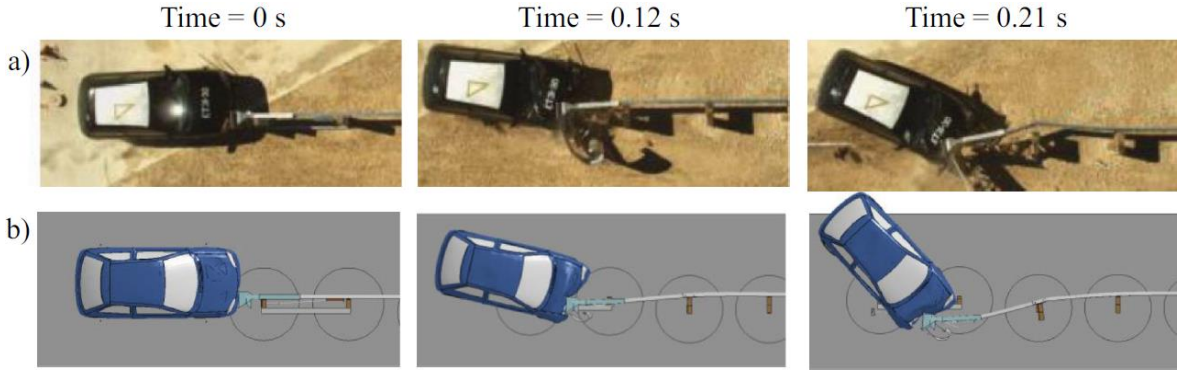

Figure 3-8 NCHRP 350 31-30 test versus FE simulation: a) experiment; b) simulation

The temporal trends of vehicle yaw and pitch angles recorded in the FE simulation were similar to the test data (Figure 3-9). However, the maximum yaw angle in the simulation (182°) was

larger than the one recorded in the test (168°). Relatively large differences were observed between the roll angles recorded in the simulation and in the test. Since the peaks of both roll and pitch angles are relatively small compared with the yaw angle, the simulation outputs were considered acceptable.

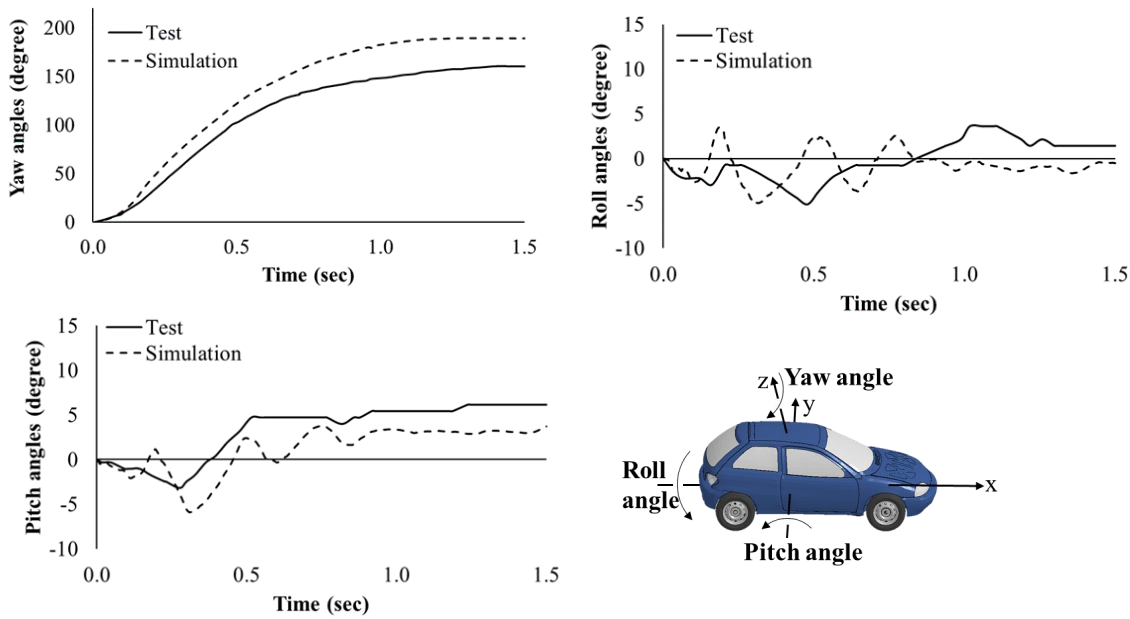

Figure 3-9 Vehicle yaw, roll, and pitch angles by time after initial impact during the NCHRP 350 31-30 simulation

3.3 Model Robustness Evaluation

The end terminal FE model showed to be stable in all vehicle collision simulations. The vehicle remained on the road after the impact, which is the main performance criteria of these safety devices. The post-impact responses of vehicles varied by the impact velocities in the simulations. The post-impact velocities were recorded as 14, 15, 17, 19, 20, and 20 km/h for the impact velocities of 97, 100, 103, 106, 109, and 113 km/h, respectively (Figure 3-10a). Similar to the trend in post-impact velocities, vehicle peak acceleration showed an increasing trend with increasing vehicle velocities (Figure 3-10b). The peak accelerations were recorded as 13.7, 14.5, 14.5, 14.8, 15.1, and 15.3 g for the impact velocities of 97, 100, 103, 106, 109, and 113 km/h, respectively.

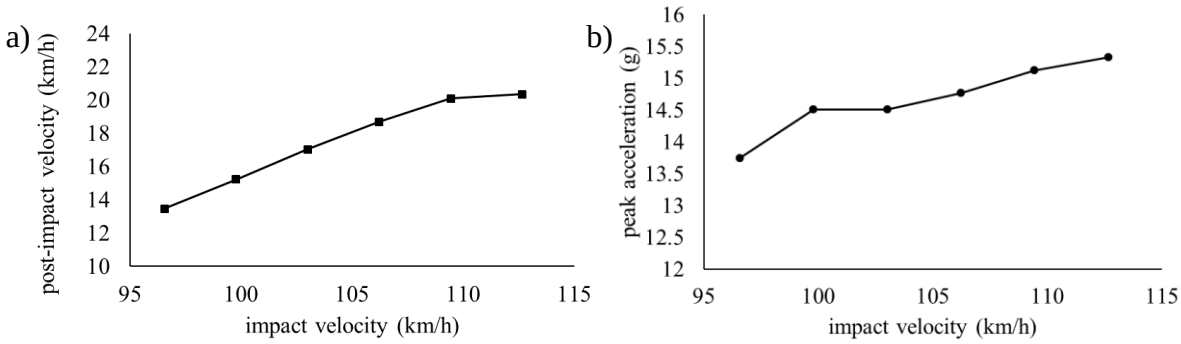

Figure 3-10 Vehicle response corresponding to impact velocity: a) post-impact velocity; b) peak acceleration of the vehicle center of gravity

3.4 Discussion

The study developed and validated an FE model of an energy-absorbing end terminal, ET-Plus, for the first time. The developed model has good mesh quality and realistic material properties as defined based on literature data. The ET-Plus FE model showed the energy-absorbing capability in an impact test with a rigid impactor. In the simulations of the two NCHRP-350 impact tests, the vehicle post-impact kinematics were found to be overall consistent between simulations and tests, especially in terms of the time history of vehicle yaw angles. The pitch and roll angles of the vehicle model showed lower peaks and matched well with the test data only during the beginning of the simulation. The models of vehicle interior parts were not available as well. Although the total mass of the vehicle model was adjusted to include the dummy and interior parts, a slight discrepancy in the vehicle moment of inertia is expected. This might have caused some kinematics differences between the simulations and physical tests, especially during vehicle rotations. Furthermore, the vehicle model was validated only in a frontal wall impact test [46], and no validation of its suspension was reported, so its accuracy in an offset test is unclear. Future research is needed to evaluate the vehicle model's performance in other crash scenarios. Other detailed vehicle models (with validated interior parts, and suspension system, etc.) are recommended to be used in the future.

A possible source of discrepancy between the time histories of vehicle angles recorded in testing and FE simulation could be caused by different methods used to derive them. In testing, the vehicle angles were calculated by numerical integration based on the measured angular velocity and acceleration data. On the other hand, the corresponding simulation data was derived directly

based on displacements of the coordinate reference points. Therefore, to get more confidence in the test data used in validation, it is recommended performing additional impact tests (to record more details and check test repeatability – only one test was available) and verification of the linear and angular velocity/acceleration data using different measurements (e.g. video analysis). Besides, time histories of vehicle linear velocity are high recommended in the future tests.

The ET-Plus FE model proved to be stable in severe impact conditions (from 97 up to 113 km/h vehicle velocity), which recommend using it in future safety studies related to guardrail end terminals. For example, the model could be used to overcome limitations in terms of pre-impact conditions of the crash tests used in current safety regulations [4, 36]. A more accurate and faster evaluation of the safety performance of ET-Plus could be determined statistically based on the results of a large number of impact FE simulations. The pre-impact conditions (e.g. the pre-impact velocity and direction, ET-Plus in-service conditions, vehicle type, etc.) of these FE simulations could be varied using a Design of Experiments (DOE) approach which would better approximate the whole real-world accident data [51-53]. Moreover, the model could be used to assist the ongoing efforts of the in-service performance evaluation of ET-Plus [37], and to improve its design by using novel energy-absorbing mechanisms (e.g. origami crash boxes [54-56]). The use of the ET-Plus FE model could reduce significantly the cost and time associated with these evaluations.

The post-impact velocity and peak acceleration were observed to increase with the increasing impact velocity, which suggest higher risks of occupant injuries at higher pre-impact vehicle velocities [48-50]. However, in addition to vehicle impact velocity, other pre-impact conditions (e.g. vehicle type, impact angle, impact offset, etc.) vary in real-world accidents as well [35]. Therefore, MASH introduced recently several new crash tests to ensure proper functionality of guardrail end terminals. Heavier vehicles (1,100 kg passenger car, and 2,270 kg pickup truck) and varying impact angles are specified in these tests [36]. Thus, additional validations of the ET-Plus FE model in these pre-impact conditions are recommended in the future when test data will be available.

Additional improvements to the ET-Plus model may include modeling the parts simplified in the current model (e.g. bolts modelled as constraints), and/or updating material/failure models of the end terminal parts (especially the guardrail posts) based on test data.

3.5 Conclusion

This paper presented the development and validation of the first ET-Plus FE model. The developed model has good dimensional accuracy and realistic material properties. The model showed energy-absorbing capability in the simulation involving a rigid impactor. The ET-Plus model was validated based on NCHRP-350 test data. The overall kinematics of vehicle model showed good visual agreement relative to test data, especially in terms of the time histories of yaw angle. Meanwhile, the end-terminal model showed good computational stability for pre-impact vehicle velocities in a range from 97 km/h up to 113 km/h. These results recommend future use of the model in safety studies related to highway safety.

4. Examination of the performance of damaged ET-Plus using FE models

This section is based in full on the previously published article

"Meng, Y., Hu, W., & Untaroiu, C. (2020). An examination of the performance of damaged energy-absorbing end terminals. *Accident Analysis & Prevention*,147, 105789."

4.1 Introduction

A guardrail end terminal is the end part of a guardrail system, which decelerates the impacting vehicle and prevents the rail from spearing through the car in an end-on collision. Although these systems were designed to decrease the severity of crashes and protect vehicle occupants, the consequences of vehicle collisions with end terminals can still be severe. In 2017, 113 deaths occurred in vehicle-to-end terminal crashes [57].

All the newly installed guardrail end terminals on federal-aid highway projects have to be shown crashworthy according to a set of test procedures required for all the highway safety products outlined by the National Cooperative Highway Research Program (NCHRP) [4] and recently the American Association of State Highway and Transportation Officials (AASHTO) Manual for Assessing Safety Hardware (MASH) [36], for the federal government to reimburse the state for the federal share of the installation expense. The crash test guidelines assure that these devices

function well for the specified test conditions, but the performance of these devices under real-world conditions could differ from the crash test results due to factors such as impact conditions, site conditions, and installation or maintenance issues (National Academies of Sciences, Engineering, and Medicine, 2018). It has been observed that some in-service guardrail end terminals are improperly installed or maintained [58]. The performance of damaged end terminals is unclear and needs to be evaluated to better understand how damages contribute to crash outcomes.

Finite Element (FE) simulations are widely used in traffic safety research due to their accuracy and low costs relative to physical tests. Several FE models have been developed for end terminals [22, 23], but no study has been performed to evaluate the safety performance of guardrail end terminals with pre-existing damages. The objectives of this study are to examine damage conditions of in-service end terminals, and to evaluate the performance of the damaged relative to undamaged end terminals in simulated crashes.

4.2 Methods

4.2.1 Examination of common damage types of end terminals

Common damage patterns of guardrail end terminals were investigated using data collected from the National Automotive Sampling System – Crashworthiness Data System (NASS-CDS). NASS-CDS contains detailed data of police-reported tow-away crashes, such as post-crash photos [59]. NASS-CDS does not code the types of fixed objects. The study reviewed 3,238 crash cases, which were randomly selected from all the cases involving fixed objects occurring from 2000 to 2014 (28,482 cases). Based on post-crash photos, 695 crash cases that involved an impact to an end terminal were identified. The observed damages to the end terminals in these cases were classified into minor and severe damages based on the NCHRP repair manual [60]. Minor damage includes a slightly deformed (Figure 4-1a) or misaligned impact head (Figure 4-1b) while all the other components could work properly. Severe damage includes a significantly deformed impact head and barriers, and may include broken posts as well (Figure 4-1c). In some cases of severe damages, the end terminal was completely destroyed (Figure 4-1d). All the end terminals in these example figures were ET-Plus, but the damage patterns could apply to all the end terminals.

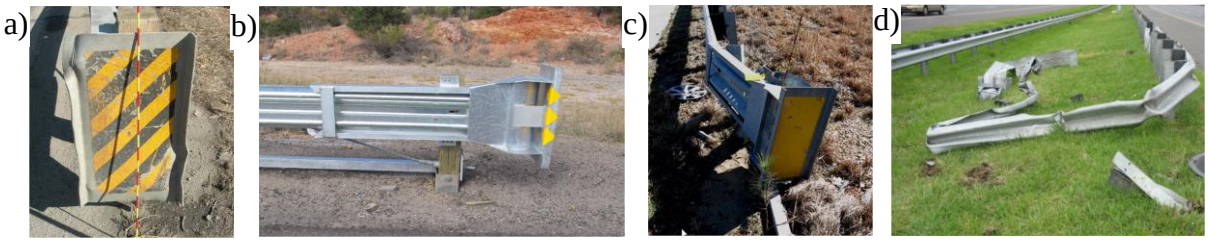

Figure 4-1 Examples of common damage patterns of end terminals: a) minor damage with scratched or bent impact head; b) minor damage with misaligned impact head; c) severe damage with less than two posts broken; d) severe damage with at least two posts broken

Note: 1.; 2. Photos were collected from NASS-CDS cases: a) Case #779014928; b) Case #526015936; c) Case # 532018933; d) Case # 766011850

4.2.2 Examination of conditions of in-service end terminals

The conditions of in-service end terminals mounted along roads in portions of six U.S. States were evaluated by using a sample from the Second Strategic Highway Research Program - Roadway Information Database (SHRP2-RID). This database covers more than 25,000 miles of roads and about 46,000 end terminals in the six Naturalistic Driving Study (NDS) sites (Florida, Indiana, New York, North Carolina, Pennsylvania, and Washington). The type and location of each end terminal are provided in this database, but their conditions are not included. The study randomly selected 298 end terminals from the SHRP2-RID. The number of samples selected from each NDS site was proportional to the total number of end terminals in each site.

The selected end terminals were located and examined to identify damage, if any, in Google Street View (GSV). One end terminal captured on one specific date in GSV was considered as a case in this study. There could be more than one case for the same end terminal, since an end terminal can be captured on different dates in the GSV. Of the 298 sampled end terminals, 92 had one case each, and the remaining 206 had 2 to 12 cases each. A total of 1,000 cases were resulted. The damage type and photo date were recorded for each case. Due to low resolution of GSV pictures before 2011, only the cases between 2011 and 2018 were investigated. The counts and proportions of undamaged, minorly damaged, and severely damaged end terminals were calculated among all the cases.

4.2.3 Development of Finite Element models for damaged ET-Plus

ET-Plus end terminals are one of the most common energy-absorbing guardrail end terminal mounted along U.S. highways [61]. ET-Plus end terminals with minor and severe damages were modeled in the study. A previously developed and validated FE model of an ET-Plus end terminal, with an installation height of 0.7 m [61], was used to develop damaged ET-Plus end terminals by FE simulations in the LS-DYNA software (LSTC, Livermore, CA, USA). Based on the examination of the 695 NASS-CDS crash cases, the minor and severe damage patterns were further divided into two minor damage patterns (M1 and M2) (Figure 4-2) and three severe damage patterns (S1, S2, and S3) (Figure 4-3), based on the direction of the deformed impact head.

The minorly damaged ET-Plus terminal models were those with deformed impact heads misaligned relative to the barrier. Minor damages such as a scratch or bend on the impact head were not modeled in this study since they were considered to have a minimal influence on the system response to the impact. The M1 ET-Plus had an impact head bending upward (Figure 4-2b), with the angle between the impact head and the barrier ranging between 1.5° to 2° (based on measurements of several M1 ET-Plus cases from GSV and NASS-CDS). An angle of 1.75° was used in the M1 ET-Plus model. To develop this model, a rotational velocity of 0.1° per second was assigned to the impact head of the undamaged ET-Plus model (*Initial_velocity in LS-DYNA) until the angle was reached. The node location, element stress, and strain were recorded and used in the M1 ET-Plus model. All other model parameters (contact, constraints, etc.) were the same as those in the undamaged ET-Plus model.

The M2 ET-Plus had an impact head bending downward, with the angle between the impact head and the barrier ranging between 2° and 3° (Figure 4-2c). The M2 ET-Plus model was developed using a similar method to the M1 model, with an angle of 2.5° between the impact head and the barrier.

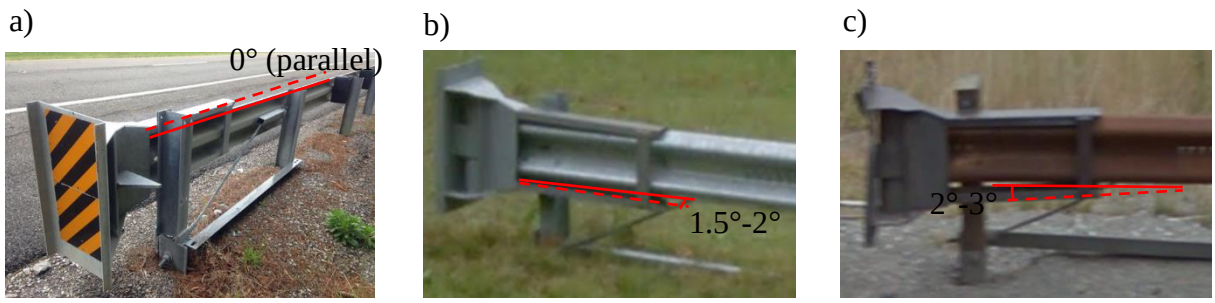

Figure 4-2 Undamaged and minorly damaged ET-Plus: a) Undamaged; b) M1; c) M2

Note: The red solid line indicates the edge of the barrier;

the red dashed line indicates the edge of the impact head

Three severely damaged ET-Plus models with at most one broken post were modeled in this study (Figure 4-3). All of these models have severe deformations in the barrier parts, with different deformation directions of the ET-Plus impact head: S1 with the impact head not bending upward or downward, S2 with the impact head bending downward, and S3 with the impact head bending upward. If the first two posts (post #1 and #2) are broken, the impact head drops, which compromises severely the end terminal's safety function. As a result, these cases were not modelled.

To develop the S1 damaged ET-Plus model, a vehicle-to-undamaged ET-Plus collision was simulated. In the simulation, an initial velocity of 100 km/h was assigned to the vehicle model (1997 Geo Metro) [62], and no offset between the vehicle and the barrier was used. The simulation was run until post #1 was broken and post #2 was not yet damaged. The node location, element stress, and element strain were recorded, and used for the initial conditions of S1 ET-Plus (Figure 4-3a).

To develop the S2 and S3 ET-Plus models, a rotational velocity of 0.1° per second was assigned to the impact head directly as prescribed motion (*Boundary_prescribed_motion_set in LS-DYNA). A simulation run to model the rotation of the impact head until the target angle between the impact head and barrier was reached (3° in S2 ET-Plus, and 5° in S3 ET-Plus) (Figure 4-3b, c). Although the angles varied widely in the investigated cases, small angles were used in the

simulation since greater angles would likely lead to extreme results. Similar to the S1 model, the node location as well as the element stress/strain were recorded and used in the S2 and S3 ET-Plus models.

Figure 4-3 Severely damaged ET-Plus: a) S1; b) S2; c) S3

Note: The red solid line indicates the edge of the barrier;

the red dashed line indicates the edge of the impact head

4.2.4 Evaluation of the safety performance of damaged ET-Plus

The safety performance of damaged ET-Plus terminals was evaluated using vehicle-to-terminal collision simulations (Figure 4-4). All of the simulations in this study were set up based on NCHRP 350, test level (TL) 3, test condition 30 (NCHRP 350 test No. 3-30), since this test was used to validate the undamaged ET-Plus model in a previous study [63]. The validation study used a vehicle model (1997 Geo Metro, 813 kg) similar to the test vehicle (1999 Geo Metro, 796 kg). All the simulated impact conditions (impact velocity, impact angle, impact position) are the same as the ones in crash tests (Table A1). The energy was recorded and compared to NCHRP-recommended criteria to verify the simulation stability [64]. Overall, the total energy remained essentially constant (varied less than 4%), the ratio of hourglass energy and the total energy was less than 3% (Figure B1). Meanwhile, the overall kinematics of the vehicle model showed qualitative agreement relative to test data [63]. Roadside Safety Verification and Validation Program (RSVVP) were used to assess the similarity of test data and simulation results using Sprague-Geer Metrics and Analysis of variance (ANOVA) Metrics [64, 65]. The simulation time histories of yaw angles had a good agreement with the test data (M = -2.7, P = 0.9; Average = 5, Standard Deviation =2.5) while the roll and pitch angle only pass the Sprague-Geer Metrics tests (Table B1).

A 1997 Geo Metro model was positioned parallel to the guardrail with an offset of 1/4 of the vehicle width (~397 mm) [38, 62]. The initial velocity of the vehicle model was 100 km/h in all the simulations. The end terminal model, either an undamaged or a damaged ET-Plus model, was impacted at the impact head.

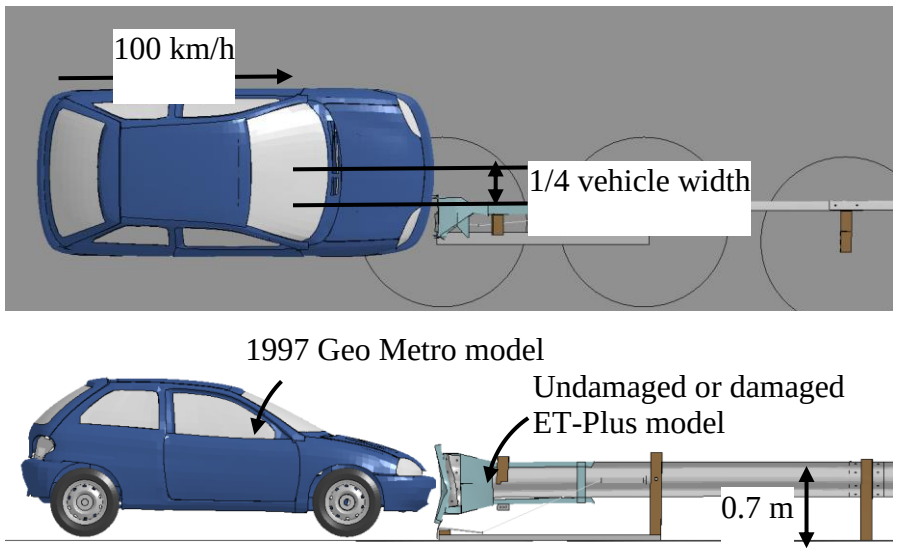

Figure 4-4 Vehicle-to-ET-Plus collision simulation

Note: S1 ET-Plus model was used in the figure for illustration

The safety performance of the damaged ET-Plus terminals was evaluated using three factors according to NCHRP 350 and MASH: structural adequacy, occupant risk, and vehicle trajectory [4, 38, 66]. Since differences between the two guidelines were observed, saferty criteria from both guidelines were used in this study.

Factors related to structural adequacy evaluate the end terminal's ability to stop or redirect the vehicle. No quantitative criterion is stated in NCHRP 350 or MASH. In the study, the collision duration and vehicle deceleration rate were used to evaluate the structrual adequacy. The collision duration was defined as the time interval from the first impact with the end terminal until the vehicle separated from the end terminal. There are six accelerometers defined in the Geo Metro vehicle model [67]. The one in the midline, the closest to the vehicle Center of Gravity (CG), was used to record vehicle velocity in this study (Node ID 2200259). First, the

velocity change during the collision duration was derived, and then the average vehicle deceleration rate was calculated as the ratio of the velocity change to the collision duration.

In terms of occupant risk, in NCHRP 350, the test vehicle is required to remain upright during a collision (no rollover). Additionally, no peneration between the end terminal and the occupant compartment of the test vehicle is allowed. During the validation of end-terminal model against the data recorded in NCHRP 350 tests [63], good predictions were observed in terms of overall vehicle's global kinematics, but some inaccuracies were found in local data such as higher predictions of vehicle's acceleration caused probably by the model simplifications (e.g. no interior seats, uncertanties regarding the location of vehicle's CG center of gravity vs. model' CG, etc). Therefore, to predict quantitative occupant risk measures such as occupant occupant impact velocities (OIV) and occupant ridedown acceleration (ORA) ,which are calculated based on the acceleration time history of vehicle's center of gravity (CG), we think the vehicle model requires some improvements. The MASH further adds limits for vehicle pitching and rolling angles to ensure the vehicle remains upright (no more than 75°) and to limit the intrusion into the occupant space of each vehicle area (Table 4-1). To evaluate the occupant risk, the general response of the vehicle model was examined. It was also checked if the vehicle model rolled over, and if there was peneration between the vehicle and ET-Plus right before the seperation. The maximum displacements toward the occupant space, as measured in a vehicle-fixed coordinate reference frame, for every node representing the structures listed in Table 4-1 and shown in Figure 4-5 were computed. The displacement of the node with the greatest vector-resultant displacement in each vehicle area was recorded for comparison with the AASHTO limits. (Figure 4-5). The lateral displacements of nodes representing the A- and B-pillars were evaluated separately. In addition, the maximum yaw angle of the vehicle was measured during the collision.

Table 4-1 MASH evaluation criteria for vehicle by area [61]

Vehicle area	Maximum deformation
Roof	102 mm
Windshield	76 mm and no tear of plastic liner
A- and B-pillars	127 mm (resultant)
	76 mm (lateral)
Wheel/foot well and toe pan areas	229 mm
Side front panel	305 mm
Front side door area (above seat)	229 mm
Front side door area (below seat)	305 mm
Floor pan and transmission tunnel areas	305 mm

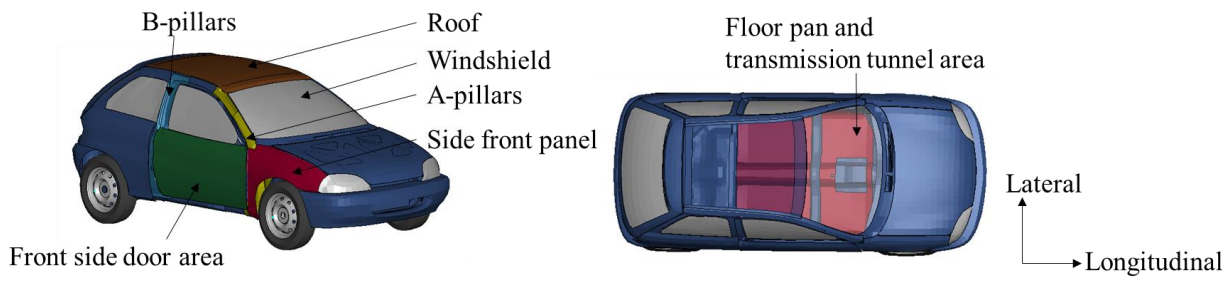

Figure 4-5 Vehicle areas to measure deformations

The vehicle trajectory predicts if the vehicle would experience a secondary collision with either a fixed object or another vehicle. Based on both NCHRP 350 and MASH, the vehicle trajectory behind the end terminal is acceptable. Meanwhile, the NCHRP 350 prefers the vehicle not to intrude into the adjacent traffic lane after the impact. No measurable criterion to evaluate vehicle trajectory is provided in NCHRP 350 or MASH. In this study, the possibility of a secondary collision was inspected. The vehicle velocity as it separated from the ET-Plus and the maximum lateral distance between the vehicle and guardrail were recorded in each simulation to predict whether the vehicle would intrude into the adjacent traffic lane.

4.3 Results

4.3.1 Distributions of damaged guardrail end terminals

Of the 1,000 cases reviewed, 733 (73%) cases had no visible damage, 184 (18%) cases had minor damage, and 83 cases (8%) had severe damage (Table 4-2). Sixty nine percent of the damaged cases were the same end terminals observed more than once, and 28 percent of the 298 sampled end terminals were observed damaged on any of the dates in the GSV.

Table 4-2 End terminal damage conditions by NDS site

State	End terminal sample #	Case #	Undamaged cases # (%)	Cases with minor damages # (%)	Cases with severe damages # (%)
IN	39	73	43 (59%)	22 (30%)	8 (11%)
FL	36	205	186 (91%)	9 (4%)	10 (5%)
WA	60	158	137 (87%)	11 (7%)	10 (6%)
PA	73	160	113 (70%)	38 (24%)	9 (6%)
NY	24	37	34 (92%)	2 (5%)	1 (3%)
NC	66	367	220 (60%)	102 (28%)	45 (12%)
Total # (%)	298	1000	733 (74%)	184 (18%)	83 (8%)
Mean ± SD of percentage			77%±16%	16%±12%	7%±3%

Several cases reviewed suggested that some end terminals were improperly maintained (Figure 4-6). For example, an ET-Plus in North Carolina was observed to be minorly damaged in a 2012 GSV picture, severely damaged in GSV pictures taken during 2014-2016, and repaired in a 2016 GSV picture (Figure 4-6a). It is possible that this ET-Plus end terminal was in use while damaged for almost 4 years. Another example of improper maintenance is a BCT end terminal observed to be minorly damaged in 2012 and still damaged in the photo taken in 2017 (Figure 4-6b).

Figure 4-6 Examples of damaged end terminals in use along U.S. roads: a) an ET-Plus end terminal that was damaged during 2012-2016; b) a BCT end terminal which was damaged since 2012

4.3.2 Development of damaged ET-Plus models

No element failure was observed during the development of the 2 minorly damaged ET-Plus models (Figure 4-7), so both impact head damaged models had the same number of nodes/elements as the undamaged model (17,943 nodes and 15,706 elements).

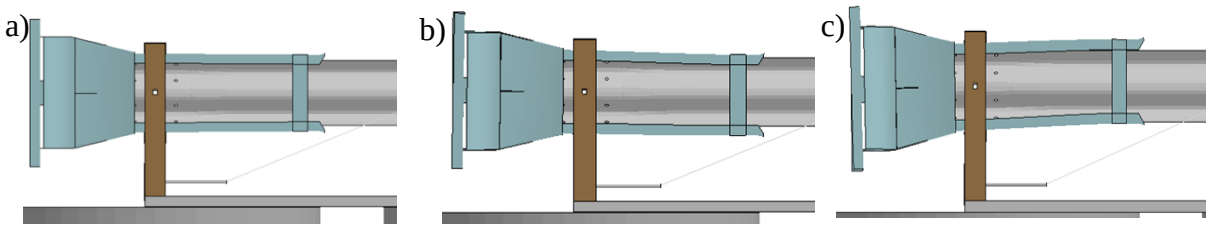

Figure 4-7 Undamaged and minorly damaged ET-Plus models: a) Undamaged; b) M1; c) M2

For the 3 severely damaged ET-Plus models (S1, S2, and S3), large deformation was observed in the impact head and rail parts but no failure was observed during the development phase (Figure 4-8). For the S1 models, post #1 was broken, so 716 solid elements were removed. No failure

was observed in any posts beyond post #1. For the S2 and S3 models, no failure in any post element was observed.

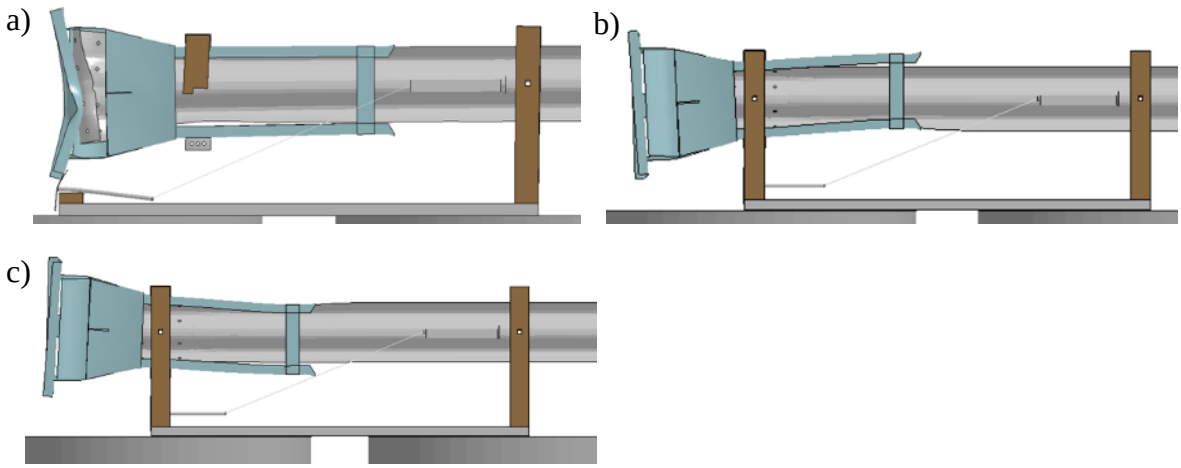

Figure 4-8 Severely damaged ET-Plus models: a) S1; b) S2; c) S3

4.3.3 Evaluation of the safety performance of damaged ET-Plus

Overall, in the vehicle-to-damaged ET-Plus collision simulations, higher average deceleration rates of vehicles (Table 4-3) and more severe vehicle local deformations (Table 4-4) were usually observed when compared with the vehicle-to-undamaged ET-Plus collision simulation results.

The collision with M1 ET-Plus was more severe than the collision with an undamaged ET-Plus. This was likely caused by a secondary collision with the barrier (observed in the M1 case at 0.87 s in the simulation) (Figure 4-9). Meanwhile, the vehicle model had a 43% larger yaw angle and a 22% shorter lateral distance (Table 4-3) compared with the angle recorded in the impact with an undamaged ET-Plus model. The separation velocity of the vehicle was also 28% higher. Almost all the measured vehicle deformations, except the floor pan and transmission tunnel areas, were larger than those observed in the vehicle model that impacted the undamaged ET-Plus (Table 4-4).

a)

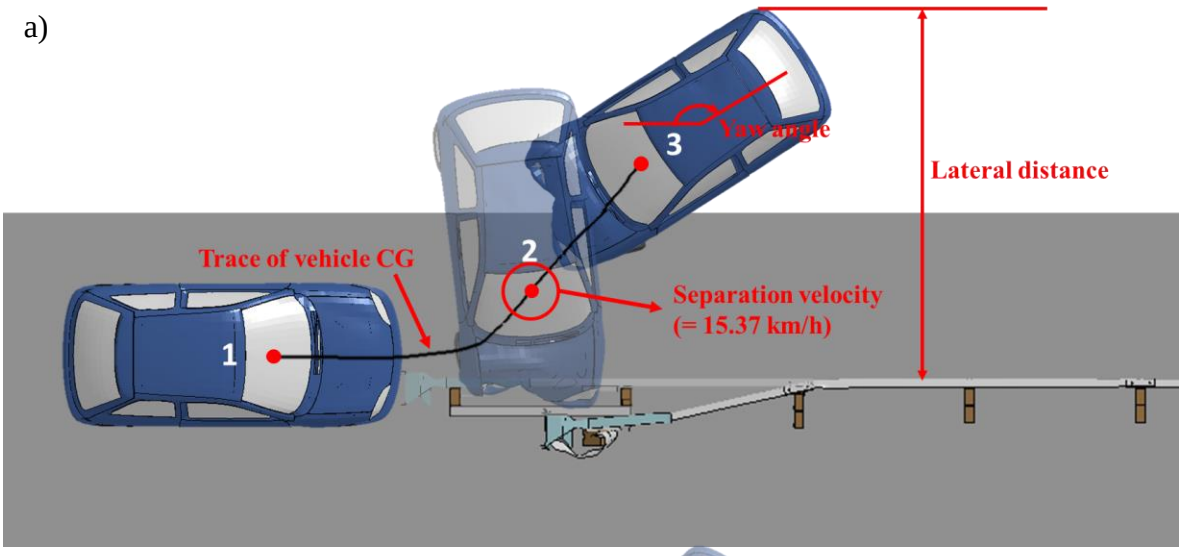

b)

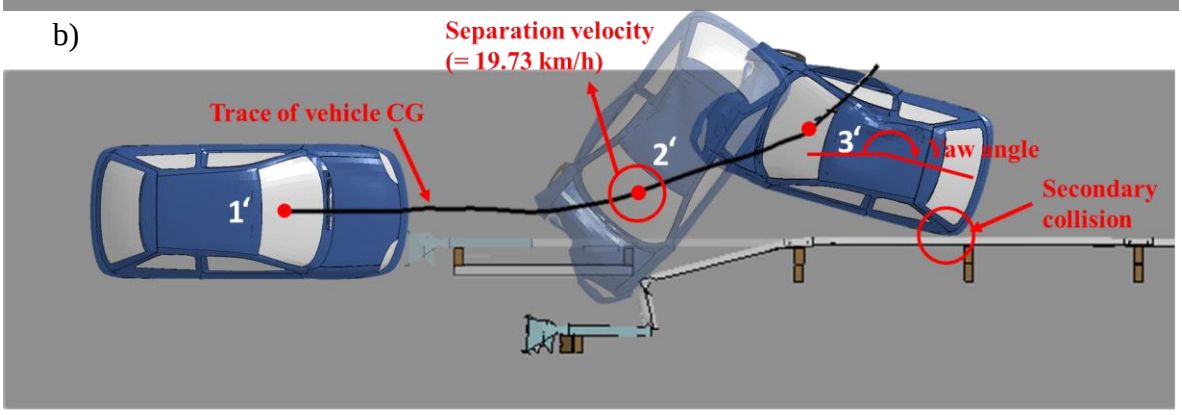

Figure 4-9 Vehicle-to-ET-Plus collision simulations: a) undamaged ET-Plus; b) M1 ET-Plus

Note: Fig. a) 1. Vehicle impacted undamaged ET-Plus; 2. Vehicle separated from the guardrail; 3. Vehicle completely stopped.

Fig. b) 1’ Vehicle impacted M1 ET-Plus; 2’. Vehicle separated from the guardrail; 3’: Secondary collision occurred.

The vehicle model impacting the M2 ET-Plus had an 8% higher deceleration rate when compared with the impact with the undamaged ET-Plus (Table 4-3). Large deformations were observed in the side front panel (200 mm) and the floor pan and transmission tunnel areas (251 mm).

In the impact cases with severely damaged end terminals, the vehicle models had higher average deceleration rates during collision, which resulted in lower structural adequacy. Specifically, the vehicle impacting the S1, S2, and S3 ET-Plus models decelerated 23%, 28%, and 52% faster than the vehicle impacting the undamaged ET-Plus model (Table 4-3). In addition, the separation velocities varied widely in each simulation with the severely damaged ET-Plus models. The vehicle models impacting the S1, S2, and S3 ET-Plus models had a 29% higher, 67% lower, and similar separation velocity relative to corresponding data from the vehicle-to-undamaged end terminal simulation (Table 4-3).

The vehicle local deformations were also different between impact simulations with the severely damaged ET-Plus models and the undamaged ET-Plus (Table 4-4) model. In the collision simulations with the S1 ET-Plus and S2 ET-Plus, all the measured vehicle deformations were larger than those observed in the impact with the undamaged ET-Plus, except the vehicle roof deformation in the S2 ET-Plus simulation. In the S3 ET-Plus simulation, the maximum deformation of the windshield, A-pillars (lateral), B-pillars (lateral), and side front panel were larger than those measured in the simulation with the undamaged ET-Plus.

Table 4-3 Vehicle responses during collision simulations

ET-Plus status	**Structural adequacy**		**Occupant risk**			**Vehicle trajectory**		
	Collision duration (s)	Vehicle avg deceleration (g)	Penetration occurs	Vehicle remains upright	Maximum yaw angle (degree)	Velocity separated from guardrail (km/h)	Secondary collision	Maximum lateral distance (m)
Undamaged	0.18	14.9	No	Yes	152	15.37	No	4.23
M1	**0.3**	7.89	No	Yes	**218**	**19.73**	**Yes**	3.29
M2	0.16	**16.1**	No	Yes	152	**16.13**	No	4.23
S1	0.135	**18.3**	No	Yes	**174**	**19.8**	No	**4.75**
S2	0.12	**19.1**	No	Yes	97	5.08	No	3.71
S3	0.12	**22.6**	No	Yes	134	**16.49**	No	4.23

Table 4-4 Vehicle maximum deformations

ET-Plus status	**Deformations by vehicle area (mm)**									
	Roof	Windshield	A-pillars (resultant)	A-pillars (lateral)	B-pillars (resultant)	B-pillars (lateral)	Side front panel	Front side door area (above seat)	Front side door area (below seat)	Floor pan and transmission tunnel areas
MASH limits	102	76	127	76	127	76	305	229	305	305
Undamaged	142	16	89	40	54	29	177	61	34	234
M1	129	**49**	**255**	**64**	**101**	**56**	**303**	**147**	**75**	222
M2	122	**18**	72	**53**	**57**	**31**	**200**	60	**35**	**251**
S1	**318**	**34**	**134**	**122**	**166**	**55**	**274**	**137**	**80**	**343**
S2	107	**72**	**368**	**140**	**82**	**34**	**288**	**167**	**148**	**245**
S3	99	**180**	67	**41**	51	**32**	**181**	51	34	230

4.4 Discussion

Although guardrail end terminals on highways are generally developed and tested for situations specified in crash testing guidelines, there are concerns about the in-service performance of these devices under real-world conditions (Joint AASHTO-FHWA Task Force on Guardrail Terminal Crash Analysis, 2015). Factors such as improper installation or maintenance could limit the performance of these devices. The study examined the conditions of a sample of in-service guardrail end terminals in the six NDS sites during 2011–2018, and found that 26% of the 1,000 cases had minor or severe damage. Five damaged ET-Plus FE models were developed to investigate possible changes in their safety performance relative to an undamaged ET-Plus model. It was found that the performance of ET-Plus guardrail end terminals was adversely affected by the minor and severe damage examined.

This study aimed to evaluate the effects of end terminal damages to the vehicle responses during crashes. Higher average vehicle deceleration rates were observed in simulated collisions with four of the five modeled damaged ET-Plus end terminals (except M1) compared with the undamaged ET-Plus. This suggests that these damaged ET-Plus end terminals do not absorb energy properly during collisions, and consequently could increase the collision severity [68, 69]. While a lower average deceleration was observed in the collision with a minorly damaged ET-Plus (M1), a secondary collision with the guardrail was observed, which also would increase the collision severity relative to the undamaged end terminal [70, 71]. The large vehicle deformations recorded in the simulations indicated a higher risk of occupant injury during the collisions with damaged end terminals relative to collisions with undamaged end terminals [72, 73].

The vehicle-to-ET-Plus collision simulations in this study were developed for the crashes occurred on the nose of the device, which were also used during the validation of the end terminal model (NCHRP 350 test 3-30) [63]. While most of the validation results were shown in the previously published paper [63], supplementary data were shown in Appendix A, B, and C in the current study. While limited test data is available, the time histories of vehicle angles were compared. In the future, the vehicle accelerations are highly recommended to be used to model validation (once it is available) because they are the foundation of OIV and ORA. Meanwhile, the NCHRP 350 test 3-30 was recently updated according to the MASH guideline. While MASH

uses many of the same impact conditions as NCHRP 350, some conditions were revised, for example in test 3-30 the vehicles have different weights. In this study, a vehicle model weight of about 820 kg was used based on an NCHRP 350 guideline. Additional models for a passenger car weighing about 1,100 kg should be used in future simulations based on the MASH guideline [66]. Meanwhile, first the undamaged end-terminal model could be validated under more crash scenarios (e.g. NCHRP 350 test 31, 33-39) in future studies. Then, the performance of damaged models could be investigated in other conditions using validated vehicle models in these impact conditions. For example, a pickup truck with a weight of 2,000 kg is required for NCHRP 350 test 31and 33. Other velocities (e.g. 50 km/h for TL 1 and 70 km/h for TL 2 tests), angles (e.g. 5°, 15°, and 25° used in MASH tests 32-37), and impact locations (e.g. barrier, and reverse direction used in MASH tests 34-37) could be incorporated into the future simulations as well [74].

In this study, occupant risks were evaluated based on the vehicle responses and maximum deformation during the collision simulations. However, this evaluation has some limitations. First, quantitative occupant risk measures such as OIV and ORA data was not used in this study due to some inaccuracies observed in the predicted acceleration of vehicle model' CG during the crash caused probably by the model simplifications. Therefore, more refinement of vehicle model are suggested in future. Second, the end-terminal was validated against NCHRP350 test data, without to quantify vehicle local deformations. To get more confidence in the model, it is suggested performing a validation against MASH test data which should include detailed information about post-impact vehicle deformation when this data will be available. In conclusion, while we consider valuable especially the comparison of the overall vehicle kinematics in the impact with undamaged and various damaged end terminal models, for more accurate predictions, especially at local level, more refinement of vehicles and model validations are suggested to be performed in future.

Some human [75, 76] and dummy FE models [77-79] have been developed and validated in previous studies. They can be added to the vehicle model in the future so the occupant risk could be estimated more accurately. For example, by using these human and dummy models, the occupant risk of injury could be evaluated using specific metrics such as the Occupant Injury Measure (OIM) [80] and/or the Whole Body Injury Metric (WBIM) [79, 81].

There are several limitations of the damaged ET-Plus FE models developed in this study. Firstly, both wood and metal posts are used in the ET-Plus systems, but only wood posts were modeled in this study. Since the material of the posts is critical in an impact, developing ET-Plus models with metal posts is necessary in the future when validation data becomes available. Secondly, only five typical damage patterns focusing on impact head changes were investigated in this study. Other damage patterns of impact head caused probably by no-vehicle impacts (e.g. vehicle impacting, snowplowing, mowing or paving, and exposure to the environment, etc. [82]) were also observed, and their investigation is recommended in the future. Additionally, the effects of other end terminal components (e.g. anchor cable, ground strut, and block-outs) in the damaged end terminal are also valuable to be evaluated in the future. Finally, only 298 in-service end terminals from six states were examined in this study. A larger sample from more areas is needed to better estimate the conditions of in-service end terminals along U.S. roads.

The study findings point to the need for in-service performance evaluations (ISPEs) and appropriate maintenance and repair practices of guardrail end terminals, to avoid degrading the performance of in-service end treatments. ISPEs of these devices are needed to ensure that these devices work effectively to reduce injuries and fatalities under various real-world conditions (National Academies of Sciences, Engineering, and Medicine, 2018). An ISPE uses detailed information on crashes, hardware installation and conditions, and site characteristics to assess and monitor the field performance of road safety devices. The evaluation helps highway agencies to determine if a device is functioning as expected, properly installed and maintained, or appropriate for the location. The evaluation also provides information for validating and refining existing crash test procedures. The causes of the observed damage to guardrail end terminals are not clear. Further investigation on how the damage occurs are recommended in future, to help road agencies devise strategies to reduce the occurrences.

The impact simulation models developed in this study could be further specified and validated by using ISPE findings and crash test results to simulate additional crash scenarios involving roadside safety devices. These models could evaluate the device performance in crash situations that are physically impractical to test as well as the effects of various site characteristics on device performance (National Academies of Sciences, Engineering, and Medicine, 2018). The simulation models could also be used to supplement the crash tests to certify new hardware

designs. Designs of roadside safety devices, of which the impact performance is less affected by damage occurring in service, are encouraged. The numerical investigation presented in this study is the first step in investigating the effects of damaged end terminals to vehicle responses. Future research examining the effects of various damage patterns on roadside safety devices by using validated models (especially car models) or crash tests is needed, to guide highway agencies' maintenance and repair practices, and eventually to support developing criteria for the replacement of damaged end terminals.

5. Injury assessment using dummy models during car-to-end terminal crashes

This section is based in full on the previously published article

"Meng, Y., Untaroiu, C. (2020). Numerical investigation of occupant injury risks in car-to-end terminal crashes using dummy-based injury criteria and vehicle-based crash severity metrics. *Accident Analysis & Prevention*, 145, 105700."

5.1 Introduction

In the USA, in 2018, a total of 7,422 deaths resulted from a vehicle leaving the roadway and hitting a fixed object alongside the road (e.g. trees, utility poles, traffic barriers, etc.). While fatalities in these crashes decreased almost 16% in the latest decade, the percentage of these fatalities from total motor vehicle crash deaths remained almost constant (20%) [1]. To prevent or deter vehicle access to off-road areas, guardrails are usually installed along highways. However, crashes with guardrails cause 10% of deaths in fixed-object crashes (9% caused by guardrail barrier, 1% caused by guardrail ends), which suggests that these systems need improvements in safety performance [1].

Guardrail end terminal safety performance is currently evaluated in the U.S based on tests according to the Manual for Assessing Safety Hardware (MASH) guideline [5]. While anthropomorphic test devices (ATD) are commonly used in other regulation crash tests (e.g. FMVSS) to evaluate occupant protection [10-12], no ATD data is measured during the MASH

tests [5]. Therefore, occupant injury risks of a certain body region cannot be evaluated, but only on a full-body injury risk based on the flail-space model (FSM). In this simplified injury model, the occupant is modelled as point mass based on a conservative assumption that the occupant is unrestrained during the crash [9].

Availability of airbags (100%) in current vehicles and high seat belt usage rates (~90%) raise some questions regarding the validity of FSM model proposed in 1981, when there was only a 20% seatbelt usage rate [13, 14]. Therefore, the relationship between vehicle responses during the crashes and the occupant injury probabilities was investigated based on real crash data [13, 15, 16] and sled test data [83]. However, there is no consensus regarding the relationship between the vehicle-based criteria and occupant injury risks (especially at body region level). While several researches showed that the FSM has little ability to assess occupant injury [15, 16], generally, it is accepted that the vehicle-based crash severity metrics provide a more conservative injury assessment than dummy-based criteria [17-19]. In addition, several previous studies showed that the occupant impact velocity (OIV) is related to the occupant injury [13] and the occupant ridedown acceleration (ORA) is a good predictor for head injuries [83]. Thus, to better understand the relationship between vehicle-based metrics (e.g. FSM) and dummy-based injury assessments, more research studies are required to be performed.

The European procedures (EN1317) were developed for seatbelt restrained occupants. Two vehicle-based metrics, Acceleration Severity Index (ASI) and Theoretical Head Impact Velocity (THIV), are required in all the tests. Although several studies were performed to investigate the predictability of these criteria, most of them were developed based on the old version of ASI which was calculated based on 50-ms average accelerations [27, 84-90]. Little research was performed to investigate the influence of revised ASI, which is based on filtered vehicle accelerations. The studies involving revised ASI were either a case study without regression analysis [91] or only focused on the relationship between ASI and THIV [92]. Thus, the relationship between the revised EN1317 vehicle-based severity metrics and the dummy-based injury assessments need to be investigated as well.

With recent updates in computational technology, numerical models became economical and repeatable alternatives to assess the potential for occupant injury risk. Dummy models were widely used to assess injuries on component levels in varied traffic crashes [24-28]. However,

there are no simulation-based studies developed to evaluate the occupant risk in the crashes involving a guardrail end terminal. The previous studies focused on either general safety performance of a guardrail [29-31] or the occupant risk assessments during the crashes with guardrail barriers (not end terminal systems) [25, 27, 32-34].

The main objective of this study was to numerically investigate for the first time the injury risks of vehicle occupants during car-to-end terminal crashes with various pre-impact conditions using dummy-based criteria and to compare with the vehicle-based crash severity metrics. The driver injury probabilities using FE simulations on both full-body and component levels were calculated and the influence of pre-impact conditions on the injury probabilities were also assessed. Finally, the injury probabilities assessed by dummy-based injury criteria were compared to the FSM and EN1317 vehicle-based metrics.

5.2 Methods

5.2.1 FE simulations of car-to-end terminal crashes

To assess the driver injury risk during vehicle-to-end terminal crashes, FE simulations were performed in LS-DYNA software (LSTC, Livermore, CA). A Toyota Yaris FE model, previously validated in varied crash tests [93], was used in all the simulations (Figure 5-1a). The vehicle model weighs 1100 kg which conforms to the MASH guideline requirements for a 1100C test vehicle [94]. Vehicle interior parts, including the steering wheel and seats were modeled in detail. A seatbelt and airbag model were added to the original Yaris model in this study. The geometric and material parameters were taken from previously-published models [95, 96]. A 50th percentile male (M50) Hybrid III dummy FE model was employed in the simulations (Figure 5-1b) [77, 96]. A preliminary simulation was performed to position the dummy model onto the driver seat. The vehicle model was supported by a rigid plate while the dummy model was dropped by gravity. A contact was defined between the vehicle seat model and the dummy model to avoid penetration. The preliminary simulation ran till the dummy stabilized on the seat and no penetration between the dummy head and vehicle hood was observed. The seat deformations, strains, and stress at the final time point were recorded from the preliminary simulations and were used as the initial conditions of the crash simulations. The seatbelt model was modified to fit the dummy model using LS-Prepost software (LSTC, Livermore, CA). A FE

model of ET-Plus end terminal, the most common energy-absorbing guardrail end terminal used along U.S. roads (Figure 5-1a). was used in all the simulations. The guardrail model was developed based on an installment height of 27 ¾ inches. Wood material was assigned to the post models. The model was previously validated [97] with passenger car-to-ET-Plus crash simulations and it showed the energy-absorbing capability during crashes.

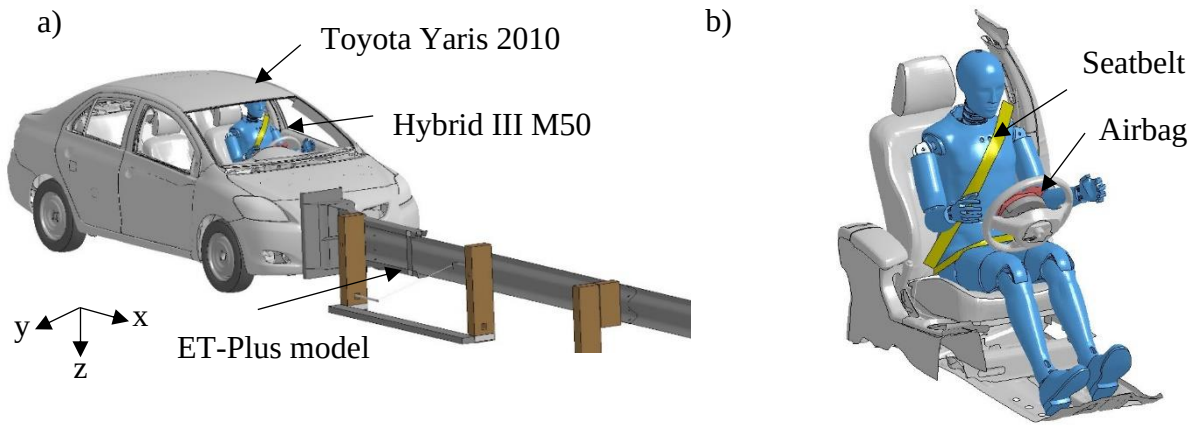

Figure 5-1 a) Vehicle-to end terminal crash setup b) FE dummy seated in the driver position

Similar to the MASH guideline, the pre-impact velocity, impact angle, and impact offset were used to describe impact scenarios [5]. Five pre-impact velocities were assigned on the vehicle as 65, 80, 100, 112, 120 km/h (which corresponding to 40, 50, 62, 70, 75 mph). The highest impact speed was assigned as 120 km/h since it is the maximum road speed limit in many U.S. states [98]. The median pre-impact velocity was assigned as100 km/h, which is the impact velocity in MASH guidelines. In two configurations, the impact angles and offsets were assigned based on MASH guideline (tests 30, 32). In one scenario, the impact angle was assigned as 0° and the offset was assigned as ¼ of vehicle width (test 30). In another scenario, the impact angle was assigned as 15° and no offset was used (test 32). Additional, two configurations using the same impact angles (0°, and 15°) and the same impact offsets (none, and ¼ of vehicle width) were used. As a result, four impact configurations (Figure 5-2) and a total of 20 vehicle-to-end terminal impact FE simulations were performed in this study.

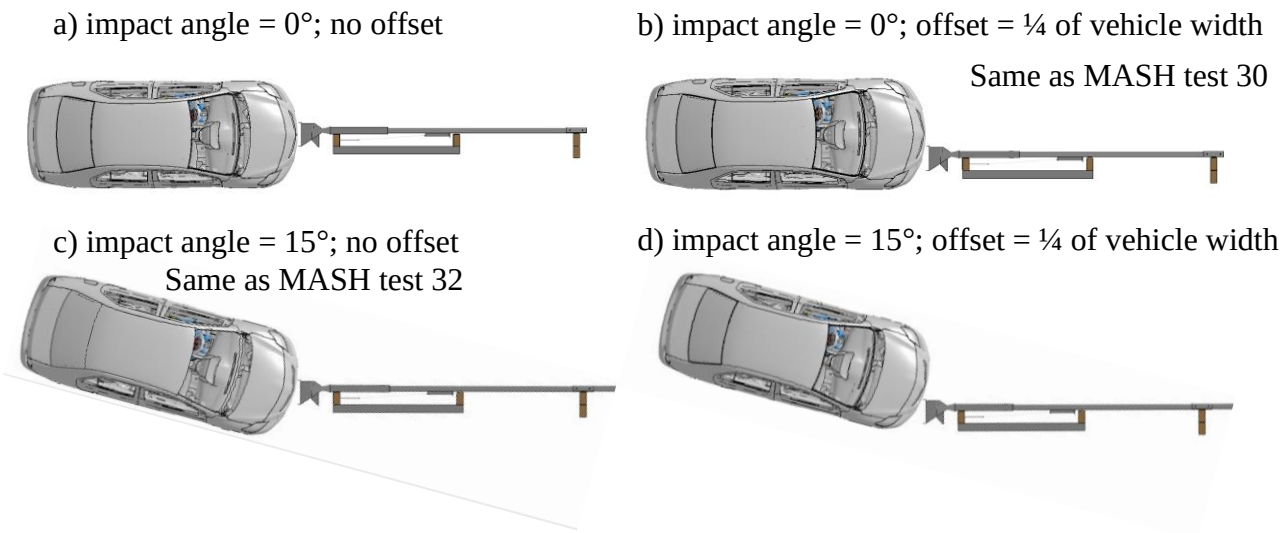

Figure 5-2 Vehicle-ET-Plus impact scenarios

Note: Pre-impact velocities of 65, 80, 100, 112, 120 km/h were assigned for each scenario

5.2.2 Occupant injury assessments using dummy-based injury criteria

In each simulation, the kinematic and kinetic responses of the dummy were recorded and the driver injury risks were assessed on body region levels (HIC_{15} and HIC_{36} for the head, N_{ij} for the neck, maximum chest deflection and chest acceleration for the chest, and the maximum femur load for the thigh). All these injury criteria values were compared to the FMVSS 208 injury limits which were developed for the mid-size male during frontal crashes (Table 5-1) [99, 100]. Correlation coefficients were calculated to investigate the relationship between pre-impact conditions and the dummy-based injury criteria using LS-OPT software (LSTC, Livermore, CA).

Table 5-1 Dummy-based injury criteria and their injury threshold values

Components	Injury criteria	Limits
Head	HIC36	1000
	HIC15	700
Neck	Nij	1
Thoracic	Chest deflection	63 mm
	Chest acceleration	60 g
Thigh	Femur load	10 kN

The risk of the occupant having a serious injury (AIS 3+) was estimated on both body-region and full-body using published injury probability functions (Equations below) [101-103]. A stochastic contribution analysis, based on Sobol's indices approach [104-106], was then performed to investigate the influences of each pre-impact vehicle condition (pre-impact velocity, offset, and angle) to the injury probabilities The values of injury probabilities were also compared with the vehicle-based crash severity metrics.

$$P(Head) = \Phi\left(\frac{\ln(HIC_{15}) - 7.45231}{0.73998}\right) \tag{5-1}$$

$$P(Neck) = \frac{1}{1+e^{3.227-1.969\times N_{ij}}} \tag{5-2}$$

$$P(Chest) = \frac{1}{1+e^{-(-7.125+0.08\times As+0.064\times ChestDef)}} \tag{5-3}$$

$$P(Leg) = \frac{1}{1+e^{4.9795-0.326\times F}} \tag{5-4}$$

$$P(AIS\ 3+) = 1 - (1 - P(Head)) \times (1 - P(Neck)) \times (1 - P(Chest) \times (1 - P(Leg)) \tag{5-5}$$

In the above equations, the units of the chest deflection (ChestDef), the chest acceleration (As), and femur load (F) were mm, g, and kN, respectively.

5.2.3 Occupant injury assessments using vehicle-based crash severity metrics

The FSM is a vehicle-based injury criteria used in MASH [5] to predict occupant injury in the crash tests with roadside safety hardware. This US criteria assumes that the occupant injuries are related to the impact to the vehicle interior parts during the crash [9]. The unbelted occupant is allowed to flail 0.6 m longitudinally and 0.3 m laterally into the vehicle interior space. Accelerations of the vehicle's center of the gravity in the longitudinal and lateral directions ($a_{x,y}$) are recorded and used to calculate flailed distance (X, Y) as follows:

$$X, Y = \int_0^t \int_0^t a_{x,y} dt^2 \tag{5-6}$$

Then the OIV were calculated as

$$OIV_{x,y} = \int_0^{t^*} a_{x,y} dt \tag{5-7}$$

where the time (t^*) was calculated while either $X = 0.6\ m$ or $Y = 0.3\ m$ was reached.

The longitudinal and lateral ORA ($ORA_{x,y}$) were then calculated as peak 10 ms average acceleration of the vehicle after t^*. The recommended threshold values for OIV and ORA are 12.2 m/s and 20.49 g, respectively for both longitudinal and lateral.

To investigate the injury predictability of current vehicle-based evaluation methods, the calculated OIV and ORA were compared to the assessed dummy-based injury probabilities determined from FE simulations using non-linear regression in JMP (version 15.0.0, SAS Institute Inc., Cary, NC). The results were fitted to a logistic curve (Eq. 5-8).

$$y = \frac{1}{1+\exp\left(-a\cdot(x-b)\right)} \tag{5-8}$$

where y is the injury probability, x is the vehicle-based crash severity metrics. The p-value of a and R^2 were calculated. With a p-value < 0.05, the correlation between the vehicle metric and the injury probability is statistically significant [107]. Therefore, the vehicle metric can be used to predict injury probability. Meanwhile, R^2 was used to measure how close the results are to the fitted regression curve. Higher the R^2 is, more predictability the vehicle metrics has.

Compared to FSM which was developed for unbelted occupants, the ASI, accepted mostly in the European standards [108, 109], was developed for belted occupants. Similar to the ORA, the ASI, was calculated based on vehicle CG accelerations (Eq. 5-9).

$$ASI = \max\left(\sqrt{\left(\frac{\bar{a}_x}{\hat{a}_x}\right)^2 + \left(\frac{\bar{a}_y}{\hat{a}_y}\right)^2 + \left(\frac{\bar{a}_z}{\hat{a}_z}\right)^2}\right) \tag{5-9}$$

where $\bar{a}$ is the acceleration filtered with a four-pole phaseless Butterworth low-pass filter which has a cut-off frequency of 13 Hz. The limit acceleration, $\hat{a}$, values are 12, 9, and 10 g for x, y, and z direction, respectively. The crash severity is classified as A, B, and C while the ASI is no more than 1.0, 1.4, and 1.9.

THIV is another vehicle-based metrics accepted in the EN1317 guideline and can be calculated using the following equations (Eq. 10-13) [108]. The THIV is required to be less than or equal to 44 km/h to pass the tests [110].

$$\begin{cases} \ddot{X}_C = a_x cos\Psi - a_y sin\Psi \\ \ddot{Y}_b = a_x sin\Psi + a_y cos\Psi \end{cases} \tag{5-10}$$

$$\begin{cases} x_b = (x_0 - X_c)cos\Psi + (y_0 - Y_c)sin\Psi \\ y_b = -(x_0 - X_c)sin\Psi + (y_0 - Y_c)cos\Psi \end{cases} \tag{5-11}$$

$$\begin{cases} \dot{x}_b = -\dot{X}_c cos\Psi - \dot{Y}_c sin\Psi + y_b\dot{\Psi} \\ \dot{y}_b = -\dot{X}_c sin\Psi - \dot{Y}_c cos\Psi - x_b\dot{\Psi} \end{cases} \tag{5-12}$$

$$THIV = \sqrt{\dot{x}_b(t^{**})^2 + \dot{y}_b(t^{**})^2} \tag{5-13}$$

where a_x and a_y are the recorded longitudinal and lateral vehicle accelerations in local coordinates while Ψ is the angle between the vehicle midline and guardrail. The t^{**} is the time of impact which was recorded while the occupant was moved 0.6 m forward or 0.3 m laterally. In this study, the longitudinal distance between vehicle CG and dummy head CG (x_0) was measured at the beginning of the crash simulation and recorded as -0.17 m while the lateral distance (y_0) was assumed to be zero as required in the guideline [108]. Similar to the metrics determined by the FSM, ASI and THIV were regressed to the assessed injury probabilities in JMP.

5.3 Results

5.3.1 Occupant injury assessments using dummy-based injury criteria

In 20 car-to-ET-Plus crash simulations, the vehicle was smoothly redirected after the impact and no rollover events were recorded. No penetration was observed between the guardrail end terminal and the vehicle models. Seatbelt and airbag models were observed to work properly. A typical car-to-ET-Plus crash simulation is shown in Figure 5-3.

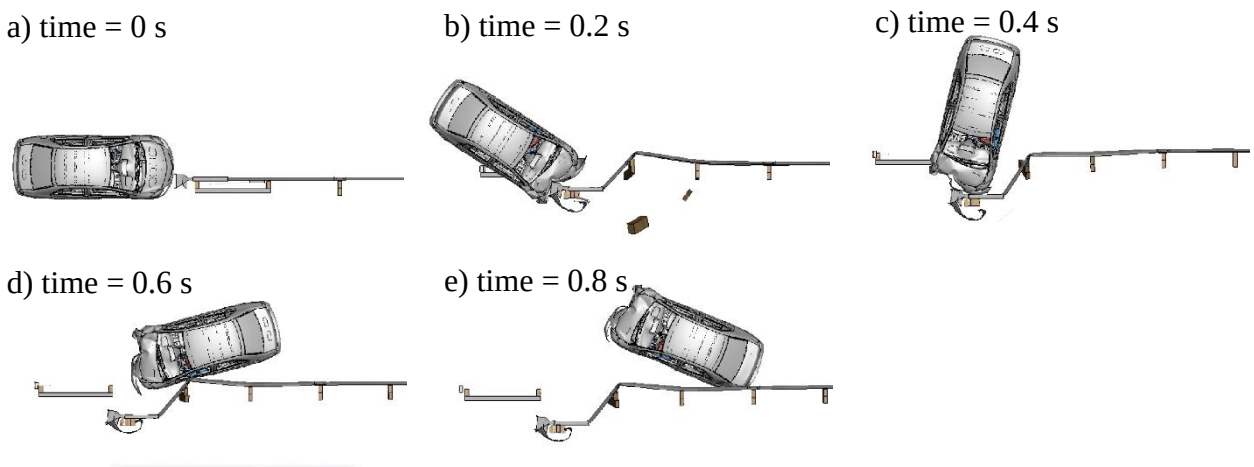

Figure 5-3 A car-to-ET-Plus crash simulation under MASH test 30 conditions (impact speed: 100 km/h; impact angle: 0°; offset: ¼ of vehicle width)

The values of dummy injury criteria values (Table D1) were under the FMVSS 208 limits. Strong correlations between pre-impact velocity and the head injury criteria (both HIC_{36} and HIC_{15}) and chest deflection were observed (Table 5-2). The chest acceleration, which was measured on the spine [111], was correlated with velocity positively and offset negatively. The Nij had a strong correlation with both pre-impact velocity and angle. Meanwhile, the femur load was observed to have a strong negative correlation with the offset between vehicle midline and the guardrail. The 95% confidence intervals of these correlation coefficients are shown in Figure E1.

Table 5-2 Correlation coefficients between pre-impact conditions and dummy region-body injury criteria

		Biomechanics injury criteria					
		HIC_{36}	HIC_{15}	N_{ij}	ChestDef	As	Femur load
Pre-impact conditions	Velocity	0.49	0.52	0.56	0.75	0.57	0.36
	Angle	0.28	0.30	0.57	-0.26	-0.04	-0.37
	offset	-0.30	-0.19	-0.06	-0.49	-0.66	-0.63

The mean occupant full-body serious injury (AIS3+) probability was estimated at 17%. The mean values of serious injury probabilities were estimated at 1%, 9%, 5% and 2% for the head, neck, chest, and thigh, respectively (Table 5-3). Based on the results of stochastic contribution analysis (Figure 5-4), the velocity had the highest influence for the change in almost all the injury probabilities (except thigh). The influences of vehicle velocity on the injury probabilities were recorded as 59%, 79%, 62%, and 44% in full-body, head, neck, and chest levels, respectively. Meanwhile, the offset between vehicle midline and the guardrail barrier had the highest influence on the thigh injuries (56%).

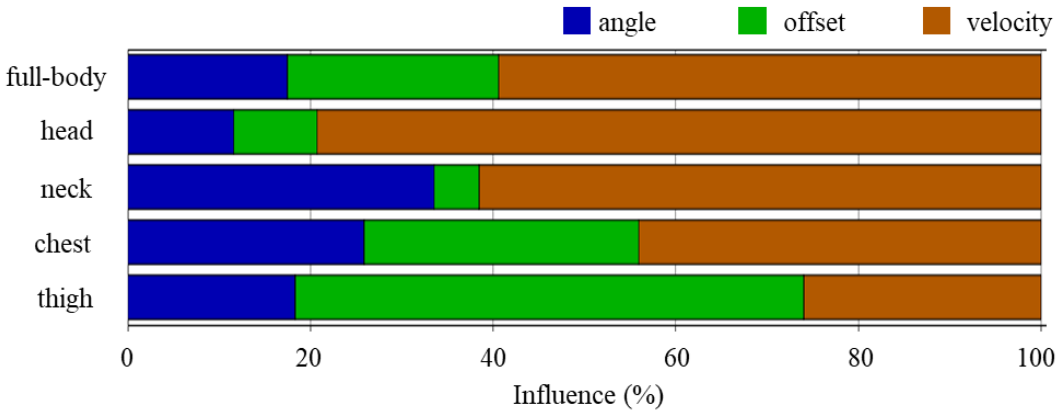

Figure 5-4 The influences of pre-impact angle, offset, and velocity on dummy region-body injury probabilities

5.3.2 Occupant injury assessments using vehicle-based crash severity metrics

The values of injury risks predicted by the dummy-based approach and vehicle-based crash severity metrics were compared in Table 5-3. The OIV/ORA values recorded in 5 crash simulations were below maximum values suggested in MASH. 11 simulations pass only the ORA criteria, 1 simulation passes only OIV criteria and the other 3 failed both MASH criteria. The mean longitudinal and lateral OIVs were recorded to be 12.8 m/s and 1.5 m/s, respectively. Additionally, the mean longitudinal and lateral ORAs were recorded to be 13.06 g and 6.43 g, respectively. The majority of recorded THIVs (14 out of 20) exceeded the limits suggested in European criteria (EN1317). Meanwhile, only two simulations failed the ASI criteria while all the others had an ASI ≤ 1.9. The average THIV and ASI were recorded as 47 km/h and 1.6.

Table 5-3 Injury probabilities assessed by dummy-based and vehicle-based crash severity metrics

Pre-impact conditions			Injury probabilities assessed by dummy-based criteria					Vehicle-based crash severity metrics					
Velocity (km/h)	Offset	Angle (°)	Full-body	Head	Neck	Chest	Thigh	OIVx (m/s)	OIVy (m/s)	ORAx (g)	ORA y (g)	ASI	THIV (km/h)
65	1/4	0	8%	0%	6%	2%	1%	12.5	0.3	16.47	3.87	1.5	43
65	1/4	15	11%	2%	8%	1%	1%	10.6	2.0	3.45	5.07	1.0	44
65	0	0	9%	0%	6%	2%	2%	12.8	0.4	16.43	1.98	1.5	46
65	0	15	9%	0%	6%	2%	1%	13.1	2.7	6.09	3.54	1.7	49
80	1/4	0	8%	0%	5%	2%	1%	12.1	0.2	12.28	3.67	1.3	44
80	1/4	15	16%	0%	13%	1%	1%	11.2	2.7	3.72	4.86	1.4	47
80	0	0	9%	0%	5%	3%	2%	12.7	0.5	12.88	2.87	1.6	56
80	0	15	10%	0%	7%	2%	2%	13.2	2.7	11.72	5.25	1.6	47
100	1/4	0	12%	0%	8%	2%	2%	11.9	0.2	19.60	7.10	1.2	46
100	1/4	15	14%	1%	10%	2%	1%	12.0	2.6	6.32	8.51	1.6	49
100	0	0	21%	4%	10%	6%	2%	13.0	0.6	25.30	7.01	1.7	58
100	0	15	18%	0%	11%	7%	2%	13.4	2.5	12.18	7.77	1.6	53
112	1/4	0	11%	0%	7%	3%	2%	12.2	0.3	20.69	9.21	1.5	45
112	1/4	15	22%	4%	16%	2%	1%	12.8	2.7	3.89	3.20	1.7	39
112	0	0	25%	5%	7%	14%	2%	14.6	0.3	23.27	8.98	2.0	46
112	0	15	28%	5%	13%	10%	2%	12.7	2.3	8.95	6.55	1.8	48
120	1/4	0	9%	0%	5%	3%	2%	12.6	0.3	19.50	7.94	1.4	44
120	1/4	15	20%	4%	14%	2%	1%	13.1	3.0	9.22	16.78	1.8	42
120	0	0	43%	2%	12%	32%	3%	16.2	0.6	22.86	9.21	2.1	46
120	0	15	31%	2%	18%	12%	2%	14.2	2.8	6.47	5.13	1.9	48
Average			17%	1%	9%	5%	2%	12.8	1.5	13.06	6.43	1.6	47
Limits								12.2	12.2	20.49	20.49	1.9	44

OIV longitudinal was identified as a good predictor for full-body injury probability (p-value <0.0001) (Table 5-4). The full-body injury probabilities matched the fitted curve with an R^2 of 0.61 (Figure 5-5a). Meanwhile, the curve showed a good agreement with a previously published curve which was developed based on real crash data (Figure 5-5b). The real crash data

were collected by EDRs in a previous study [86]. Meanwhile, the predictability of ORA, ASI, and THIV to the injury probabilities were evaluated (Table 5-4).

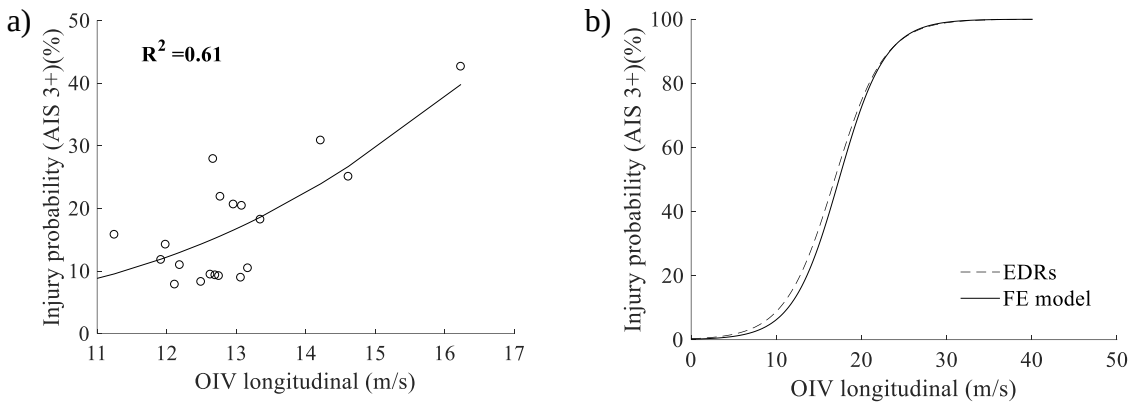

Figure 5-5 Correlation between OIV longitudinal and AIS 3+ dummy injury probability

Table 5-4 Correlations of vehicle-based severity metrics and the injury probabilities assessed by dummy-based criteria

Vehicle-based severity metrics	Injury probabilities assessed by dummy-based criteria	a	b	p-value of a	R^2
OIVx (m/s)	Full-body	0.3979	17.0699	<0.0001	0.62
	Head	0.2162	32.5275	0.2516	0.07
	Neck	0.0969	36.1951	0.2221	0.07
	Chest	0.7227	17.2739	<0.0001	0.91
	Thigh	0.1477	41.0257	<0.0001	0.59
ORAx (g)	Full-body	0.0136	131.3400	0.5325	0.02
	Head	-0.0084	-494.2429	0.8520	0.00
	Neck	-0.0287	-66.2585	0.0524	0.17
	Chest	0.0995	44.2423	0.0532	0.19
	Thigh	0.0195	225.9959	0.0030	0.33
ASI	Full-body	2.4603	2.3074	<0.0001	0.75
	Head	2.3219	3.4692	0.0191	0.30
	Neck	0.8531	4.2617	0.0182	0.24

	Chest	6.2174	2.2351	<0.0001	0.92
	Thigh	0.5546	9.0897	0.0017	0.33
THIV (km/h)	Full-body	0.1064	62.8157	<0.0001	0.62
	Head	0.0804	100.3388	0.0986	0.13
	Neck	0.0299	122.7241	0.1496	0.10
	Chest	0.2203	62.3675	<0.0001	0.86
	Thigh	0.0350	165.9634	<0.0001	0.46

Note: 1. Bold numbers are the ones less than 0.05 (good correlation)
2. Shaded body-region can be predicted by vehicle-based severity metrics

The OIV longitudinal was found to have little correlation to head and neck injuries since the p-values were 0.25 and 0.22, respectively. On the other hand, good correlations between OIV longitudinal and chest/femur injuries were observed (p-values <0.0001, R2=0.91 for chest, 0.59 for femur) (Figure 5-6). The ORA was identified as a weak predictor for all the injuries except thigh (p-value = 0.0030) (Figure F1).

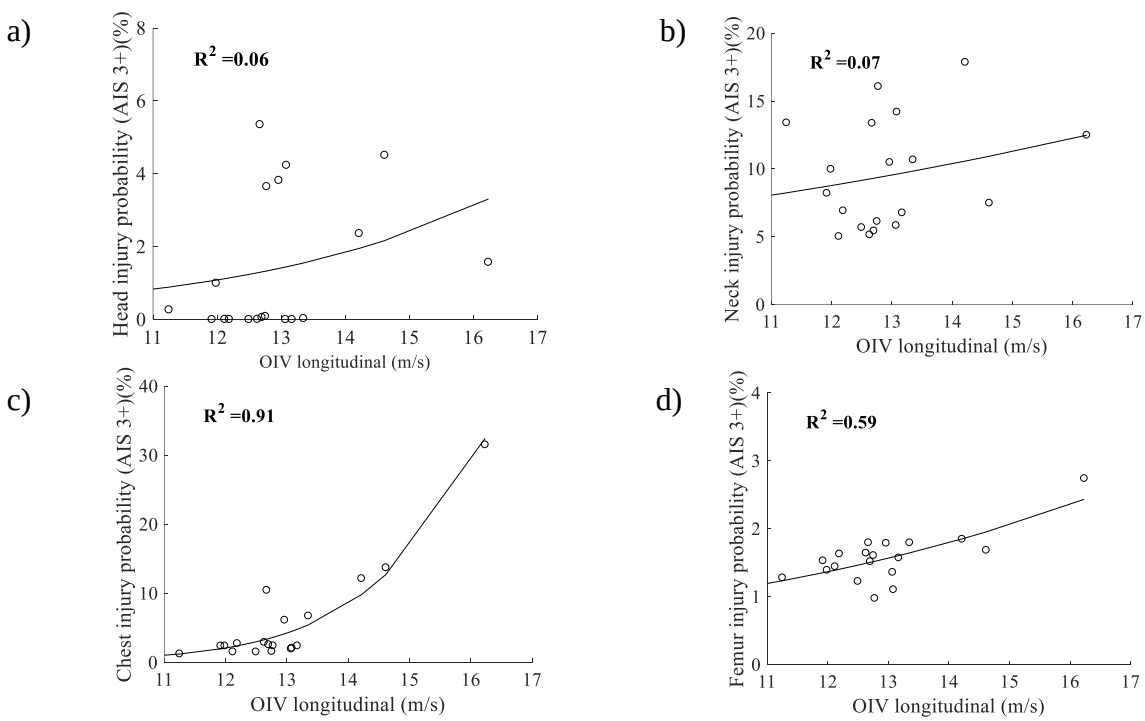

Figure 5-6 Correlation between OIV longitudinal and dummy region-body injury probabilities: a) head; b) neck; c) chest; d) femur

The ASI was observed to be a good predictor for all the injuries since all the p-value are less than 0.05 (Figure G1). However, the assessed head, neck, and thigh injury probabilities fitted the

curves with a R2 around 0.30, which is much lower than the ones recorded in the curves for full-body (0.75) or chest (0.92). The THIV has a good correlation with full-body, chest, and thigh injury probabilities while it has a poor correlation with the others (Figure H1).

5.4 Discussion

The safety performance of ET-Plus under the MASH test conditions (no. 30 and 32) was investigated using numerical methods for the first time. It was observed that ET-Plus would only pass MASH test 30. The recorded value of OIV longitudinal in MASH test 32 (13.4 m/s) was larger than the 12.2 m/s limit. This result indicated that the pass of the National Cooperative Highway Research Program (NCHRP) tests cannot guarantee the pass of the MASH tests. Therefore, it is recommended to test the NCHRP-tested end terminals under the MASH test conditions in the future. While our ET-Plus model was validated only under NCHRP conditions [63], a limitation of this study is the lack of validation of ET-Plus model under MASH conditions, which is recommended to be performed when the corresponding test data will be available.

In the car-to-end terminal crash FE simulations, the offset between vehicle mid-line and barrier was found to have the most prominent effect on occupant thigh injury risk. Similar trends were observed in a previous study [112] which was developed based on crash data. In the previous study, the leg injury risk (AIS 2+ and 3+) was observed to be higher in left-offset crashes than in frontal impact crashes while the other body-region injuries (arm, thorax, head) have a similar injury risk in all the crashes. Meanwhile, vehicle pre-impact velocity was observed to have the most influence on full-body, head, neck, and chest injuries. The positive relationship between vehicle velocity and full-body injury agreed with a previous study which was developed based on real-world fixed-object crashes [113]. In the previous study, a positive exponential relationship was found between speed limit and fatality rate. On the other hand, the relationship between vehicle velocity and body-region injuries was rarely evaluated. Although positive relationship was found between the change of velocity (del-v) and body-region injuries in several studies [114, 115], the effects of the pre-impact velocity to occupant risk in crashes with fixed-objects was evaluated quantitatively for the first time in the current study.

The injury assessed by vehicle-based crash severity metrics was observed to be more conservative than the ones determined by dummy-based injury criteria. Specifically, all the

dummy-based injury criteria values (Table D1) were observed to be under the FMVSS 208 limits whereas only a small proportion of the results pass either MASH or EN1317 criteria (5 of 20 crashes pass MASH criteria, 6 of 20 crashes pass EN1317 criteria). Similar difference was reported in previous studies [18, 19]. In particular, it was suggested that to account for the difference, ORA should be used to evaluate occupant risk during crashes with fixed-objects and the allowable limit of ORA longitudinal should be set as 31 g instead of 20.49 g [19]. In this study, the maximum ORA longitudinal was recorded as 25.30 g which is less than the suggested value. If the suggested limit was considered, the occupant injury risks evaluated from vehicle-based crash severity metrics and dummy-based injury criteria showed agreement.

The regression curve for OIV longitudinal and full-body injury probability showed good agreement with previously published EDRs data [86]. Therefore, the reliability of the numerical injury assessment method was verified. Both studies used logistic curves, which are a statistical model commonly used to predict injury probabilities [116, 117]. The discrepancies observed between the curves generated by our simulation results and EDR data may be caused by the different vehicle type used in each study: GM cars in the EDR study and a Toyota Yaris car model in the current work. In addition to showing similar trends compared to the real-world crash data, our current numerical approach has the advantage of being flexible in terms of choosing the crash conditions (e.g. velocity, angle, vehicle type, guardrail type) and having higher repeatability.

While the vehicle-based crash severity metrics have predictability for full-body injury risk, they have weak correlation to body-region injuries. This could be caused by the unconstrained occupant condition used in calculating the vehicle-based crash severity metrics, while the effects of seatbelt and airbags were considered in the dummy-based injury criteria. For example, the usage of airbags may decrease head and neck injury probability [118]. The U.S. criteria (OIV and ORA) were observed to correlate to only chest and thigh injuries. A stronger correlation was found between the European criteria (ASI and THIV) and injury probabilities because the ASI is correlated to all the body-region injuries. Meanwhile, it should be mentioned that ASI could not be used to make a precise prediction of head, neck, or thigh injuries because of the low R^2 [119]. Although chest injuries were considered to be unpredictable by the change of vehicle velocity in a previous study [17], our observations showed that chest injuries can be predicted by vehicle

responses (OIV longitudinal and ASI). In sum, this study showed that most of the body-region injuries (except chest injury) are not predictable by vehicle-based crash severity metrics but only by dummy-based injury criteria.

Other than the full-body injury probabilities presented in Sec. 5.3.2, P_{joint} was used by US New Car Assessment Program (NCAP) to estimate the occupant injury risk during 5-star rating crashes tests [120]. Therefore, the P_{joint} is also worth investigation. With similar statistical regressions performed, the OIV longitudinal, ORA longitudinal and THIV were observed to be poorly correlated to the P_{joint} because of high p-values (0.11, 0.14, and 0.06, respectively). Nonetheless, the ASI was observed to be a good predictor for the P_{joint} (p-value = 0.01). It indicated that P_{joint} is harder to be predicted comparing to the full-body injury probability. Therefore, studies focusing on the relationship between US NCAP criteria and vehicle-based metrics are needed in the future, which is out of the scope of this study.

Overall, the numerical evaluation method developed in this study has several advantages. It can be used for various impact conditions, and the detailed injury probabilities can be assessed on component levels. However, this study has several limitations and could be improved in the future. First, the crash conditions used in the simulations were simplified from real crashes. Only one vehicle and one end terminal model were used in the simulations which cannot stand for all the crashes. Other than the sedan vehicle considered in this study, a pickup truck (2270 kg) could also be employed in the MASH tests. Meanwhile, the pre-impact velocity was selected from 65 to 120 km/h in the simulations because they are in the range of the speed limits used along U.S. roads. The crashes with a low impact speed were not studied although they may occur [121]. Second, a Hybrid III dummy model was used in all vehicle-to-end terminal FE simulations in this study. The dummy-based occupant injuries were estimated based on the FMVSS 208 injury criteria which is developed for frontal barrier impact. For the dummy involved in a crash with a guardrail end terminal, especially the oblique crashes, the maximum allowable values may vary somewhat from the FMVSS208 thresholds. In this study, the FMVSS 208 criteria were used because there is no direct criterion established for the occupant injury in crashes with a guardrail end terminal. The FMVSS 208 was considered to be acceptable in this study since the maximum allowable values were developed for the Hybrid III M50 dummy specifically [99, 100]. Another

limitation of this study is that the dummy model was assigned to drive seat only while the passengers may face a different risk in the crashes.

The numerical model presented in this study is the first step in evaluating occupant injuries in crashes with guardrail end terminals, which can support the current evaluation methods based on crash tests. In the future, other guardrail models, other vehicle models, and/or the dummy models assigned to different positions may be incorporated into the current simulations. Pickup truck models, especially the ones that conform to the MASH requirements, are recommended to be used in the future. Considering a wider range of velocities, offsets, and/or angles may help investigate the influences of pre-impact conditions to the occupant injuries. Additional improvements to this study may be the acceptance of other dummy-based injury criteria parameters (thoracic trauma index, combined thoracic index, pelvic acceleration, etc.), which can assist occupant injury assessments [122, 123]. Meanwhile, an EDR study focusing on vehicle-to-fixed object crashes is recommended to be performed in the future. With more data provided, the simulations would be better validated, the dummy injury probabilities would be better predicted, and the safety performance of vehicle and roadside safety hardware would be better evaluated.

5.5 Conclusion

Car-to-end terminal crash FE simulations involving a dummy model were performed for the first time in this study. The driver injury risks during a crash with ET-Plus were evaluated on both full-body and component levels. The pre-impact velocity was observed to influence the driver injuries the most. Statistical analysis was performed to compare the vehicle-based crash severity metrics and dummy-based injury criteria based on 20 crash simulations. The ASI was identified as the best vehicle-based severity metric, which is correlated to all the injuries probabilities. The results pointed out the limitations of the current vehicle-based injury prediction methods, which are accepted by MASH or EN1317, that head, neck, and thigh injuries cannot be predicted. The numerical dummy-based injury assessment methodology was recommended to be added to the current injury evaluation methods. The models could also supplement the development of new crash tests with various impact conditions and the optimization of the design of guardrail end terminals.

6. Injury assessment using GHBMC occupant model during car-to-end terminal crashes

The content of this section was submitted on June 22, 2022 to *Accident Analysis & Prevention*

6.1 Introduction

A total of 8,603 fatalities were caused by fixed-object crashes in 2020 in U.S. which represent 22% of total traffic fatalities and increased by 14% last decade (7,529 fatalities recorded in 2010) [124]. Guardrails were developed to reduce the impact severity of the roadway departure crashes. In U.S and Europe, the guardrail end terminals safety performance are currently assessed according to either the Manual for Assessing Safety Hardware (MASH) guideline [5] or the EN1317 guideline [108]. In both guidelines, the crash severity is evaluated in full-scale crash tests based on vehicle-based metrics, developed based on vehicular velocities and accelerations. While test data recorded by Anthropomorphic Test Devices (ATDs, also known as crash dummies) are used to evaluate the occupant injury risks under varied impact conditions such as: frontal impact [125, 126], rear impact [127], and side impact [125, 128], no ATD data are available in the guardrail tests.

Computational simulations are currently performed to analyze vehicles' and occupants' dynamic performance during a crash [129]. In these simulations, ATD models and human body models are widely-used to assess the occupant injury risks [26, 27]. Especially, human body models could provide detail local load/stress distributions, and consequently predict the risk of injuries on various human body-regions [130]. However, the use of human body models in the simulations of vehicle to guardrail end terminal crashes were not reported in literature.

In this study, for the first time, a human body FE model is used in the simulations of car-to-end terminal crashes to assess risk of occupant injuries and to develop a better understanding of injury mechanisms. The effects of impact velocity, angle, and offsets on occupant injury risks were also evaluated using both the vehicle-based severity metrics[5, 108] and ATD biomechanics injury measures [131]. Then, the correlation between vehicle-based metrics and occupant injury risks were investigated as well.

6.2 Method

To perform vehicle-to-end terminal crash simulations, a Global Human Body Models Consortium (GHBMC) occupant model, a Toyota Yaris model, and an ET-Plus model were integrated in LS-DYNA software (Ansys, Canonsburg, PA). The geometry of the GHBMC model (M50-OS, version2-2) was based on the data measured from a 50th percentile male volunteer (174 cm in height and 79 kg in weight) [132, 133]. The model was validated in body-region and full-body levels under various impact conditions, such as frontal impact and lateral impact, and was observed to have capabilities to assess occupant injury risks [134-137]. A Toyota Yaris (model year 2010) model was used in all the crash simulations since it corresponds to the sedan vehicle 1100C used in the MASH tests [138]. Meanwhile, an ET-Plus model was used in this study since it is the most common energy-absorbing guardrail end terminal used in U.S [139]. All these models were validated and had good capabilities to predict their kinetic and kinematic during the crash simulations [87, 134, 138, 139].

A simulation was initially performed to position the GHBMC model onto the driver seat (Figure 6-1). A contact between GHBMC outer surface and vehicle interior surfaces (seat and floor surfaces) were defined, and then the human body model was dropped by gravity until it settles into the seat model. At the end of each settle simulation, the deformed geometries and corresponding strains were exported using a “dynain” file in the software LS-DYNA, and then were used as the initial conditions in the crash simulations. A seatbelt model was also developed and routed around the positioned GHBMC model [140].

Figure 6-1 GHBMC model seated in driver position

Design of Experiments (DOE) is a useful tool to investigate the effects of inputs on the outputs of a system [141]. The inputs of this study include the pre-impact velocity, impact angle, and impact offset. Pre-impact velocity, assigned on the vehicle model, range from 65 to 120 km/h (Figure 6-2) and includes the pre-impact velocity used in the MASH tests (100 km/h) [5]. Two impact angles (0° and 15°) and two impact offset (0 and ¼) were used in the simulations (Figure 2). The impact angle was measured between the midline of the vehicle and the midline of the guardrail model. The offset was defined as the percentage of the vehicle width between these midlines. Overall, a total of 20 vehicle-to-end terminal crash simulations (5 velocities, 2 offsets, 2 angles) were performed in this study.

a) impact angle = 0°; no offset

b) impact angle = 0°; offset = ¼ of vehicle width
Same as MASH test 30

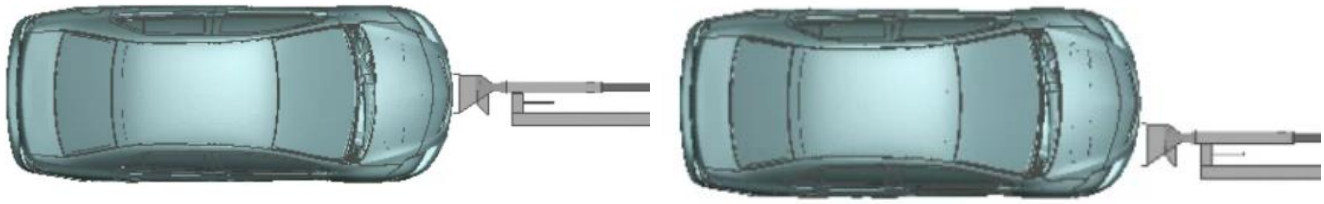

c) impact angle = 15°; no offset
Same as MASH test 32

d) impact angle = 15°; offset = ¼ of vehicle width

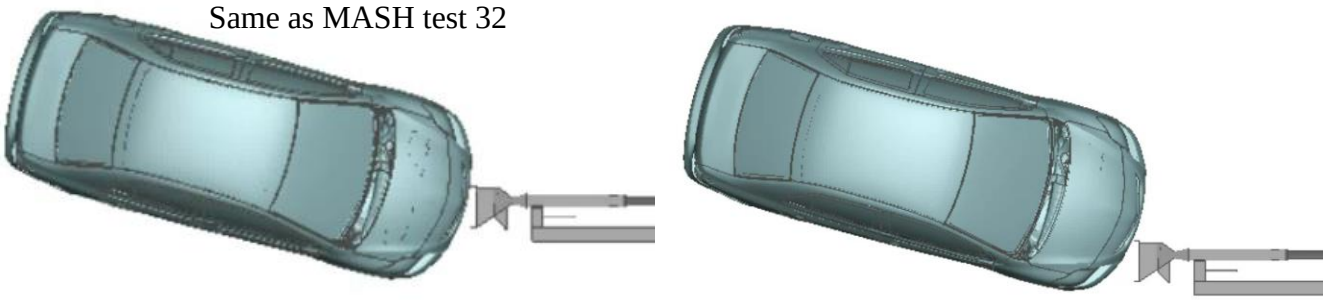

Figure 6-2 Setup of vehicle-to-end terminal crash simulations

Note: Pre-impact velocities of 65, 80, 100, 112, 120 km/h were assigned for each scenario

The kinetics and kinematics of GHBMC model were recorded to assess driver injury risk on both body-region and full-body levels. The GHBMC recorded responses include head accelerations and angular velocities, neck force and moment, chest deflection, and femur loads. Injury measures were calculated for each body region: head (HIC_{15}) , brain (BrIC), neck (Nij, N_t, and N_c), chest (CD), thigh (F_F), and leg (F_{UT}, F_{LT}, and RTI) (Table 6-1) [142, 143]. The injury risks were then assessed based on each injury measure using well-defined injury probabilities (Table I1) [103, 144-146]. To make the full-body injury risk (OIM) comparable to the previously-published dummy results [131], the OIM was defined as the accumulation of head, neck, chest and thigh injury risk.

Table 6-1 GHBMC Injury measures [142, 143]

Body region	Injury measure	Values associated to 25% percentage injury risk	Values associated to 50% percentage injury risk
Head	Head injury criteria (HIC_{15})	1047	1724
Brain	Brain injury criteria (BrIC)	0.8	1.0
Neck	Neck injury criteria (Nij)	1.1	1.6
	Neck tension force (N_t)	4.2 kN	4.6 kN
	Neck compression force (N_c)	4.2 kN	4.6 kN
Chest	Chest deflection (CD)	49.1 mm	62.3 mm
Thigh	Femur force (F_F)	11.9 kN	15.3 kN
Leg	Upper tibia force (F_{UT})	5.9 kN	7.3 kN
	Lower tibia force (F_{LT})	5.2 kN	6.8 kN
	Revised tibia index (RTI)	1.0	1.2

Meanwhile, vehicle-based severity metrics were recorded and calculated based on the U.S and Europe guidelines. Specifically, Occupant injury velocity (OIV) and Occupant Ridedown Acceleration (ORA), Acceleration Severity Index (ASI), and Theoretical Head Impact Velocity (THIV) were calculated [5, 108, 131]. The correlation between vehicle-based severity metrics and model-based body injury probabilities was investigate using JMP software (SAS, Cary NC).

6.3 Results

The vehicle models were smoothly redirected after the impact and no rollover events were recorded in all 20 car-to-end terminal crash simulations. Seatbelt and airbag models worked properly, so no impact between head and vehicle headliner was observed. The GHBMC occupant performances can be roughly classified into two types, depending on the occurrence of an occupant-vehicle interior impact. For the simulation without occupant-vehicle interior impact, the occupant model was observed to move forward, hit the airbag and rebound (Figure 6-3a). In

other simulations, the occupant model also hit the airbag first, then it hit either the windshield, the window, or the headrest model (Figure 6-3b-d).

GHBMC kinematics data were recorded in each body region. High amount of variabilities were observed in head acceleration (74 ± 45g), and femur force (0.7 ± 0.3 kN) while the head angular velocity, neck force, chest deflection, and tibia forces spread in relative small ranges (Table 6-2).

Table 6-2 GHBMC kinematics data recorded in the simulations

Pre-impact conditions			GHBMC kinematics data (Max. value)						
Velocity (km/h)	Offset	Angle (°)	a_{res} (g)	ω_{res} (rad/s)	N_t /N_c (kN)	CD (mm)	F_F (kN)	F_{UT} (kN)	F_{LT} (kN)
65	1/4	0	25	26	0.7	25	0.4	2.0	3.1
65	1/4	15	66	31	0.9	26	0.5	1.5	2.8
65	0	0	47	37	1.3	34	0.4	1.5	2.5
65	0	15	56	33	1.2	31	0.4	1.6	2.5
80	1/4	0	41	32	1.2	37	0.5	2.1	2.9
80	1/4	15	81	40	1.1	33	0.8	1.3	2.4
80	0	0	50	40	1.4	43	0.5	1.9	2.5
80	0	15	54	32	0.9	28	0.5	2.2	3.0
100	1/4	0	50	38	1.5	31	1.0	2.4	3.7
100	1/4	15	83	39	1.3	35	0.8	2.0	3.3
100	0	0	53	37	1.6	36	0.6	2.7	4.6
100	0	15	54	37	1.1	38	0.6	3.0	5.0
112	1/4	0	203	30	1.3	35	0.7	2.6	3.5
112	1/4	15	85	38	1.1	36	0.6	1.8	3.3
112	0	0	64	30	1.4	47	0.9	3.1	5.3
112	0	15	46	35	0.8	39	0.8	3.6	5.4
120	1/4	0	200	31	1.3	46	0.7	2.3	3.6
120	1/4	15	94	37	1.0	42	0.7	3.5	4.8
120	0	0	59	37	0.9	45	1.8	3.2	5.1
120	0	15	76	30	1.1	45	0.9	3.2	5.7
Average			74	35	1.2	37	0.7	2.4	3.8
Standard Deviation			45	4	0.2	6	0.3	0.7	1.1

Note: a_{res}: head resultant acceleration; ω_{res}: head angular velocity; N_t /N_c: Neck tension/ compression force; CD: chest deflection; F_F: femur force; F_{UT}: upper tibia force; F_{LT}: lower tibia force

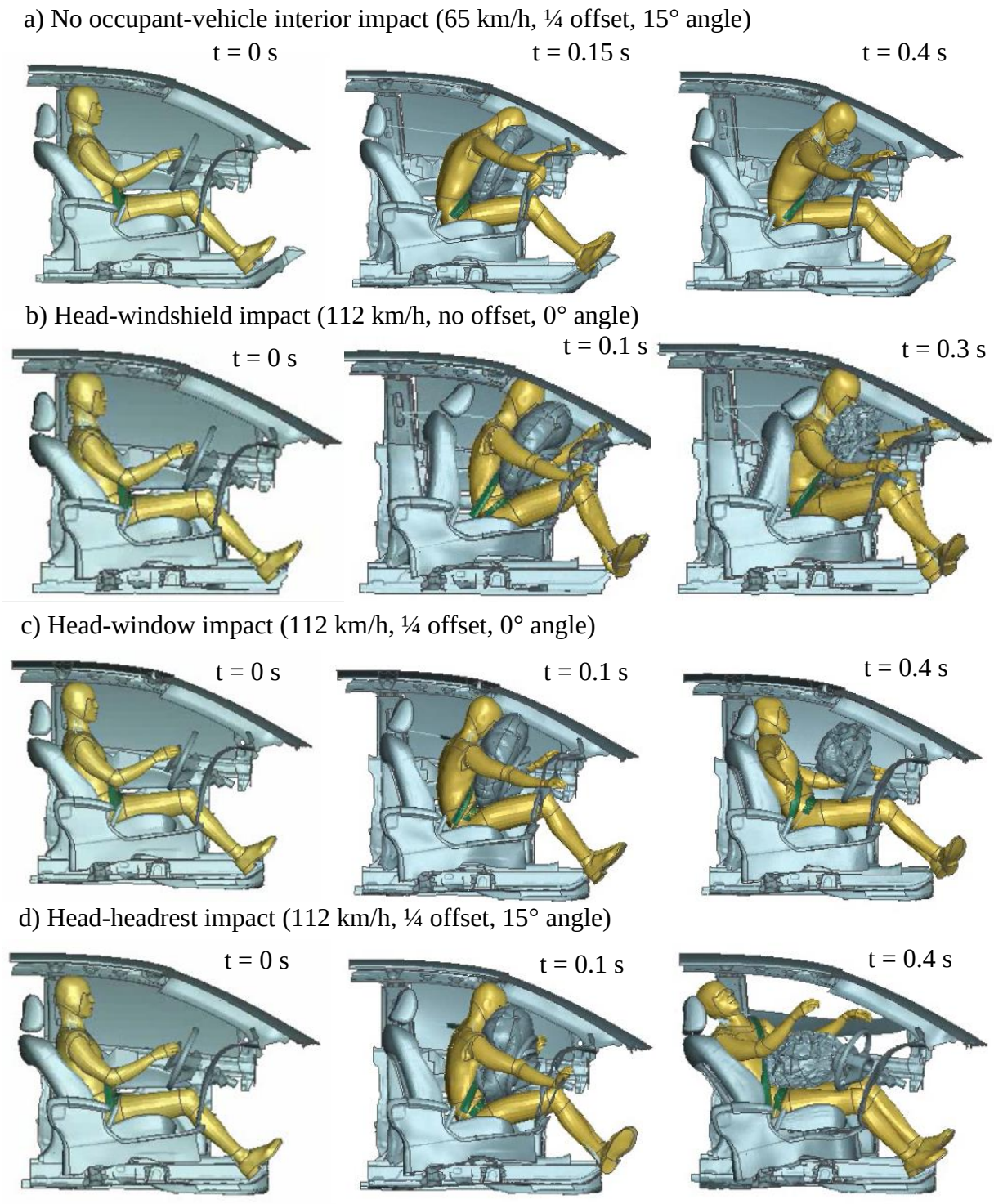

Figure 6-3 GHBMC performances during crash simulations

The effects of the pre-impact conditions on each injury measures were assessed using the Correlation Metrix. The values of maximum femur load (F_F < 1.8 kN) were much lower than the

corresponding values of 25% injury risks (11.9 kN), so F_F was removed from the correlation analysis. Positive correlations were observed between pre-impact velocity and all the body-region injury risks (Table 6-3). Therefore, a higher pre-impact velocity would increase all the body-region injury risks. In a crash with a larger offset, the occupant may face higher head, brain, and neck injury risks (increased HIC15, BrIC, and Nij). Meanwhile, the BrIC and lower tibia force had positive correlations with pre-impact angles.

Table 6-3 Correlations between pre-impact conditions and injury measures

		GHBMC injury measures								
		HIC36	HIC15	BrIC	Nij	Nt	Nc	CD	FUT	FLT
Pre-impact conditions	Velocity	0.53	0.56	0.17	0.09	0.09	0.22	0.74	0.77	0.77
	Offset	-0.07	0.36	0.44	0.09	-0.09	-0.18	-0.31	-0.33	-0.38
	Angle	-0.46	-0.18	0.56	-0.43	-0.45	-0.15	-0.2	-0.01	0.06

Vehicle-based crash severity metrics were then assessed based on the equations shown in Table I1. Only 3 simulations passed all the MASH criteria (OIV < 12.2 and ORA < 20.49). Among all the cases, 15 simulations had a OIVx exceeded the MASH threshold, and 6 simulations were observed to have a large ORAx (Table 6-4). Meanwhile, all the 15 simulations which have a high OIV were observed to fail the THIV criteria indicated that the thresholds used in the U.S (OIV) and Europe (THIV) guidelines showed good agreements.

Table 6-4 Injury probabilities and vehicle-based crash severity metrics from the simulations

Pre-impact conditions			Injury probabilities assessed by GHBMC kinematics data					Vehicle-based crash severity metrics					
Velocity (km/h)	Offset	Angle (°)	Head	Neck	Chest	Thigh	Full-body	OIVx (m/s)	OIVy (m/s)	ORAx (g)	ORAy (g)	ASI	THIV (km/h)
65	1/4	0	0.00%	5.44%	2.54%	0.79%	8.56%	10.5	0.4	12.16	6.18	1.0	38
65	1/4	15	0.05%	5.86%	2.89%	0.80%	9.36%	10.9	0.9	3.60	6.84	1.0	40

65	0	0	0.19%	6.77%	7.05%	0.78%	14.18%	**12.5**	0.6	17.07	3.37	1.4	**45**
65	0	15	0.23%	6.95%	5.13%	0.77%	12.60%	**13.0**	2.2	7.04	4.82	1.6	**48**
80	1/4	0	0.05%	7.27%	9.27%	0.80%	16.58%	**12.5**	0.6	11.86	4.05	1.4	**45**
80	1/4	15	1.25%	6.49%	6.55%	0.89%	14.47%	10.7	2.3	4.32	6.18	1.3	39
80	0	0	0.36%	6.84%	15.76%	0.80%	22.43%	**12.6**	0.3	14.93	2.98	1.5	**45**
80	0	15	0.15%	6.16%	3.58%	0.80%	10.38%	**12.3**	2.9	10.61	4.78	1.4	**45**
100	1/4	0	0.26%	8.02%	5.47%	0.94%	14.09%	11.9	0.1	**21.46**	10.15	1.3	43
100	1/4	15	1.35%	7.16%	7.58%	0.87%	16.09%	**12.4**	3.0	6.89	9.56	1.6	**47**
100	0	0	0.76%	7.75%	8.54%	0.83%	16.97%	**13.2**	0.0	**29.59**	8.82	1.8	**47**
100	0	15	0.06%	6.85%	10.55%	0.82%	17.41%	**13.6**	3.2	11.11	7.21	1.6	**50**
112	1/4	0	9.26%	7.31%	7.64%	0.86%	22.98%	11.8	0.4	**23.47**	10.73	1.5	42
112	1/4	15	1.84%	5.90%	8.75%	0.84%	16.43%	**13.6**	1.6	9.37	14.93	1.8	**49**
112	0	0	1.30%	6.64%	20.97%	0.91%	27.85%	**14.8**	1.0	**28.51**	8.35	2.0	**53**
112	0	15	0.00%	5.77%	10.93%	0.90%	16.82%	**13.3**	2.5	6.19	4.75	1.9	**50**
120	1/4	0	15.31%	7.54%	20.51%	0.85%	38.28%	**12.3**	0.0	**21.63**	9.50	1.6	**45**
120	1/4	15	3.68%	6.22%	14.51%	0.85%	23.43%	**14.5**	2.0	10.96	20.00	1.8	**53**
120	0	0	0.52%	5.99%	18.65%	1.22%	24.85%	**15.1**	0.6	**22.37**	6.80	2.1	**54**
120	0	15	0.54%	6.11%	19.22%	0.93%	25.27%	**13.0**	3.2	5.73	7.84	1.7	**48**
Avera			1.86%	6.65%	10.30%	0.86%	18.45%	12.7	1.4	13.94	7.89	1.6	46
Limits								12.2	12.2	20.49	20.49	1.9	44

Note: 1. OIVx/ORAx: OIV/ORA longitudinal; OIVy/ORAy: OIV/ORA lateral

2. Bold numbers are the ones exceed the limits.

To quantify the contributions of the pre-impact conditions on the injury risks, Sobol' indices were calculated for body-region and full-body injury probabilities (Figure 6-4). Overall, the pre-impact velocity had the highest influence for the change in almost all the injury probabilities (except brain and neck). The pre-impact angle had the highest influence on the neck injuries (88% and 92% for the injury risks predicted by Nij and Nt, correspondingly). The brain injuries were mainly affected by pre-impact offset (50%) and angle (49%). Overall, the OIM were affected by velocity, offset, and angles by 90.5%, 0.3%, and 9.1%.

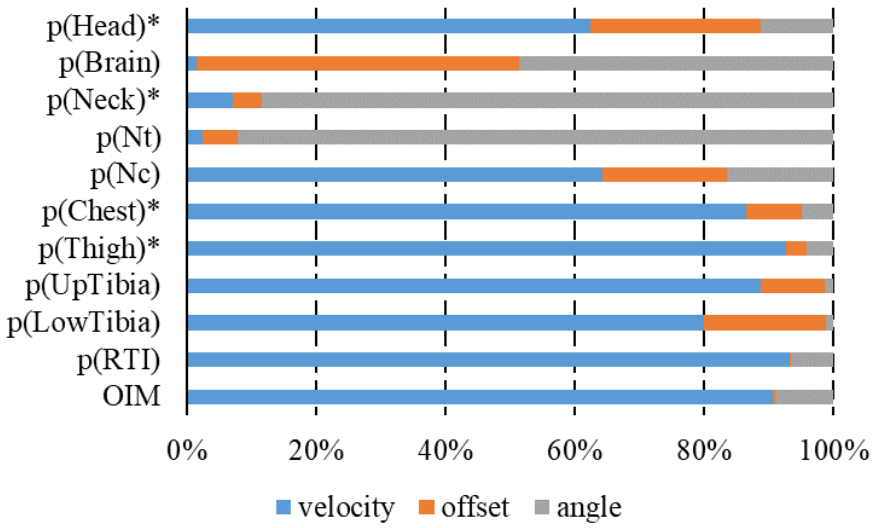

Figure 6-4 The influence of the pre-impact velocity, offset, and angles to GHBMC injury risks

Note: The injuries with * were used to calculate the OIM

The assessed full-body and body-region injury risks were regressed to each vehicle-based injury metrics using the non-linear regression (Eqn. 6-1). A univariance logistic regression was performed was performed in software JMP, where the vehicle metrics was defined as the independent variable and the injury risk (either body-region or full-body level) was defined as response variable [147-149].

$$Injury\ risk = \frac{1}{1+e^{-a\cdot(Vechile\ metrics-b)}} \tag{6-1}$$

Several regressed curves (e.g. OIVx vs. neck injury) had a negative *a*, which indicated that the injury risks was decreased while the vehicle metrics was increased. These curves were considered as unrealistic and were marked as NA in Table 6-5. The p-value of *a* was used to evaluate the correlation between vehicle-based injury criteria and biomechanics injury risks. A p-value less than 0.05 was considered as good correlation (Figure 6-5). Overall, all the vehicle-

based severity metrics had good correlations to full-body injury risks (Table 6-5). In terms of body-region injury risks, the OIVx, ASI, and THIV had good correlations to chest, thigh, up tibia, and lower tibia injuries. Meanwhile, the ORAx was observed to have a good correlation to the neck injury which was assessed based on Nij. A certain trend toward significance was observed between ORAx and chest injury risk (p-value = 0.09).

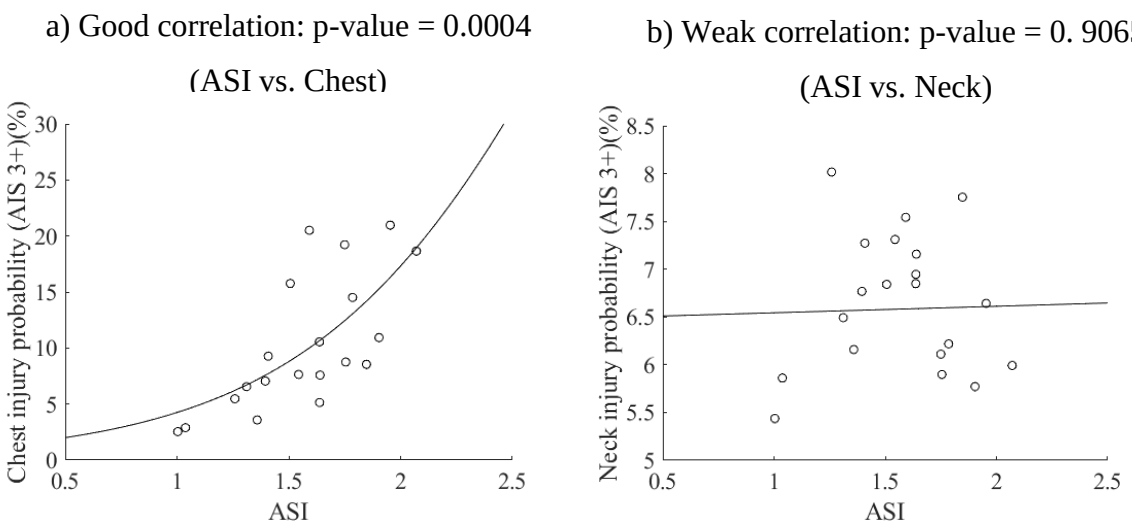

Figure 6-5 A comparison of good and weak correlations

Table 6-5 Correlations of vehicle-based injury criteria with the injury probabilities assessed by biomechanics injury measures

Vehicle-based severity metrics	Injury probabilities assessed by dummy-based criteria	*a*	*b*	p-value of *a*
OIVx (m/s)	Full-body	0.1785	21.1259	**0.0270**
	Head	0.0060	652.4542	0.9864
	Brain	0.0005	2656.9751	0.9976
	Neck	NA		
	Nt	NA		
	Chest	0.3326	19.4109	**0.0004**
	Thigh	0.0466	114.4755	**0.0140**
	Up Tibia	0.3106	25.2846	**0.0002**

	Low Tibia	0.4057	17.5057	**0.0004**
ORAx	Full-body	0.0265	70.4749	**0.0252**
	Head	0.0559	85.8150	0.2781
	Brain	NA		
	Neck	0.0074	369.4307	**0.0080**
	Nt	NA		
	Chest	0.0279	92.1987	0.0903
	Thigh	0.0041	1172.1495	0.1969
	Up Tibia	0.0110	362.5655	0.5081
	Low Tibia	0.0184	115.3702	0.3886
ASI	Full-body	0.9181	3.2082	**0.0082**
	Head	0.3900	11.7451	0.8233
	Brain	NA		
	Neck	0.0111	240.5456	0.9065
	Nt	0.0336	180.0736	0.9464
	Chest	1.5520	3.0073	**0.0004**
	Thigh	0.2249	22.6714	**0.0050**
	Up Tibia	1.5463	4.1082	**0.0001**
	Low Tibia	2.2394	2.4639	**<.0001**
THIV (km/h)	Full-body	0.0485	77.2233	**0.0323**
	Head	0.0011	3656.0774	0.9920
	Brain	NA		
	Neck	NA		
	Nt	0.0635	145.3980	0.1613
	Chest	0.0941	70.0119	**0.0005**
	Thigh	0.0125	427.3879	**0.0187**
	Up Tibia	0.0972	86.7020	**<.0001**
	Low Tibia	0.1245	62.1057	**<.0001**

Note: 1. Bold numbers are the ones less than 0.05 (good correlation)

2. Shaded body-region can be predicted by vehicle-based severity metrics

6.4 Discussion

Currently, the safety performances of end terminals in terms of the occupant injury risks are evaluated in standard crash tests based on the flail-space model in U.S. In this approach developed in early 1980s [5, 9], the occupant is assumed to be unbelted [9]. In last four decades, several occupant safety features (seatbelt, airbags, etc.) were installed in late vehicles [150], so there are concerns about the validity of the flail-space model in current impact conditions. In this study, FE simulations of vehicle-end terminal crashes involving belted human body model was performed for the first time.

In the vehicle-end terminal crashes, the pre-impact velocity was observed to have the largest effect to occupant injury risks. The positive correlation between velocity and full-body injury risk agreed with previous studies [86, 113, 114]. Based on police crash data, a positive correlation was observed between the speed limit and fatality rates [113]. Additionally, positive logistic correlations between delta-v and occupant injury risks were found for occupant injury risks at different severity levels [86, 114]. Meanwhile, positive correlations were observed between pre-impact offset and head, brain, and neck injury risks which may be caused by the higher probability of head-vehicle interior impact, especially with the window and the headrest models.

Regarding the injury prediction, all the vehicle-based metrics showed capability to predict the whole GHBMC full-body injury risk (OIM) while the ASI had the best performance (p-value as 0.0082). Meanwhile, the chest injury risk showed to be well predicted by the OIVx, ASI, and THIV, but not so well by ORAx ($p = 0.0903$). These correlations were also proved using dummy models in several previous studies [27, 131, 151]. Therefore, in the future, it is

recommended to employ ATDs in the certification tests of new end terminals, or at least to propose more advanced vehicle-based metrics into the current guidelines. A numerical simulation developed based on the current study could be used to validate these new vehicle-based metrics.

In the occupants involved in end terminal crashes, the brain and tibia injury risks were assessed numerically for the first time, and the neck injuries were assessed based not only Nij but on also axial forces. Therefore, more correlations between GHBMC and vehicle-based injury metrics were identified in this study comparing to the previously-published study using the Hybrid III dummy model [131].

Comparing the full-body injury regression curves between the GHBMC and the dummy study, agreements were observed in the OIV, ASI, and THIV although a difference was observed in ORA (Table 6-6). The dummy full body injury probability cannot be predicted by ORAx while a good correlation was observed in GHBMC. Meanwhile, comparing the identified regression curves, a lower *a* value was observed in the GHBMC ones which indicated that the predicted occupant injury risks grew slower in the human body model when the same vehicle-based metrics were used (Figure 6-6).

Table 6-6 Correlations of vehicle-based injury criteria with full-body injury risks assessed by biomechanics injury measures

Vehicle-based severity metrics	Occupant model	*a*	*b*	p-value of *a*	Correlation
OIVx (m/s)	GHBMC	0.1785	21.1259	**0.0270**	**Yes**
	Hybrid III	0.4918	16.4192	**0.0361**	**Yes**

ORAx	GHBMC	0.0265	70.4749	**0.0252**	**Yes**
	Hybrid III	0.0136	131.3400	0.5325	No
ASI	GHBMC	0.9181	3.2082	**0.0082**	**Yes**
	Hybrid III	2.1749	2.4338	**0.0165**	**Yes**
THIV (km/h)	GHBMC	0.0485	77.2233	**0.0323**	**Yes**
	Hybrid III	0.1247	60.7197	**0.0100**	**Yes**

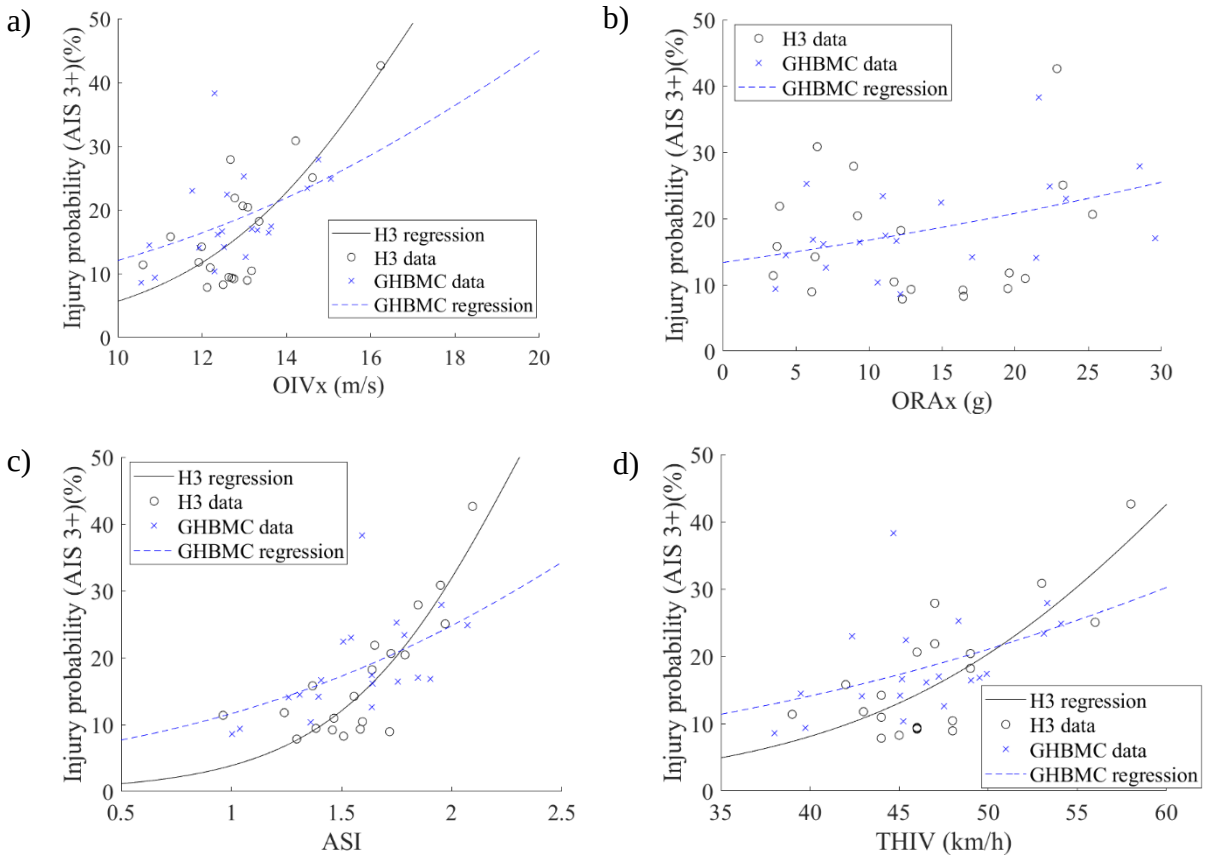

Figure 6-6 Correlations between vehicle-based metrics vs. Full body human/ATD injury probabilities: a) OIVx b) ORAx c) ASI d) THIV

This study had some limitations such that related to usage of only one end terminal model, and only one vehicle model. In future, models of a vehicle with light weight and/or pickup truck could be investigated based on current numerical approach as well. The current

scenarios were developed based on MASH guidelines (0 or 1/4 in offset, 0° or 15° in angle). Once the distributions of pre-impact conditions of the real-life crashes will be identified, the study could be repeated using a different DOE to better identify their contributors of the crash severity and occupant injury risks.

6.5 Conclusion

Twenty FE crash simulations involving end terminal, vehicle, and belted human body model was performed in this study. It was observed that current vehicle-based assessment methods, can predict full-body occupant injury risks and certain body-region injury risks while no head and brain injury can be predicted. Therefore, additional investigations are suggested for improving the current assessment guidelines of new end terminals. The numerical method developed in this study could help investigate the safety performance of new end terminals.

7. Summary

7.1 Conclusion

Guardrail end terminals are important to roadway safety, but limited research has been performed on them. The possibility of decrease of their performances in-service due to improper installation or minor damages due to impacts is unknown. This study investigated the performance of both non-damaged and damaged end terminals. Meanwhile, guardrail end terminal safety performance is currently evaluated in the U.S based on tests according to MASH guideline, in which the occupant is modelled as point mass based on a conservative assumption that the occupant is unrestrained during the crash. This study aimed to fill these knowledge gaps and had innovations as follow:

(1) **An energy-absorbing guardrail end terminal FE model was developed and validated for the first time.** The developed model could evaluate the end terminal performance in crash situations that are impractical to the physical tests as well as the effects of various pre-impact conditions on device performance.

(2) **The distributions and the common damage patterns of in-service end terminals was investigated.** The distribution data summarized in the study offers preliminary information on the status and the damages of in-service guardrail end terminals. The effects of the damaged end terminals on both vehicle responses and occupant injury risk were evaluated using simulations. While all the previous studies focused on well-maintained guardrail end terminals, this study pointed for the first time to the performance evaluation of in-service end terminals.

(3) **The driver injury risks during a crash with ET-Plus was assessed on component level quantitatively for the first time.** DOE studies were performed to investigate the relationship between crash conditions and occupant injury probabilities. The pre-impact velocity was observed to influence the driver injuries the most in both dummy and GHBMC simulations.

(4) **The correlations between vehicle-based metrics and occupant injury probabilities were determined.** Statistical analysis was performed to compare the vehicle-based crash severity metrics and dummy-based injury criteria based on 20 crash simulations. The correlation between crash severity metrics and the component level injury probabilities were identified for the first time. The ASI was identified as the best vehicle-based severity metrics which is correlated to all dummy injury probabilities and most of the GHBMC injury probabilities.

7.2 Limitations and future work

In this study, a FE model was developed for an energy-absorbing guardrail end terminal which is commonly used along U.S. roads. The whole FE model was validated, and it showed robustness in various crash simulations. However, several limitations should be acknowledged as follows:

First, the end terminal model was only validated under sedan-to-ET-Plus crash conditions. More investigations and validations were recommended to be performed in future studies, especially with a larger vehicle (e.g. SUVs and pickup trucks).

Second, the distributions of the damaged end terminals were investigated based on 1,000 selected cases in six states. While differences in damage patterns were observed in various states, it was recommended to include more samples, especially from uninvestigated areas, in future studies.

Third, all the damaged ET-Plus models were evaluated under the NCHRP test 3-30 scenarios. The performance of these models could be further investigated under various conditions. For example, different vehicles, velocities, angles, and impact locations could be incorporated to current simulations.

Fourth, only driver injury risks were assessed in the crash simulations with a dummy/human body model. A passenger model was recommended to be added in future crash simulations since it may face a different injury risk in the crashes.

7.3 Publications and copyright

The following journal papers and conference proceedings were written as part of this work.

1.Meng, Y., Hu, W., & Untaroiu, C. (2019). Finite Element modeling of an energy-absorbing guardrail end terminal. *SAE International Journal of Commercial Vehicles* 12 (02-12-04-0021), 271-280. The copyright license is in Appendix K

2. Meng, Y., Hu, W., & Untaroiu, C. (2020). An examination of the performance of damaged energy-absorbing end terminals. *Accident Analysis & Prevention*,147, 105789. No copyright required to republish the contents in dissertation, details are shown in Appendix J

3. Meng, Y., Untaroiu, C. (2020). Numerical investigation of occupant injury risks in car-to-end terminal crashes using dummy-based injury criteria and vehicle-based crash severity metrics. *Accident Analysis & Prevention*, 145, 105700. No copyright required to republish the contents in dissertation, details are shown in Appendix J

4. Meng, Y., Untaroiu, C. Numerical Investigation of Driver Injury Risks in Car-to-End Terminal Crashes using a Human Finite Element Model. Submitted to *Transportation Engineering* on July 9th , 2022

5. Meng, Y., & Untaroiu, C. Occupant Injury Risk Assessment during a Car–to-End Terminal Crash under Crash Test Conditions and Extended Scenarios. *16th International LS-DYNA Conference*, 2020 Jun 10-11; Virtual

6. Meng, Y., & Untaroiu, C. Development and Validation of a Finite Element Model of an Energy-absorbing Guardrail End Terminal. *15th international LS-DYNA user conference;* 2018 Jun 10-12; Detroit, MI

7. Meng, Y., & Untaroiu, C. Investigation of Energy-absorbing Guardrail End Terminals along U.S. Roads: Statistics and a Computer Modeling Study. *2018 AAAM Student Symposium*; 2018 Oct 7; Nashville, TN

7. Meng, Y., & Untaroiu, C. Development and validation of a Finite Element model for an energy-absorbing guardrail end terminal. *2018 BMES annual meeting*; 2018 Oct 17-20; Atlanta, GA

The following journal papers were also published during my Ph. D.

1. Meng, Y., Yates, K., & Untaroiu, C. (2022). Effects of rear seat design on occupant injury risk during frontal crashes: A parametric study using Finite Element Analysis. Mechanics Based Design of Structures and Machines, (accepted with minor revision)

2. Meng, Y., Yates, K., & Untaroiu, C. (2022). Numerical Investigation of the Performance of Current Vehicle Rear Seats Using Finite Element Analysis. SAE International Journal of Transportation Safety, 10(2):2022.

3. Jin, H., Sharma, R., Meng, Y., Untaroiu, A., Doerzaph, Z., Dobrovolny, C., & Untaroiu, C. (2020). Evaluation of the injury risks of truck occupants involved in a crash as a result of errant truck platoons. SAE International Journal of Transportation Safety, 8(09-08-01-0001), 5-18.

4. Pak, W., Meng, Y., Schap, J., Koya, B., Gayzik, F. S., & Untaroiu, C. (2020). Development and validation of a finite element model of a small female pedestrian. Computer Methods in Biomechanics and Biomedical Engineering, 1-11.

5. Pak, W., Meng, Y., Schap, J., Koya, B., Gayzik, F. S., & Untaroiu, C. (2019). Finite element model of a high-stature male pedestrian for simulating car-to-pedestrian collisions. International Journal of Automotive Technology, 20(3), 445-453.

6. Meng, Y., Untaroiu, C. (2018). A Review of Pediatric Lower Extremity Data for Pedestrian Numerical Modeling: Injury Epidemiology, Anatomy, Anthropometry, Structural, and Mechanical Properties. Applied Bionics and Biomechanics, 2018.

7. Untaroiu, C., Pak, W., Meng, Y., Schap, J., Koya, B., & Gayzik, F. S. (2018). A Finite Element Model of a Midsize Male for Simulating Pedestrian Accidents. Journal of Biomechanical Engineering, 140(1), 011003.

References

1. IIHS, *Fatality Facts 2020 Collisions with fixed objects and animals.* Arlington, VA, 2022.
2. Johnson, N.S. and H.C. Gabler, *Injury Risk in Frontal Crashes with Guardrail and Guardrail End Terminals.* 93rd Annual Meeting of The Transportation Research Board 2013.
3. Nadeau, G., *ET-Plus Guardrail End Terminal; Request for Information.* FHWA Docket No FHWA-2014-0039, 2014. **39**: p. 77595-77596.
4. Ross Jr, H.E., et al., *Recommended Procedures for the Safety Performance Evaluation of Highway Features.* National Cooperative Highway Research Program Report 350, 1993.
5. AASHTO, *Manual for assessing safety hardware (MASH).* Washington, DC, 2009.
6. Welborn, C. *MASH Guardrail Implementation and Design*. in *MDT Preconstruction Conference*. 2018. Montana.
7. National Academies of Sciences, E. and Medicine, *In-service Performance Evaluation of Guardrail End Treatments*. 2018: National Academies Press.
8. Joint AASHTO-FHWA Task Force on Guardrail Terminal Crash Analysis. *Safety analysis of extruding W-Beam guardrail terminal crashes*. 2015 [cited 2020 Apr. 8].
9. Michie, J.D., *Collision Risk Assessment Based on Occupant Flail Space Model*. 1981: The Institute.
10. Hollowell, W.T., et al., *Review of potential test procedures for FMVSS No. 208.* National Highway Traffic Safety Administration, 1998.
11. IIHS, *Moderate Overlap Frontal Crashworthiness Evaluation Crash Test Protocol (Version XVII).* Arlington, VA, 2016.
12. Saunders, J., M. Craig, and D. Parent, *Moving deformable barrier test procedure for evaluating small overlap/oblique crashes.* SAE International Journal of Commercial Vehicles, 2012. **5**(2012-01-0577): p. 172-195.
13. Gabauer, D. and H.C. Gabler, *Methodology to evaluate the flail space model by using event data recorder technology.* Transportation research record, 2004. **1890**(1): p. 49-57.
14. NHTSA, *Seat Belt Use in 2019—Overall Results*, in *Traffic Safety Facts - Research Note*. 2019, National Highway Traffic Safety Administration: National Highway Traffic Safety Administration.
15. Council, F.M. and J.R. Stewart, *Attempt to define relationship between forces to crash-test vehicles and occupant injury in similar real-world crashes.* Transportation Research Record, 1993. **1419**: p. 78-85.
16. Ray, M.H., J.D. Michie, and M. Hargrave, *Events that produce occupant injury in longitudinal barrier accidents.* Transportation Research Record, 1986. **1065**: p. 19-30.
17. Hinch, J., et al., *Impact attenuators: a current engineering evaluation.* Transportation Research Record, 1988. **1198**: p. 76-89.
18. Schulz, N., et al., *A Base Study to Investigate Mash Conservativeness of Occupant Risk Evaluation.* ASCE-ASME J Risk and Uncert in Engrg Sys Part B Mech Engrg, 2019.

19. Silvestri-Dobrovolny, C., et al. *A Base Study to Investigate MASH Conservativeness of Occupant Risk Evaluation*. in *ASME 2016 International Mechanical Engineering Congress and Exposition*. 2016. American Society of Mechanical Engineers Digital Collection.
20. Atahan, A.O., *Finite element simulation of a strong-post W-beam guardrail system.* Simulation, 2002. **78**(10): p. 587-599.
21. Whitworth, H., et al., *Finite element modeling of the crash performance of roadside barriers.* International Journal of Crashworthiness, 2004. **9**(1): p. 35-43.
22. Ray, M. and G. Patzner, *Finite-element model of modified eccentric loader terminal (MELT).* Transportation Research Record: Journal of the Transportation Research Board, 1997(1599): p. 11-21.
23. Reid, J.D. and D.L. Sicking, *Design and simulation of a sequential kinking guardrail terminal.* International journal of impact engineering, 1998. **21**(9): p. 761-772.
24. Dobrovolny, C.S., et al., *Implications of Truck Platoons for Roadside Hardware and Vehicle Safety.* 2019.
25. Jin, H., et al., *Evaluation of the Injury Risks of Truck Occupants Involved in a Crash as a Result of Errant Truck Platoons.* 2018.
26. Kirkpatrick, S.W., R. MacNeill, and R.T. Bocchieri. *Development of an LS-DYNA occupant model for use in crash analyses of roadside safety features*. in *Transportation Research Board 82nd Annual Meeting, Washington, DC, Jan*. 2003. Citeseer.
27. Li, N., et al., *A numerical study of occupant responses and injuries in vehicular crashes into roadside barriers based on finite element simulations.* Advances in Engineering Software, 2015. **90**: p. 22-40.
28. Seyedi, M., et al., *Experimental and Numerical Analysis of Injury Risk in Cutaway Bus Side Impact Test.*
29. Atahan, A.O. and M.M. Erdem, *Evaluation of 12 m long turned down guardrail end terminal using full-scale crash testing and simulation.* Latin American Journal of Solids and Structures, 2016. **13**(16): p. 3107-3125.
30. Sicking, D.L. and K.K. Mak, *Improving roadside safety by computer simulation.* Public Roads, 2001. **64**(4): p. 9-12.
31. Teng, T.-L., C.-C. Liang, and T.-T. Tran, *Development and validation of a finite element model for road safety barrier impact tests.* Simulation, 2016. **92**(6): p. 565-578.
32. Iwamoto, M., et al., *Development of a human body finite element model with multiple muscles and their controller for estimating occupant motions and impact responses in frontal crash situations*. 2012, SAE Technical Paper.
33. Kan, C.-D., et al., *Crashworthiness evaluation using integrated vehicle and occupant finite element models.* International journal of crashworthiness, 2001. **6**(3): p. 387-398.
34. Vavalle, N.A., et al., *Quantitative validation of a human body finite element model using rigid body impacts.* Annals of biomedical engineering, 2015. **43**(9): p. 2163-2174.
35. Insurance Institute for Highway Safety (IIHS). *Collisions with fixed objects and animals 2017*. 2018.
36. American Association of State Highway and Transportation Officals (AASHTO), *Manual for assessing safety hardware (MASH) Second Edition*. 2016.
37. Eigen, A.M. *In-Service Performance Evaluation Resources (ISPE) Federal Highway Administration Pilot In-Service Performance Evaluation of Guardrail End Treatments*. 2018.

38. Ferren, J., *Full-scale crash evaluations of the ET Plus end terminal with 4-inch wide guide channel installed with a rail height of 27 3/4 inches*. 2015.
39. Guo, J., et al., *Efficient modeling of panel-like structures in perforation simulations.* Computers & structures, 2003. **81**(1): p. 1-8.
40. Hallquist, J.O., *LS-DYNA theory manual.* Livermore software Technology corporation, 2006. **3**: p. 25-31.
41. Wright, A.E. and M.H. Ray, *Characterizing guardrail steel for LS-DYNA3D simulations.* Transportation research record, 1996. **1528**(1): p. 138-145.
42. Murray, Y.D., *Development of a wood material model for roadside safety applications.* Aptek Inc., Colorado Springs, 2003: p. 1-10.
43. Murray, Y.D., *Manual for LS-DYNA wood material model 143*. 2007, United States. Federal Highway Administration.
44. Wright, A. and M. Ray, *Characterizing guardrail steel for LS-DYNA3D simulations.* Transportation Research Record: Journal of the Transportation Research Board, 1996(1528): p. 138-145.
45. Oberg, E., F.D. Jones, and H.L. Horton, *Machinery's handbook: a reference book for the mechanical engineer, draftsman, toolmaker and machinist*. 1964: Industrial Press.
46. Opiela, K., S. Kan, and D. Marzougui, *Handbook of Development & Validation of a Finite Element Model for the 1997 Geo Metro Passenger Sedan.* 1997.
47. Ferren, J., *Full-scale crash evaluations of the ET Plus end terminal with 4-inch wide guide channel installed with a rail height of 31 inches*. 2015.
48. Martin, J.-L., *Relationship between crash rate and hourly traffic flow on interurban motorways.* Accident Analysis & Prevention, 2002. **34**(5): p. 619-629.
49. Renski, H., A. Khattak, and F. Council, *Effect of speed limit increases on crash injury severity: analysis of single-vehicle crashes on North Carolina interstate highways.* Transportation Research Record: Journal of the Transportation Research Board, 1999(1665): p. 100-108.
50. McKenzie, J. and J. Williams, *The dynamic behaviour of the head and cervical spine during 'whiplash'.* Journal of biomechanics, 1971. **4**(6): p. 477-490.
51. Atahan, A.O., et al., *Development of of a continuous motorcycle protection barrier system using computer simulation and full-scale crash testing.* Accident Analysis and Prevention, 2018. **116**: p. 103-115.
52. Untaroiu, C.D., et al., *Crash reconstruction of pedestrian accidents using optimization techniques.* International Journal of Impact Engineering, 2009. **36**(2): p. 210-219.
53. Meng, Y.Z., et al., *A finite element model of a six-year-old child for simulating pedestrian accidents.* Accident Analysis and Prevention, 2017. **98**: p. 206-213.
54. Zhou, C.H., et al., *Origami Crash Boxes Subjected to Dynamic Oblique Loading.* Journal of Applied Mechanics-Transactions of the Asme, 2017. **84**(9).
55. Zhou, C.H., et al., *Dynamic axial crushing of origami crash boxes.* International Journal of Mechanical Sciences, 2016. **118**: p. 1-12.
56. Zhou, C.H., Y. Zhou, and B. Wang, *Crashworthiness design for trapezoid origami crash boxes.* Thin-Walled Structures, 2017. **117**: p. 257-267.
57. Insurance Institute for Highway Safety (IIHS). *Collisions with fixed objects and animals 2017*. 2019; Available from: https://www.iihs.org/iihs/topics/t/roadway-and-environment/fatalityfacts/fixed-object-crashes/2017.

58. Trinity highway. *Make safety a priority*. 2018 [cited 2018 12/17/2018]; Available from: http://www.etplusfacts.com/Virginia.
59. Gabauer, D.J. and H.C. Gabler. *Differential rollover risk in vehicle-to-traffic barrier collisions*. in *Annals of Advances in Automotive Medicine/Annual Scientific Conference*. 2009. Association for the Advancement of Automotive Medicine.
60. National Cooperative Highway Research Program, *A guide for W-Beam guardrail damage assessment (draft): A field manual for highway maintenance personnel*. 2014.
61. Meng, Y. and C.D. Untaroiu, *Investigation of Energy-absorbing Guardrail End Terminals along U.S. Roads: Statistics and a Computer Modeling Study*, in *AAAM 2018 Student Symposium*. 2018: Nashville, TN.
62. Bruski, D., et al. *On the validation of the LS-DYNA Geo Metro numerical model*. in *MATEC Web of Conferences*. 2019. EDP Sciences.
63. Meng, Y., W. Hu, and C.D. Untaroiu, *Finite Element Modeling of an Energy-Absorbing Guardrail End Terminal.* SAE International Journal of Commercial Vehicles, 2019. **12**(02-12-04-0021).
64. National Academies of Sciences Engineering Medicine, *Procedures for Verification and Validation of Computer Simulations Used for Roadside Safety Applications*. 2011, Washington, DC: The National Academies Press. https://doi. org/10.17226 ….
65. Ray, M.H., et al., *Recommended procedures for verification and validation of computer simulations used for roadside safety applications.* Final Report , Project, 2008(22-24).
66. American Association of State Highway and Transportation Officials (AASHTO), *Manual for assessing safety hardware (MASH) Second edition*. 2016.
67. The National Crash Analysis Center (NCAC), *Development & Validation of a Finite Element Model for the 1997 Geo Metro Passenger Sedan*. 2008.
68. Mizuno, K., et al., *Optimization of vehicle deceleration to reduce occupant injury risks in frontal impact.* Traffic injury prevention, 2014. **15**(1): p. 48-55.
69. Ito, D., Y. Yokoi, and K. Mizuno, *Crash pulse optimization for occupant protection at various impact velocities.* Traffic injury prevention, 2015. **16**(3): p. 260-267.
70. Vitet, S. and H. Schebdat, *Safety Benefit Evaluation of Secondary Collision Mitigation Braking.* 25th International Technical Conference on the Enhanced Safety of Vehicles (ESV) National Highway Traffic Safety Administration, 2017.
71. Gabauer, D.J., *Secondary collisions following a traffic barrier impact: frequency, factors, and occupant risk.* Annals of Advances in Automotive Medicine/Annual Scientific Conference, 2010. **54**: p. 223.
72. Vaca, F.E., et al., *Crash injury prediction and vehicle damage reporting by paramedics.* Western journal of emergency medicine, 2009. **10**(2): p. 62.
73. Eigen, A.M. and D. Glassbrenner, *The relationship between occupant compartment deformation and occupant injury*. 2004.
74. Mak, K.K. and R.P. Bligh, *Assessment of NCHRP Report 350 test conditions.* Transportation Research Record: Journal of the Transportation Research Board, 2002. **1797**(1): p. 38-43.
75. Iwamoto, M., et al., *Development of a finite element model of the total human model for safety (THUMS) and application to injury reconstruction.* Proceedings of the international IRCOBI Conference, 2002.
76. Yue, N., J. Shin, and C.D. Untaroiu, *Development and validation of an occupant lower limb finite element model*. 2011, SAE Technical Paper.

77. Noureddine, A., A. Eskandarian, and K. Digges, *Computer modeling and validation of a Hybrid III dummy for crashworthiness simulation.* Mathematical and computer modelling, 2002. **35**(7-8): p. 885-893.
78. Untaroiu, C., et al. *Evaluation of a finite element model of the THOR-NT dummy in frontal crash environment*. in *Proceedings of 21st International Conference on Experimental Safety Vehicles (ESV)*. 2009.
79. Putnam, J.B., et al., *Validation and sensitivity analysis of a finite element model of THOR-NT ATD for injury prediction under vertical impact loading.* AHS International 69th Annual Forum, 2013: p. 38-47.
80. Cassatta, S., et al., *Advanced Restraint Systems (ARS) Final Report* 2013, NHTSA.
81. Adam, T. and C.D. Untaroiu, *Identification of occupant posture using a Bayesian classification methodology to reduce the risk of injury in a collision.* Transportation Research Part C-Emerging Technologies, 2011. **19**(6): p. 1078-1094.
82. Gabauer, D. and H.C. Gabler, *Review of Current Damage-Level Criteria for Longitudinal Barrier Repair.* Proceedings of the 87 th Annual Meeting of the Transportation Research Record, 2008.
83. Gabauer, D. and R. Thomson. *Correlation of vehicle and roadside crash test injury criteria*. in *19th International Technical Conference on the Enhanced Safety of Vehicles (ESV)-Washington DC June*. 2005.
84. Burbridge, A. and R. Troutbeck, *A model for predicting Acceleration Severity Index in impacts with road safety barriers.* International journal of crashworthiness, 2019. **24**(4): p. 442-452.
85. Gabauer, D. and H.C. Gabler, *Evaluation of threshold values of acceleration severity index by using event data recorder technology.* Transportation research record, 2005. **1904**(1): p. 37-45.
86. Gabauer, D.J. and H.C. Gabler, *Comparison of roadside crash injury metrics using event data recorders.* J Accident Analysis Prevention, 2008. **40**(2): p. 548-558.
87. Prodduturu, H.R., *Correlation between Roadside Safety Hardware and Vehicle Safety Standards Evaluation Criteria*. 2016.
88. Shojaati, M. *Correlation between injury risk and impact severity index ASI*. in *Proceedings of the 3rd Swiss Transport Research Conference*. 2003.
89. Tsoi, A.H. and H.C. Gabler, *Evaluation of vehicle-based crash severity metrics.* Traffic injury prevention, 2015. **16**(sup2): p. S132-S139.
90. Naish, D.A. and A. Burbridge, *Occupant severity prediction from simulation of small car impact with various concrete barrier profiles.* International journal of crashworthiness, 2015. **20**(5): p. 510-523.
91. Chell, J., et al., *Limitations of the European barrier crash testing regulation relating to occupant safety.* Accident Analysis & Prevention, 2019. **133**: p. 105239.
92. Anghileri, M., M. Luminari, and G. Williams, *ROBUST Project Deliverable D. 2.1. Analysis of test data from European laboratories*. 2005.
93. Marzougui, D., et al., *Extended validation of the finite element model for the 2010 Toyota Yaris Passenger Sedan.* National Crash Analysis Center, George Washington University, Washington, DC, Report No. NCAC 2012-W-005, 2012.
94. Opiela, K., S. Kan, and D.S. Marzougui, *Development & Validation of a Finite Element Model for the 2010 Toyota Yaris Passenger Sedan.* National Crash Analysis Center,

George Washington University, Washington, DC, Report No. NCAC 2011-T-001, 2011(NCAC 2011-T-001).
95. Guha, S. *Occupant modeling workshops & other learning aids*. 2010 [cited 2020 01/29]; Available from: http://www.lstc.com/training_workshops.
96. Masiá, J., B. Eixerés, and J. Dols, *Models for airbag simulation in vehicles adapted for disabled drivers.* Zaragoza, 2008.
97. Meng, Y., W. Hu, and C. Untaroiu, *Finite Element Modeling of an Energy-Absorbing Guardrail End Terminal.* SAE International Journal of Commercial Vehicles, 2019. **14**(4).
98. NHTSA, *Summary of State Speed Laws Twelfth Edition: Current as of October 8, 2012.* National Committee on Uniform Traffic Laws and Ordinances, 2013.
99. Nason, N., *Petition for Rulemaking Regarding Federal Motor Vehicle Safety Standard No. 208 (49 CFR 571.208) Occupant Crash Protection.* 2007.
100. Kuppa, S., J. Rupp, and L. Schneider, *Knee-Thigh-Hip Injuries and Knee/Femur compliance of the Hybrid III, Thor-Lx, and Human cadavers*. 2000, NHTSA.
101. Cassatta, S., et al., *Advanced Restraint Systems (ARS) Final Report*. 2013.
102. Gennarelli, T.A. and E. Wodzin, *AIS 2005: a contemporary injury scale.* Injury, 2006. **37**(12): p. 1083-1091.
103. Eppinger, R., et al., *Development of Improved Injury Criteria for the Assessment of Advanced Automotive Restraint Systems-II.* National Highway Traffic Safety Administration: Washington, 1999.
104. Sobol, I.M., *Sensitivity estimates for nonlinear mathematical models.* Mathematical modelling and computational experiments, 1993. **1**(4): p. 407-414.
105. Chan, K., A. Saltelli, and S. Tarantola. *Sensitivity analysis of model output: variance-based methods make the difference*. in *Proceedings of the 29th conference on Winter simulation*. 1997.
106. Stander, N., et al., *LS-OPT user's manual–a design optimization and probabilistic analysis tool for the engineering analyst.* Livermore Software Technology Corporation, Livermore, 2007.
107. Greenland, S., et al., *Statistical tests, P values, confidence intervals, and power: a guide to misinterpretations.* European journal of epidemiology, 2016. **31**(4): p. 337-350.
108. CEN, *Road restraint systems Part 1: Terminology and general criteria for test methods*. 2010, CEN–European Committee for standardization, Central Secretariat: rue de ….
109. CEN, *Road Restraint Systems Part 2: Performance Classes, Impact Test Acceptance Criteria and Test Methods for Safety Barriers Including Vehicle Parapets (EN 1317-2)*. 2010, European Committee for Standardization Brussels.
110. CEN, *Road restraint systems, part 7: Performance classes, impact test acceptance criteria and test methods for terminals of safety barriers*. 2012, CEN–European Committee for standardization, Central Secretariat: rue de ….
111. Abrate, S., *Impact engineering of composite structures*. Vol. 526. 2011: Springer Science & Business Media.
112. Stucki, S.L., W.T. Hollowell, and O. Fessahaie, *Determination of frontal offset test conditions based on crash data*. 1998: National Highway Traffic Safety Administration.
113. Doecke, S.D., et al., *Safe speed limits for a safe system: The relationship between speed limit and fatal crash rate for different crash types.* Traffic injury prevention, 2018. **19**(4): p. 404-408.

114. Gabauer, D.J. and H.C. Gabler. *Comparison of delta-v and occupant impact velocity crash severity metrics using event data recorders*. in *Annual proceedings/association for the advancement of automotive medicine*. 2006. Association for the Advancement of Automotive Medicine.
115. Weaver, A.A., et al., *Estimated injury risk for specific injuries and body regions in frontal motor vehicle crashes.* Traffic injury prevention, 2015. **16**(sup1): p. S108-S116.
116. Hosmer Jr, D.W., S. Lemeshow, and R.X. Sturdivant, *Applied logistic regression*. Vol. 398. 2013: John Wiley & Sons.
117. Petitjean, A., et al., *Injury risk curves for the WorldSID 50th male dummy*. 2009, SAE Technical Paper.
118. Wallis, L.A. and I.J.E.m.j. Greaves, *Injuries associated with airbag deployment.* 2002. **19**(6): p. 490-493.
119. Lewis-Beck, M.S. and A. Skalaban, *The R-squared: Some straight talk.* Political Analysis, 1990. **2**: p. 153-171.
120. NHTSA, *Consumer Information; New Car Assessment Program.* Federal Register, 2008(Part II).
121. FHWA. *Frequently Asked Questions: Barriers, Terminals, Transitions, Attenuators, and Bridge Railings*. 2017 [cited 2020 Feb. 25]; Available from: https://safety.fhwa.dot.gov/roadway_dept/countermeasures/faqs/qa_bttabr.cfm#btcc2.
122. Yoganandan, N., et al., *Biomechanics of side impact: injury criteria, aging occupants, and airbag technology.* Journal of biomechanics, 2007. **40**(2): p. 227-243.
123. Kent, R., J. Patrie, and N. Benson. *The Hybrid III dummy as a discriminator of injurious and non-injurious restraint loading*. in *Annual Proceedings/Association for the Advancement of Automotive Medicine*. 2003. Association for the Advancement of Automotive Medicine.
124. IIHS, *Fatality Facts 2019 Collisions with fixed objects and animals.* Arlington, VA, 2022.
125. Hershman, L.L., *The US new car assessment program (NCAP): Past, present and future.* 2001.
126. Federal Register, *49 CFR 571.208 - Standard No. 208; Occupant crash protection*. 2011.
127. Federal Register, *49 CFR § 571.202a - Standard No. 202a; Head restraints; Mandatory applicability begins on September 1, 2009*. 2020.
128. Federal Register, *49 CFR § 571.214 - Standard No. 214; Side impact protection*. 2020.
129. Nava, M.A., *Vehicle dynamics using computer simulations and event data recorders*. 2016, California State University, Sacramento.
130. Gehre, C. and N. Praxl, *Evaluation of a dummy design by using a human body model*, in *9th European LS-DYNA Conference*. 2013: Manchester, UK.
131. Meng, Y. and C. Untaroiu, *Numerical investigation of occupant injury risks in car-to-end terminal crashes using dummy-based injury criteria and vehicle-based crash severity metrics.* Accident Analysis & Prevention, 2020. **145**: p. 105700.
132. Gayzik, F.S., et al. *Development of a full human body finite element model for blunt injury prediction utilizing a multi-modality medical imaging protocol*. in *12th International LS-DYNA User Conference*. 2012.
133. Schwartz, D., et al., *Development of a computationally efficient full human body finite element model.* Traffic injury prevention, 2015. **16**(sup1): p. S49-S56.

134. Schap, J.M., B. Koya, and F.S. Gayzik, *Objective evaluation of whole body kinematics in a simulated, restrained frontal impact.* Annals of Biomedical Engineering, 2019. **47**(2): p. 512-523.
135. Park, G., et al., *Validation of shoulder response of human body finite-element model (GHBMC) under whole body lateral impact condition.* Annals of Biomedical Engineering, 2016. **44**(8): p. 2558-2576.
136. Decker, W., et al., *Modular use of human body models of varying levels of complexity: validation of head kinematics.* Traffic injury prevention, 2017. **18**(sup1): p. S155-S160.
137. Boyle, K.J., et al. *A human modelling study on occupant kinematics in highly reclined seats during frontal crashes*. in *Proceedings of the International Research Conference on the Biomechanics of Impact, IRCOBI, Florence, Italy, 11th September-13th September. IRC-19-43*. 2019.
138. Marzougui, D., et al., *Extended validation of the finite element model for the 2010 Toyota Yaris passenger sedan (MASH 1100kg vehicle)*. 2013.
139. Meng, Y., W. Hu, and C. Untaroiu, *Finite element modeling of an energy-absorbing guardrail end terminal.* SAE International Journal of Commercial Vehicles, 2020. **12**(4).
140. Manual, L.-D.K.U.s. and I. Volume, *Manual Version 971*. Livermore Software Technology Corporation, 2007. **7374**: p. 354.
141. Kennard, R.W. and L.A. Stone, *Computer aided design of experiments.* Technometrics, 1969. **11**(1): p. 137-148.
142. Zhao, J., M. Katagiri, and S. Lee. *Methodology for Occupant Injury Risk Assessment with GHBMC Human Body Models*. in *2019 GHBMC Users' Workshop*. 2019. Detroit, MI, U.S.
143. Johnson, D., B. Koya, and F.S. Gayzik, *Comparison of Neck Injury Criteria Values Across Human Body Models of Varying Complexity.* Frontiers in bioengineering and biotechnology, 2020: p. 985.
144. Kuppa, S., et al., *Lower extremity injuries and associated injury criteria*. 2001, SAE Technical Paper.
145. Hu, J., et al., *Frontal crash simulations using parametric human models representing a diverse population.* Traffic injury prevention, 2019. **20**(sup1): p. S97-S105.
146. Takhounts, E.G., et al., *Development of brain injury criteria (BrIC).* Stapp car crash journal, 2013. **57**: p. 243.
147. Albuquerque, F.D.B.d. and D.M. Awadalla, *Roadside fixed-object collisions, barrier performance, and fatal injuries in single-vehicle, run-off-road crashes.* Safety, 2020. **6**(2): p. 27.
148. Molan, A.M., M. Rezapour, and K. Ksaibati, *Modeling traffic barriers crash severity by considering the effect of traffic barrier dimensions.* Journal of modern transportation, 2019. **27**(2): p. 141-151.
149. Wang, J.-S., *MAIS (05/08) Injury Probability Curves as Functions of Delta V*. 2022.
150. Obeng, K., *Injury severity, vehicle safety features, and intersection crashes.* Traffic injury prevention, 2008. **9**(3): p. 268-276.
151. Long, K., et al., *Safety evaluation for roadside crashes by vehicle–object collision simulation.* Advances in Mechanical Engineering, 2018. **10**(10): p. 1687814018805581.

Appendix

Appendix A Information for crash test and simulation

Table A.1 Basic information for crash test and the validation simulation

General Information	**Known Solution (Crash test)**	**Analysis Solution (FE simulation)**
Test Number:	27-30	NA
Vehicle:	1999 Geo Metro	1997 Geo Metro
Impact Conditions		
Vehicle Mass:	796 kg	813 kg
Speed:	102.5 km/h	102.5 km/h
Angle:	0.1 degree	0.1 degree
Impact Point:	Impact head of ET-Plus; ¼ offset	Impact head of ET-Plus; ¼ offset

Appendix B Energy-time histories for Geo-Metro simulations

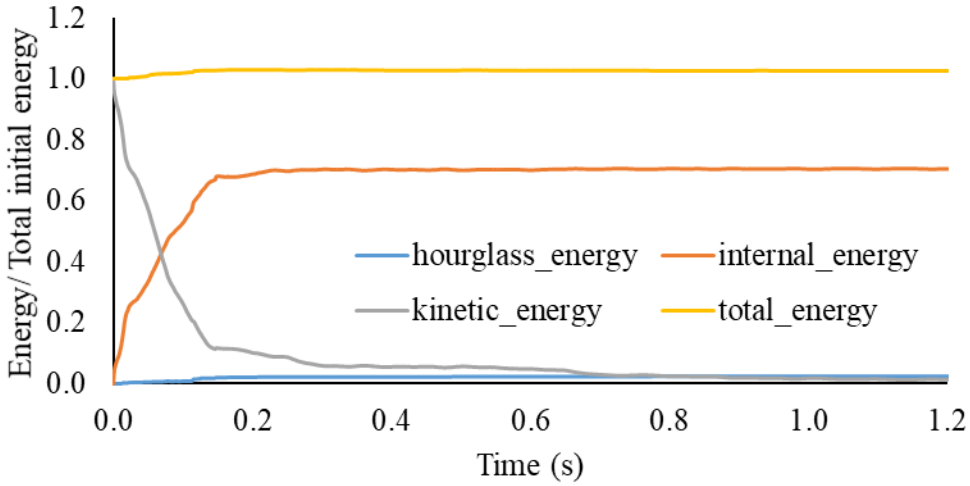

Figure B.1 Plot of global energy-time histories for Geo-Metro-undamaged ET-Plus crash simulation

Table B.1 Analysis solution verification table for the validation simulation

Verification Evaluation Criteria*	**Change (%)**	**Pass?**
Total energy of the analysis solution (i.e., kinetic, potential, contact, etc.) must not vary more than 10 percent from the beginning of the run to the end of the run.	3.20	Yes
Hourglass Energy of the analysis solution at the end of the run is less than five percent of the total initial energy at the beginning of the run.	2.39	Yes
The part/material with the highest amount of hourglass energy at any time during the run is less than five percent of the total initial energy at the beginning of the run.	0.84	Yes
Mass added to the total model is less than five percent of the total model mass at the beginning of the run.	0	Yes
The part/material with the most mass added had less than 10 percent of its initial mass added.	0	Yes
The moving parts/materials in the model have less than five percent of mass added to the initial moving mass of the model.	0	Yes
There are shooting nodes in the solution?	No	Yes
There are solid elements with negative volumes?	No	Yes

* The criteria are based on Procedures for Verification and Validation of Computer Simulations Used for Roadside Safety Applications [64]

Appendix C Quantitative evaluation of the validation simulation

Table C.1 Quantitative evaluation of the validation simulation

Verification Evaluation Criteria			**Pass?**
Sprague-Geer Metrics	M (Criteria =40)	P (Criteria =40)	
Yaw angle	-2.7	0.9	Yes
Roll angle	-23.3	37.4	Yes
Pitch angle	-22.3	27.2	Yes
ANOVA Metrics	Average (Criteria =5)	SD* (Criteria =35)	
Yaw angle	-1.8	2.5	Yes
Roll angle	28.5	25.2	No**
Pitch angle	8.1	26.4	No**

Note: *SD: Standard Deviation; ** Roll and pitch angles only match the test data at the beginning of the crash [63]

Appendix D Dummy-based injury criteria recorded in each simulation

Table D.1 Dummy-based injury criteria recorded in each simulation

Pre-impact vehicle conditions			Dummy-based injury criteria					
Velocity	Offset	Angle	HIC36	HIC15	Nij	Chest Deflection (mm)	Chest Acceleration (g)	Femur load (kN)
65	1/4	0	67	31	0.21	20	21	1.8
65	1/4	15	353	353	0.41	15	17	1.6
65	0	0	289	169	0.25	19	23	2.7
65	0	15	105	55	0.23	22	23	2.1
80	1/4	0	88	88	0.15	20	21	2.3
80	1/4	15	219	219	0.69	15	22	1.9
80	0	0	242	155	0.19	24	24	2.5
80	0	15	125	69	0.31	22	26	2.6
100	1/4	0 *	96	50	0.41	27	21	2.5
100	1/4	15	308	308	0.52	23	24	2.2
100	0	0	465	465	0.55	29	31	3.0
100	0	15**	198	133	0.56	29	33	3.0
112	1/4	0	113	85	0.32	28	22	2.7
112	1/4	15	457	457	0.80	24	24	1.1
112	0	0	412	492	0.36	35	38	2.8
112	0	15	523	523	0.69	34	35	3.0
120	1/4	0	111	99	0.16	29	22	2.7
120	1/4	15	481	481	0.73	22	24	1.5
120	0	0	441	351	0.65	39	48	4.3
120	0	15	412	397	0.86	32	38	3.1
FMVSS 208 limits			**1000**	**700**	**1**	**63**	**60**	**10**

Note: * Corresponding to the test conditions used in the MASH guideline (test 30)
** Corresponding to the test conditions used in the MASH guideline (test 32)

Appendix E Coefficient of correlation plot between pre-impact conditions and dummy body-region injury criteria

a) HIC_{36}

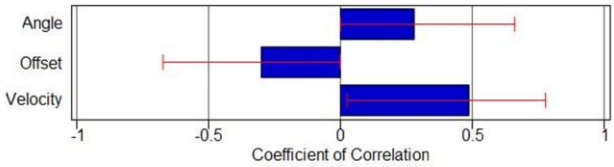

b) HIC_{15}

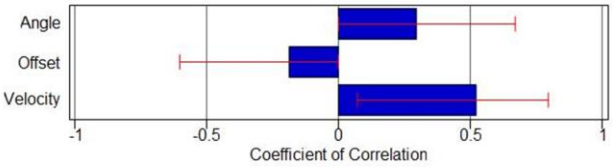

c) Chest deflection

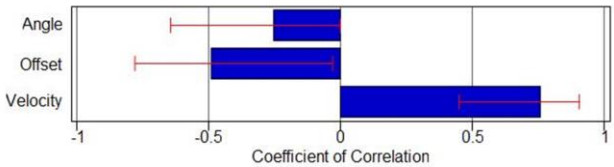

d) Chest acceleration

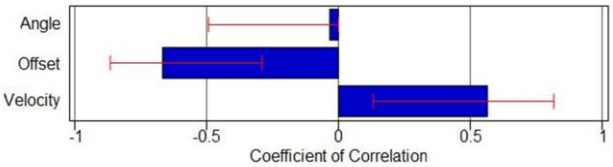

e) Femur load

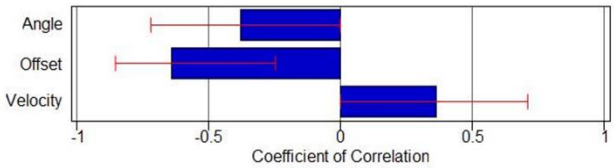

Figure E.1 Coefficient of correlation plot between pre-impact conditions and dummy body region injury criteria: a) HIC36; b) HIC15; c) Chest deflection; d) Chest acceleration; e) Femur load

Appendix F Correlation between ORA longitudinal and dummy body-region injury probabilities

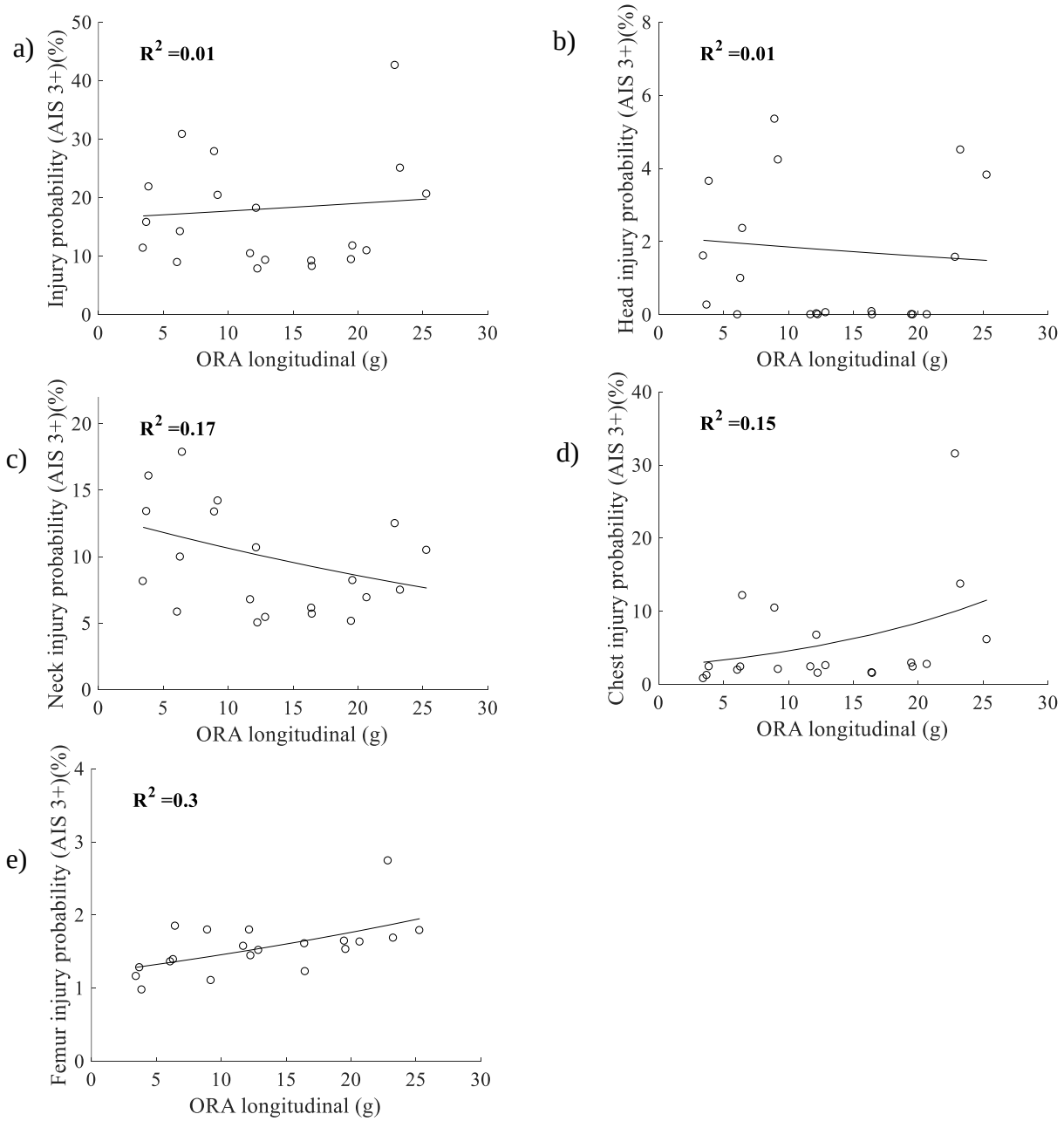

Figure F.1 Correlation between ORA longitudinal and dummy body-region injury probabilities: a) full body; b) head; c) neck; d) chest; e) femur

Appendix G Correlation between ASI and dummy body-region injury probabilities

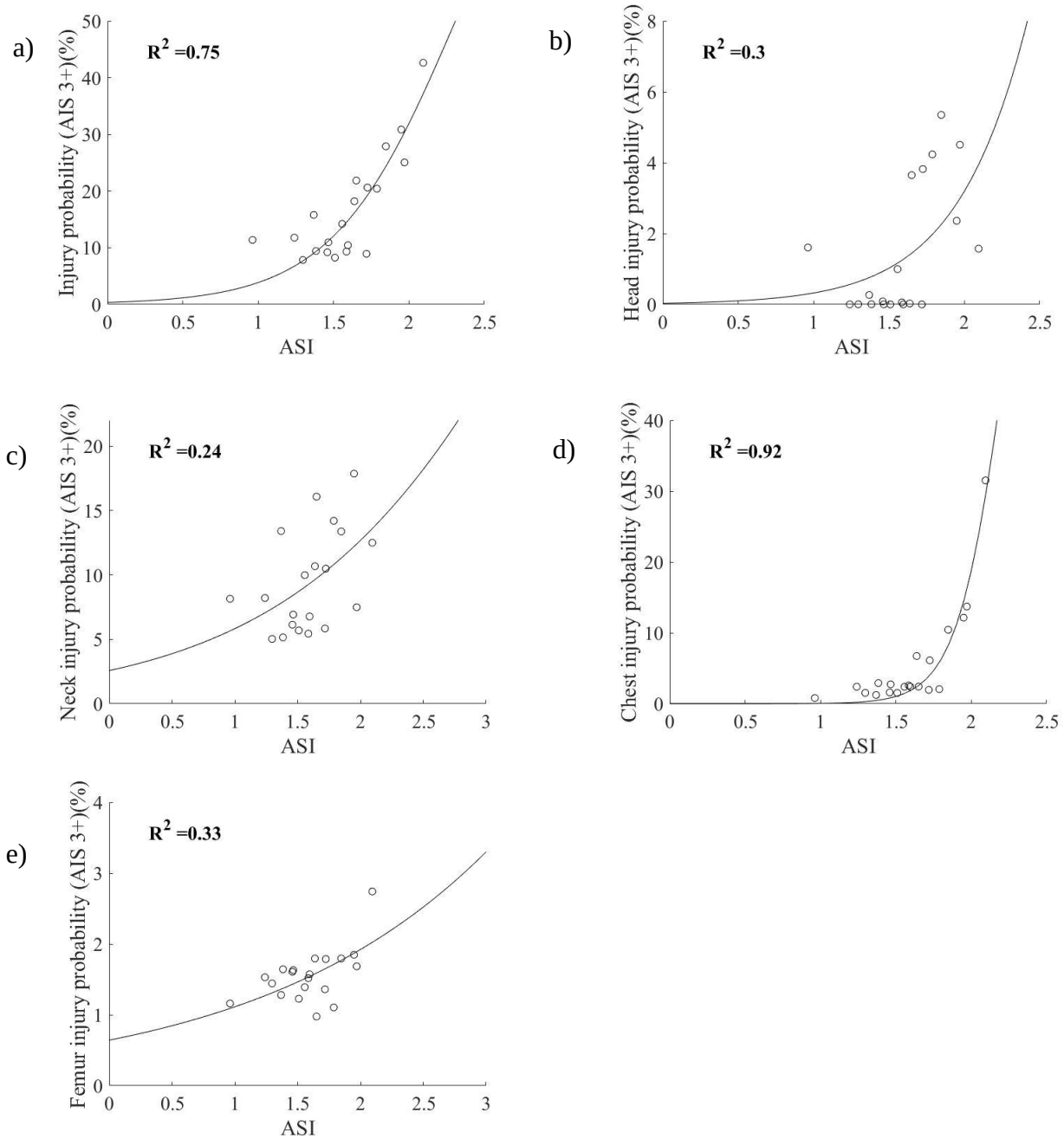

Figure G.1 Correlation between ASI and dummy body-region injury probabilities: a) full body; b) head; c) neck; d) chest; e) femur

Appendix H Correlation between THIV and dummy body-region injury probabilities

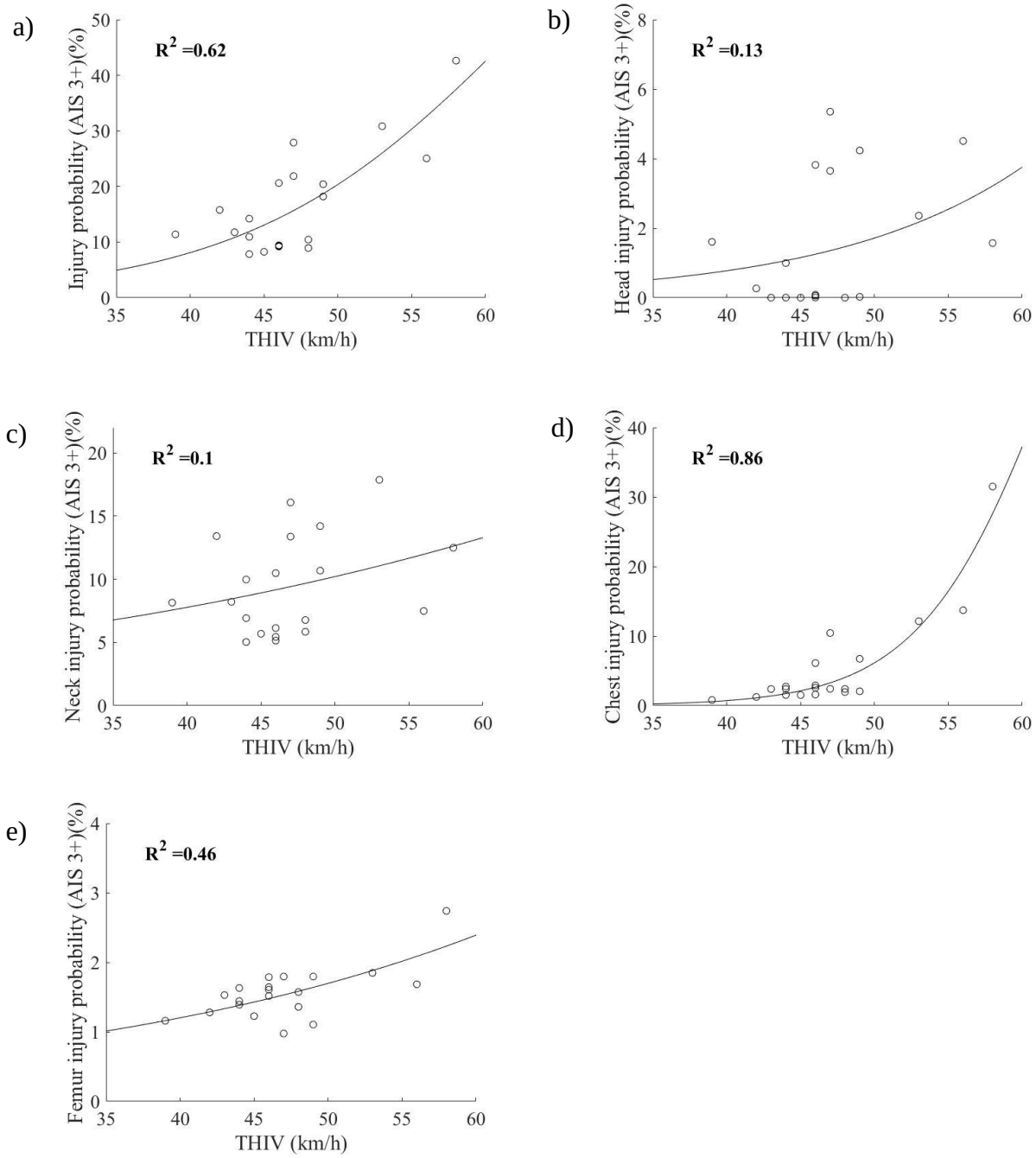

Figure H.1 0-2Correlation between THIV and dummy body-region injury probabilities: a) full body; b) head; c) neck; d) chest; e) femur

Appendix I GHBMC injury risks equations

Table I.1 Equations to assess GHBMC injury risks

Body region	Injury risks	Injury severity	Reference
Head	$P(Head) = \Phi(\frac{\ln(HIC_{15}) - 7.45231}{0.73998})$	AIS 3+	[103]
Brain	$P(Brain) = 1 - e^{-(\frac{BrIC-0.523}{0.513})^{1.8}}$	AIS 3+	[146]
Neck	$P(Neck) = \frac{1}{1 + e^{3.227-1.969\times N_{ij}}}$	AIS 3+	[103]
	$P(NeckForce) = \frac{1}{1 + e^{10.9745-2.375*Nt\ or\ Nc}}$	AIS 3+	[103]
Chest	$P(Chest) = \frac{1}{1 + e^{10.5456-1.568*CD^{0.4612}}}$	AIS 3+	[145]
Thigh	$P(Thigh) = \frac{1}{1 + e^{4.9795-0.326\times F}}$	AIS 3+	[144]
Upper tibia	$P(Upper\ Tibia) = \frac{1}{1 + e^{0.5204-0.0819*F_{UT}+0.0686*mass}}$ In which, mass =79 kg	AIS 2+	[144]
Lower tibia	$P(Lower\ Tibia) = \frac{1}{1 + e^{4.572-0.67*F_{LT}}}$	AIS 2+	[144]
Leg	$P(Leg) = 1 - \exp(-e^{\frac{\ln(RTI)-0.2728}{0.2468}})$	AIS 2+	[144]
Full-body	$OIM = 1 - \left(1 - P(Head)\right) \times \left(1 - P(Neck)\right) \times \left(1 - P(Chest)\right) \times \left(1 - P(Thigh)\right)$	NA	[131]

Appendix J Copyright from *Accident Analysis and Prevention*

The papers "An examination of the performance of damaged energy-absorbing end terminals" and "Numerical investigation of occupant injury risks in car-to-end terminal crashes using dummy-based injury criteria and vehicle-based crash severity metrics" were published on Accident Analysis and Prevention. A copyright description is shown below, no copyright permission is required to republish the contents in dissertation.

Author:

Yunzhu Meng,Wen Hu,Costin Untaroiu

Publication:

Accident Analysis & Prevention

Publisher:

Elsevier

Date:

November 2020

Journal Author Rights

Please note that, as the author of this Elsevier article, you retain the right to include it in a thesis or dissertation, provided it is not published commercially. Permission is not required, but please ensure that you reference the journal as the original source. For more information on this and on your other retained rights, please visit: https://www.elsevier.com/about/our-business/policies/copyright#Author-rights

Appendix K Copyright from *SAE International Journal of Commercial Vehicles*

The paper "Finite Element Modeling of an Energy-Absorbing Guardrail End Terminal" was published on SAE International journal of commercial vehicles. The copyright license is as below:

CCC Marketplace™

This is a License Agreement between Yunzhu Meng ("User") and Copyright Clearance Center, Inc. ("CCC") on behalf of the Rightsholder identified in the order details below. The license consists of the order details, the Marketplace Order General Terms and Conditions below, and any Rightsholder Terms and Conditions which are included below.

All payments must be made in full to CCC in accordance with the Marketplace Order General Terms and Conditions below.

Order Date	23-Jun-2022	Type of Use	Republish in a thesis/dissertation
Order License ID	1240310-1		
ISSN	1946-3928	Publisher	SAE International
		Portion	Chapter/article

LICENSED CONTENT

Publication Title	SAE International journal of commercial vehicles	Rightsholder	SAE International
		Publication Type	Journal
Article Title	Finite Element Modeling of an Energy-Absorbing Guardrail End Terminal	Issue	4
		Volume	12
Author/Editor	Society of Automotive Engineers.	URL	http://saecomveh.saejournals.org/
Date	01/01/2009		
Language	English		
Country	United States of America		

REQUEST DETAILS

Portion Type	Chapter/article	Rights Requested	Main product
Page range(s)	271-280	Distribution	United States
Total number of pages	10	Translation	Original language of publication
Format (select all that apply)	Electronic	Copies for the disabled?	No
Who will republish the content?	Author of requested content	Minor editing privileges?	No
		Incidental promotional use?	No
Duration of Use	Life of current edition		
Lifetime Unit Quantity	Up to 499	Currency	USD

NEW WORK DETAILS

Title	Investigation of W-beam energy-absorbing guardrail end terminal safety performance using Finite Element modeling	Institution name	Virginia Tech
		Expected presentation date	2022-08-01
Instructor name	Yunzhu Meng		

ADDITIONAL DETAILS

Order reference number	N/A	**The requesting person / organization to appear on the license**	Yunzhu Meng

REUSE CONTENT DETAILS

Title, description or numeric reference of the portion(s)	Finite Element Modeling of an Energy-Absorbing Guardrail End Terminal	**Title of the article/chapter the portion is from**	Finite Element Modeling of an Energy-Absorbing Guardrail End Terminal
Editor of portion(s)	Untaroiu, Costin Daniel; Untaroiu, Costin Daniel; Hu, Wen; Hu, Wen; Meng, Yunzhu; Meng, Yunzhu	**Author of portion(s)**	Untaroiu, Costin Daniel; Untaroiu, Costin Daniel; Hu, Wen; Hu, Wen; Meng, Yunzhu; Meng, Yunzhu
Volume of serial or monograph	12	**Issue, if republishing an article from a serial**	4
Page or page range of portion	271-280	**Publication date of portion**	2020-02-07

Marketplace Order General Terms and Conditions

The following terms and conditions ("General Terms"), together with any applicable Publisher Terms and Conditions, govern User's use of Works pursuant to the Licenses granted by Copyright Clearance Center, Inc. ("CCC") on behalf of the applicable Rightsholders of such Works through CCC's applicable Marketplace transactional licensing services (each, a "Service").

1) **Definitions.** For purposes of these General Terms, the following definitions apply:

"License" is the licensed use the User obtains via the Marketplace platform in a particular licensing transaction, as set forth in the Order Confirmation.

"Order Confirmation" is the confirmation CCC provides to the User at the conclusion of each Marketplace transaction. "Order Confirmation Terms" are additional terms set forth on specific Order Confirmations not set forth in the General Terms that can include terms applicable to a particular CCC transactional licensing service and/or any Rightsholder-specific terms.

"Rightsholder(s)" are the holders of copyright rights in the Works for which a User obtains licenses via the Marketplace platform, which are displayed on specific Order Confirmations.

"Terms" means the terms and conditions set forth in these General Terms and any additional Order Confirmation Terms collectively.

"User" or "you" is the person or entity making the use granted under the relevant License. Where the person accepting the Terms on behalf of a User is a freelancer or other third party who the User authorized to accept the General Terms on the User's behalf, such person shall be deemed jointly a User for purposes of such Terms.

"Work(s)" are the copyright protected works described in relevant Order Confirmations.

2) **Description of Service.** CCC's Marketplace enables Users to obtain Licenses to use one or more Works in accordance with all relevant Terms. CCC grants Licenses as an agent on behalf of the copyright rightsholder identified in the relevant Order Confirmation.

3) **Applicability of Terms.** The Terms govern User's use of Works in connection with the relevant License. In the event of any conflict between General Terms and Order Confirmation Terms, the latter shall govern. User acknowledges that Rightsholders have complete discretion whether to grant any permission, and whether to place any limitations on any grant, and that CCC has no right to supersede or to modify any such discretionary act by a Rightsholder.

4) **Representations; Acceptance.** By using the Service, User represents and warrants that User has been duly authorized by the User to accept, and hereby does accept, all Terms.

5) **Scope of License; Limitations and Obligations.** All Works and all rights therein, including copyright rights, remain the sole and exclusive property of the Rightsholder. The License provides only those rights expressly set forth in the terms and conveys no other rights in any Works

6) **General Payment Terms.** User may pay at time of checkout by credit card or choose to be invoiced. If the User chooses to be invoiced, the User shall: (i) remit payments in the manner identified on specific invoices, (ii) unless otherwise specifically stated in an Order Confirmation or separate written agreement, Users shall remit payments upon receipt of the relevant invoice from CCC, either by delivery or notification of availability of the invoice via the Marketplace platform, and (iii) if the User does not pay the invoice within 30 days of receipt, the User may incur a service charge of 1.5% per month or the maximum rate allowed by applicable law, whichever is less. While User may exercise the rights in the License immediately upon receiving the Order Confirmation, the License is automatically revoked and is null and void, as if it had never been issued, if CCC does not receive complete payment on a timely basis.

7) **General Limits on Use.** Unless otherwise provided in the Order Confirmation, any grant of rights to User (i) involves only the rights set forth in the Terms and does not include subsequent or additional uses, (ii) is non-exclusive and non-transferable, and (iii) is subject to any and all limitations and restrictions (such as, but not limited to, limitations on duration of use or circulation) included in the Terms. Upon completion of the licensed use as set forth in the Order Confirmation, User shall either secure a new permission for further use of the Work(s) or immediately cease any new use of the Work(s) and shall render inaccessible (such as by deleting or by removing or severing links or other locators) any further copies of the Work. User may only make alterations to the Work if and as expressly set forth in the Order Confirmation. No Work may be used in any way that is defamatory, violates the rights of third parties (including such third parties' rights of copyright, privacy, publicity, or other tangible or intangible property), or is otherwise illegal, sexually explicit, or obscene. In addition, User may not conjoin a Work with any other material that may result in damage to the reputation of the Rightsholder. User agrees to inform CCC if it becomes aware of any infringement of any rights in a Work and to cooperate with any reasonable request of CCC or the Rightsholder in connection therewith.

8) **Third Party Materials.** In the event that the material for which a License is sought includes third party materials (such as photographs, illustrations, graphs, inserts and similar materials) that are identified in such material as having been used by permission (or a similar indicator), User is responsible for identifying, and seeking separate licenses (under this Service, if available, or otherwise) for any of such third party materials; without a separate license, User may not use such third party materials via the License.

9) **Copyright Notice.** Use of proper copyright notice for a Work is required as a condition of any License granted under the Service. Unless otherwise provided in the Order Confirmation, a proper copyright notice will read substantially as follows: "Used with permission of [Rightsholder's name], from [Work's title, author, volume, edition number and year of copyright]; permission conveyed through Copyright Clearance Center, Inc." Such notice must be provided in a reasonably legible font size and must be placed either on a cover page or in another location that any person, upon gaining access to the material which is the subject of a permission, shall see, or in the case of republication Licenses, immediately adjacent to the Work as used (for example, as part of a by-line or footnote) or in the place where substantially all other credits or notices for the new work containing the republished Work are located. Failure to include the required notice results in loss to the Rightsholder and CCC, and the User shall be liable to pay liquidated damages for each such failure equal to twice the use fee specified in the Order Confirmation, in addition to the use fee itself and any other fees and charges specified.

10) **Indemnity.** User hereby indemnifies and agrees to defend the Rightsholder and CCC, and their respective employees and directors, against all claims, liability, damages, costs, and expenses, including legal fees and expenses, arising out of any use of a Work beyond the scope of the rights granted herein and in the Order Confirmation, or any use of a Work which has been altered in any unauthorized way by User, including claims of defamation or infringement of rights of copyright, publicity, privacy, or other tangible or intangible property.

11) **Limitation of Liability.** UNDER NO CIRCUMSTANCES WILL CCC OR THE RIGHTSHOLDER BE LIABLE FOR ANY DIRECT, INDIRECT, CONSEQUENTIAL, OR INCIDENTAL DAMAGES (INCLUDING WITHOUT LIMITATION DAMAGES FOR LOSS OF BUSINESS PROFITS OR INFORMATION, OR FOR BUSINESS INTERRUPTION) ARISING OUT OF THE USE OR INABILITY TO USE A WORK, EVEN IF ONE OR BOTH OF THEM HAS BEEN ADVISED OF THE POSSIBILITY OF SUCH DAMAGES. In any event, the total liability of the Rightsholder and CCC (including their respective employees and directors) shall not exceed the total amount actually paid by User for the relevant License. User assumes full liability for the actions and omissions of its principals, employees, agents, affiliates, successors, and assigns.

12) **Limited Warranties.** THE WORK(S) AND RIGHT(S) ARE PROVIDED "AS IS." CCC HAS THE RIGHT TO GRANT TO USER THE RIGHTS GRANTED IN THE ORDER CONFIRMATION DOCUMENT. CCC AND THE RIGHTSHOLDER DISCLAIM ALL OTHER

WARRANTIES RELATING TO THE WORK(S) AND RIGHT(S), EITHER EXPRESS OR IMPLIED, INCLUDING WITHOUT LIMITATION IMPLIED WARRANTIES OF MERCHANTABILITY OR FITNESS FOR A PARTICULAR PURPOSE. ADDITIONAL RIGHTS MAY BE REQUIRED TO USE ILLUSTRATIONS, GRAPHS, PHOTOGRAPHS, ABSTRACTS, INSERTS, OR OTHER PORTIONS OF THE WORK (AS OPPOSED TO THE ENTIRE WORK) IN A MANNER CONTEMPLATED BY USER; USER UNDERSTANDS AND AGREES THAT NEITHER CCC NOR THE RIGHTSHOLDER MAY HAVE SUCH ADDITIONAL RIGHTS TO GRANT.

13) **Effect of Breach.** Any failure by User to pay any amount when due, or any use by User of a Work beyond the scope of the License set forth in the Order Confirmation and/or the Terms, shall be a material breach of such License. Any breach not cured within 10 days of written notice thereof shall result in immediate termination of such License without further notice. Any unauthorized (but licensable) use of a Work that is terminated immediately upon notice thereof may be liquidated by payment of the Rightsholder's ordinary license price therefor; any unauthorized (and unlicensable) use that is not terminated immediately for any reason (including, for example, because materials containing the Work cannot reasonably be recalled) will be subject to all remedies available at law or in equity, but in no event to a payment of less than three times the Rightsholder's ordinary license price for the most closely analogous licensable use plus Rightsholder's and/or CCC's costs and expenses incurred in collecting such payment.

14) **Additional Terms for Specific Products and Services.** If a User is making one of the uses described in this Section 14, the additional terms and conditions apply:

a) ***Print Uses of Academic Course Content and Materials (photocopies for academic coursepacks or classroom handouts).*** For photocopies for academic coursepacks or classroom handouts the following additional terms apply:

i) The copies and anthologies created under this License may be made and assembled by faculty members individually or at their request by on-campus bookstores or copy centers, or by off-campus copy shops and other similar entities.

ii) No License granted shall in any way: (i) include any right by User to create a substantively non-identical copy of the Work or to edit or in any other way modify the Work (except by means of deleting material immediately preceding or following the entire portion of the Work copied) (ii) permit "publishing ventures" where any particular anthology would be systematically marketed at multiple institutions.

iii) Subject to any Publisher Terms (and notwithstanding any apparent contradiction in the Order Confirmation arising from data provided by User), any use authorized under the academic pay-per-use service is limited as follows:

A) any License granted shall apply to only one class (bearing a unique identifier as assigned by the institution, and thereby including all sections or other subparts of the class) at one institution;

B) use is limited to not more than 25% of the text of a book or of the items in a published collection of essays, poems or articles;

C) use is limited to no more than the greater of (a) 25% of the text of an issue of a journal or other periodical or (b) two articles from such an issue;

D) no User may sell or distribute any particular anthology, whether photocopied or electronic, at more than one institution of learning;

E) in the case of a photocopy permission, no materials may be entered into electronic memory by User except in order to produce an identical copy of a Work before or during the academic term (or analogous period) as to which any particular permission is granted. In the event that User shall choose to retain materials that are the subject of a photocopy permission in electronic memory for purposes of producing identical copies more than one day after such retention (but still within the scope of any permission granted), User must notify CCC of such fact in the applicable permission request and such retention shall constitute one copy actually sold for purposes of calculating permission fees due; and

F) any permission granted shall expire at the end of the class. No permission granted shall in any way include any right by User to create a substantively non-identical copy of the Work or to edit or in any other way modify the Work (except by means of deleting material immediately preceding or following the entire portion of the Work copied).

iv) Books and Records; Right to Audit. As to each permission granted under the academic pay-per-use Service, User shall maintain for at least four full calendar years books and records sufficient for CCC to determine the

numbers of copies made by User under such permission. CCC and any representatives it may designate shall have the right to audit such books and records at any time during User's ordinary business hours, upon two days' prior notice. If any such audit shall determine that User shall have underpaid for, or underreported, any photocopies sold or by three percent (3%) or more, then User shall bear all the costs of any such audit; otherwise, CCC shall bear the costs of any such audit. Any amount determined by such audit to have been underpaid by User shall immediately be paid to CCC by User, together with interest thereon at the rate of 10% per annum from the date such amount was originally due. The provisions of this paragraph shall survive the termination of this License for any reason.

b) ***Digital Pay-Per-Uses of Academic Course Content and Materials (e-coursepacks, electronic reserves, learning management systems, academic institution intranets).*** For uses in e-coursepacks, posts in electronic reserves, posts in learning management systems, or posts on academic institution intranets, the following additional terms apply:

i) The pay-per-uses subject to this Section 14(b) include:

A) **Posting e-reserves, course management systems, e-coursepacks for text-based content,** which grants authorizations to import requested material in electronic format, and allows electronic access to this material to members of a designated college or university class, under the direction of an instructor designated by the college or university, accessible only under appropriate electronic controls (e.g., password);

B) **Posting e-reserves, course management systems, e-coursepacks for material consisting of photographs or other still images not embedded in text,** which grants not only the authorizations described in Section 14(b)(i)(A) above, but also the following authorization: to include the requested material in course materials for use consistent with Section 14(b)(i)(A) above, including any necessary resizing, reformatting or modification of the resolution of such requested material (provided that such modification does not alter the underlying editorial content or meaning of the requested material, and provided that the resulting modified content is used solely within the scope of, and in a manner consistent with, the particular authorization described in the Order Confirmation and the Terms), but not including any other form of manipulation, alteration or editing of the requested material;

C) **Posting e-reserves, course management systems, e-coursepacks or other academic distribution for audiovisual content,** which grants not only the authorizations described in Section 14(b)(i)(A) above, but also the following authorizations: (i) to include the requested material in course materials for use consistent with Section 14(b)(i)(A) above; (ii) to display and perform the requested material to such members of such class in the physical classroom or remotely by means of streaming media or other video formats; and (iii) to "clip" or reformat the requested material for purposes of time or content management or ease of delivery, provided that such "clipping" or reformatting does not alter the underlying editorial content or meaning of the requested material and that the resulting material is used solely within the scope of, and in a manner consistent with, the particular authorization described in the Order Confirmation and the Terms. Unless expressly set forth in the relevant Order Conformation, the License does not authorize any other form of manipulation, alteration or editing of the requested material.

ii) Unless expressly set forth in the relevant Order Confirmation, no License granted shall in any way: (i) include any right by User to create a substantively non-identical copy of the Work or to edit or in any other way modify the Work (except by means of deleting material immediately preceding or following the entire portion of the Work copied or, in the case of Works subject to Sections 14(b)(1)(B) or (C) above, as described in such Sections) (ii) permit "publishing ventures" where any particular course materials would be systematically marketed at multiple institutions.

iii) Subject to any further limitations determined in the Rightsholder Terms (and notwithstanding any apparent contradiction in the Order Confirmation arising from data provided by User), any use authorized under the electronic course content pay-per-use service is limited as follows:

A) any License granted shall apply to only one class (bearing a unique identifier as assigned by the institution, and thereby including all sections or other subparts of the class) at one institution;

B) use is limited to not more than 25% of the text of a book or of the items in a published collection of essays, poems or articles;

C) use is limited to not more than the greater of (a) 25% of the text of an issue of a journal or other periodical or (b) two articles from such an issue;

D) no User may sell or distribute any particular materials, whether photocopied or electronic, at more than one institution of learning;

E) electronic access to material which is the subject of an electronic-use permission must be limited by means of electronic password, student identification or other control permitting access solely to students and instructors in the class;

F) User must ensure (through use of an electronic cover page or other appropriate means) that any person, upon gaining electronic access to the material, which is the subject of a permission, shall see:

- a proper copyright notice, identifying the Rightsholder in whose name CCC has granted permission,
- a statement to the effect that such copy was made pursuant to permission,
- a statement identifying the class to which the material applies and notifying the reader that the material has been made available electronically solely for use in the class, and
- a statement to the effect that the material may not be further distributed to any person outside the class, whether by copying or by transmission and whether electronically or in paper form, and User must also ensure that such cover page or other means will print out in the event that the person accessing the material chooses to print out the material or any part thereof.

G) any permission granted shall expire at the end of the class and, absent some other form of authorization, User is thereupon required to delete the applicable material from any electronic storage or to block electronic access to the applicable material.

iv) Uses of separate portions of a Work, even if they are to be included in the same course material or the same university or college class, require separate permissions under the electronic course content pay-per-use Service. Unless otherwise provided in the Order Confirmation, any grant of rights to User is limited to use completed no later than the end of the academic term (or analogous period) as to which any particular permission is granted.

v) Books and Records; Right to Audit. As to each permission granted under the electronic course content Service, User shall maintain for at least four full calendar years books and records sufficient for CCC to determine the numbers of copies made by User under such permission. CCC and any representatives it may designate shall have the right to audit such books and records at any time during User's ordinary business hours, upon two days' prior notice. If any such audit shall determine that User shall have underpaid for, or underreported, any electronic copies used by three percent (3%) or more, then User shall bear all the costs of any such audit; otherwise, CCC shall bear the costs of any such audit. Any amount determined by such audit to have been underpaid by User shall immediately be paid to CCC by User, together with interest thereon at the rate of 10% per annum from the date such amount was originally due. The provisions of this paragraph shall survive the termination of this license for any reason.

c) ***Pay-Per-Use Permissions for Certain Reproductions (Academic photocopies for library reserves and interlibrary loan reporting) (Non-academic internal/external business uses and commercial document delivery).*** The License expressly excludes the uses listed in Section (c)(i)-(v) below (which must be subject to separate license from the applicable Rightsholder) for: academic photocopies for library reserves and interlibrary loan reporting; and non-academic internal/external business uses and commercial document delivery.

i) electronic storage of any reproduction (whether in plain-text, PDF, or any other format) other than on a transitory basis;

ii) the input of Works or reproductions thereof into any computerized database;

iii) reproduction of an entire Work (cover-to-cover copying) except where the Work is a single article;

iv) reproduction for resale to anyone other than a specific customer of User;

v) republication in any different form. Please obtain authorizations for these uses through other CCC services or directly from the rightsholder.

Any license granted is further limited as set forth in any restrictions included in the Order Confirmation and/or in these Terms.

d) ***Electronic Reproductions in Online Environments (Non-Academic-email, intranet, internet and extranet).*** For "electronic reproductions", which generally includes e-mail use (including instant messaging or other electronic transmission to a defined group of recipients) or posting on an intranet, extranet or Intranet site (including any display or performance incidental thereto), the following additional terms apply:

i) Unless otherwise set forth in the Order Confirmation, the License is limited to use completed within 30 days for any use on the Internet, 60 days for any use on an intranet or extranet and one year for any other use, all as measured from the "republication date" as identified in the Order Confirmation, if any, and otherwise from the date of the Order Confirmation.

ii) User may not make or permit any alterations to the Work, unless expressly set forth in the Order Confirmation (after request by User and approval by Rightsholder); provided, however, that a Work consisting of photographs or other still images not embedded in text may, if necessary, be resized, reformatted or have its resolution modified without additional express permission, and a Work consisting of audiovisual content may, if necessary, be "clipped" or reformatted for purposes of time or content management or ease of delivery (provided that any such resizing, reformatting, resolution modification or "clipping" does not alter the underlying editorial content or meaning of the Work used, and that the resulting material is used solely within the scope of, and in a manner consistent with, the particular License described in the Order Confirmation and the Terms.

15) **Miscellaneous.**

a) User acknowledges that CCC may, from time to time, make changes or additions to the Service or to the Terms, and that Rightsholder may make changes or additions to the Rightsholder Terms. Such updated Terms will replace the prior terms and conditions in the order workflow and shall be effective as to any subsequent Licenses but shall not apply to Licenses already granted and paid for under a prior set of terms.

b) Use of User-related information collected through the Service is governed by CCC's privacy policy, available online at www.copyright.com/about/privacy-policy/.

c) The License is personal to User. Therefore, User may not assign or transfer to any other person (whether a natural person or an organization of any kind) the License or any rights granted thereunder; provided, however, that, where applicable, User may assign such License in its entirety on written notice to CCC in the event of a transfer of all or substantially all of User's rights in any new material which includes the Work(s) licensed under this Service.

d) No amendment or waiver of any Terms is binding unless set forth in writing and signed by the appropriate parties, including, where applicable, the Rightsholder. The Rightsholder and CCC hereby object to any terms contained in any writing prepared by or on behalf of the User or its principals, employees, agents or affiliates and purporting to govern or otherwise relate to the License described in the Order Confirmation, which terms are in any way inconsistent with any Terms set forth in the Order Confirmation, and/or in CCC's standard operating procedures, whether such writing is prepared prior to, simultaneously with or subsequent to the Order Confirmation, and whether such writing appears on a copy of the Order Confirmation or in a separate instrument.

e) The License described in the Order Confirmation shall be governed by and construed under the law of the State of New York, USA, without regard to the principles thereof of conflicts of law. Any case, controversy, suit, action, or proceeding arising out of, in connection with, or related to such License shall be brought, at CCC's sole discretion, in any federal or state court located in the County of New York, State of New York, USA, or in any federal or state court whose geographical jurisdiction covers the location of the Rightsholder set forth in the Order Confirmation. The parties expressly submit to the personal jurisdiction and venue of each such federal or state court.